Monitoring, Modeling, and Regulation for Indoor and Outdoor Exercises

By

Yi Zhang

Submitted to the Faculty of Engineering and Information Technology

in partial fulfillment of the requirements for degree of

Doctor of Philosophy

at the University of Technology, Sydney

April 2013

Certificate of Authorship / Originality

I, Yi Zhang, certify that the work in this thesis has not previously been submitted for a degree, nor has it been submitted as part of the requirements of a degree, except as fully acknowledged within the text.

I also certify that this thesis has been written by me. Any help that I have received in my research work and in the preparation of the thesis itself has been acknowledged. In addition, I certify that all information sources and literature used are indicated in the thesis.

Signature of Candidate: **Production Note:**
Signature reuroved prior to publication.

Date: 25/Jan/2014

Acknowledgments

This doctoral thesis has been developed based on control and modeling for the body's cardiovascular and respiratory responses to exercise, which has provided infrastructure support for cardiorespiratory disease detection and diagnosis, home based rehabilitation monitoring, and exercise strength regulation under free living conditions. And this support is gratefully acknowledged.

I would like to express my thankfulness to all the people who have contributed in one way or another to the work presented in this doctoral thesis. In particular, I would like to mention:

My supervisor Dr. Steven W. Su, for his continuous advice and guidance along the realization of this dissertation. He gave me all of encouragements, supports, and advice in every single moment, something that I will never forget. He knew not only how to awake my interest and eagerness for the research, but also showed me to enjoy it. Those with short or eroded memories will never fade in my lifetime. My sincere acknowledgments and admiration to him.

I also would like thank Dr. Ying Guo and Dr. Branko Celler, of the Australian Commonwealth Scientific and Industrial Research Organisation (CSIRO), Information and Communication Technology (ICT) Centre, for introducing me to the various projects and applications at their research interests in the e-Health area, as well as for offering me the CSIRO ICT Research Top Up Scholarship to encourage me. I greatly appreciate having known and worked with all of you, and I hope this will continue again in the near future.

Dr. Weidong Chen, Professor of the Department of Automation at the Shanghai Jiao Tong University, for his previous fundamental works on the cardiorespiratory system modeling and control. His guidance has contributed significantly to the results in this thesis.

Dr. Hung T. Nguyen, Professor of the University of Technology, Sydney (UTS), for providing me a chance to participate in the Australian '2011 three-minute presentation' at faculty round, and '2012 UTS Faculty of Engineering and IT (FEIT) showcase'. Not to mention he always gave the constant support and guidance for my work and helped me get through this thesis on time.

Mr. Jan Szymanski, Engineer at the School of Electrical, Mechanical and Mechatronic Systems of UTS, for introducing me to the various aspects of the hardware designs in microcontroller, as well as for making invaluable comments and options during the study period of hardware implementation.

Thanks to Gunasmin Lye, Phyllis Agius, Craig Shuard, Pym Bains, Juliana Chea, and Racheal Laugery for their constant willingness to help and provide guidance with many formal procedures related to this thesis. The never-ending thesis-related forms, travel documents, human ethics approval documents, and so on, would have taken up many more valuable hours if I were not lucky enough to be able to call or visit you wonderful people when stuck. Not to mention I always enjoyed just dropping in for a chat at the same time.

Also, I would like to thank my colleagues, Azzam Haddad, Mitchell Yuwono, Jordan Nguyen, and Davood Dehestani, as well as all other members at Centre for Health Technologies (CHT) of UTS, for the very hard but also happy moments that we shared during the development of our respective thesis.

To my colleagues in the office at CB01.2015, Kevin Weng, Linda Zhou, Rosemary,

Michael Che, Umar Rashid, and Tao Zhang, I have very much appreciated having known you and working in the same environment as all of you. Each of you are kind-hearted and insanely skilled in various areas, and I wish you all the best.

My sincere acknowledgments go to all of my friends, who are always there to support me the way I am for them. And thanks to them for having kept me sane and contributed largely to the fun I have had over these years in Sydney.

I also want to thank for the support and courage from the UTS librarian gave me constantly. Their help with the, always too bureaucratic, administrative aspects of this work is sincerely appreciated.

And last but not least, I would like to thank my family. My dad has been my lifelong inspiration and mentor, and my mum has always been guiding me. Nothing will ever come between us. My grandparents are always there to encourage me and I only hope to make you proud. I love you all more than words can express and your constant love, support, and guidance over the years have allowed me to become the person I am today.

Abstract

This thesis focuses on the modeling and regulation of exercise intensity by using non-invasive portable sensors. Firstly, an innovative switching Resistance-Capacitor (RC) model has been proposed to depict the dynamics of human cardio-respiratory (CR) responses to the onset and offset of exercise. This switching model utilizes electronic terms with switching mechanism to explicitly depict dynamical characteristics at the onset/offset of exercise and the transition in between. It can not only guarantee the continuity of model output between onset and offset of exercise but also quantify lactate metabolism at onset and offset by using the term 'oxygen debt'.

Secondly, to effectively regulate human CR responses to exercise, a single-input single-output (SISO) closed-loop control framework is proposed. Within this framework, a control oriented modeling approach using support vector regression (SVR) is presented. Based on that, a novel model predictive control (MPC) algorithm is developed for the regulation of exercise intensity. Simulation study shows the proposed machine learning based model predictive control approach can achieve desired performance requirements for both the onset and offset of exercise and the transitions in between.

The third research topic is related to the monitoring of outdoor exercise. A reliable Android application based monitoring system is developed. This system includes a portable HxMBT HR sensor (Zephyr®), an easy-to-use interface, and a supervisory module. This technique is applicable to cardiovascular disease detection and diagnosis, home based rehabilitation monitoring, and exercise strength regulation under free living conditions.

Finally, in order to provide a more reliable automated treadmill system for running exercise, the multi-loop integral controllability (MIC) analysis is introduced, which extends the concept of decentralized integral controllability (DIC) from square systems

to multiple-input single-output (MISO) processes. A condition to ensure MIC for 2ISO is proposed and its sufficiency has been proved by using singular perturbation theory. Then, a sufficient MIC condition for MISO processes is provided.

Table of Contents

List of Figures

List of Tables

Chapter 1

Introduction

Exercise biomedical engineering synthesizes data from exercise physiology, exercise biomedicine, and engineering, utilizing exercise as a stressor to determine the responses from the structure and function of human body, and furthermore to develop technologies and devices for improving the longevity and quality of life. Our research interests focus on new technologies and devices to monitor, evaluate, and control of human cardiovascular and respiratory responses for safe and effective exercise and rehabilitation under free living conditions. For convenience, some terms are introduced first:

Biomedical engineering is a discipline that addresses medical and biological problems through the use of theories borrowed from the physical sciences, and technologies inherited from engineering [34].

Exercise physiology is the discipline of the acute responses and chronic adaptations to a wide range of physical exercise conditions, and of how exercise or sport influences the structure and function of human body [76] [23]. It is studied by assessing how movement affects systems of the body, mostly represented by the cardiorespiratory (CR) system, the nervous system, the musculoskeletal system, the endocrine system, and the cells and sub-cellular molecules of body (Related to our interests the topic of how moderate exercise effects on human CR system is considered).

Exercise biomedical engineering is a new body of knowledge that now integrates the studies of medicine, physiology, exercise, and health technologies. It has been widely

accepted that exercise is beneficial on the prevention and treatment of numerous chronic diseases such as stroke, cardiovascular and coronary heart diseases, diabetics, hypertension, and various degenerative disorders [109] [87] [76] [23]. Thus, this field seeks to close the gap between engineering and exercise medicine: It combines the design and problem solving skills of engineering with medical and biological sciences to advance healthcare treatment, including diagnosis, monitoring, treatment, and therapy [34].

Moreover, our studies emphasize exercise biomedical engineering more than exercise physiology or medicine. Exercise biomedical engineering needs comprehensive knowledge from exercise physiology, medicine, and engineering. For instance, the renal exercise physiologist studies the kidney as an isolated organ to determine effects of exercise on kidney function. The exercise biomedical engineers would specialize in those investigations on the kidney and related physiological responses to exercise, as well as would aim to develop potential methodologies that can provide solutions to help people living with kidney diseases.

In a word, this study discusses some problems of exercise biomedicine in general and of control engineering in particular, as well as comes up with a class of methodologies and devices arising from the monitoring, modeling, and control of human CR responses to indoor and outdoor exercises.

The remaining of this section is organized as follows. The study motivation is being presented in section 1.1, and the aims of the doctoral thesis are introduced in the section 1.2. Section 1.3 and 1.4 include the background and the thesis contribution respectively. Publications are listed in section 1.5, and the overall structure of this thesis is outlined in section 1.6.

1.1 Research Motivation

> Exercise and regular daily physical activity are of vital importance for general well being and in the management of noncommunicable diseases, particularly of obesity and diabetes. Obesity and diabetes are now worldwide public health issues. They lead to increased morbidity and mortality from a range of associated diseases including heart disease, stroke and kidney failure. Recent major randomised clinical trials internationally have demonstrated safe exercise as the best means for the prevention of type 2 diabetes in individuals. Data on obesity in Australia shows that in 2006 62% of Australian Men and 45% of women are overweight or obese. Of these almost a million are diabetic, and the number is expected to rise to more than 1.6 million in 2030. The total health expenditure attributable to diabetes was greater than $0.8 billion in 2001 and is rising rapidly. — "Obesity in Australia: a need for urgent action" [119]

The nature of the illness that beset the whole world population in recent years has undergone a transition from a predominance of communicable diseases (e.g., tuberculosis and pneumonia) to the present predominance of noncommunicable diseases (e.g., cardiovascular diseases, diabetes, cancer, hypertension, chronic respiratory diseases, and various degenerative disorders) [76] [52]. This change represents the contribution of the medical profession, both in research and clinical practice, toward the virtual control and the imminent eradication of a large portion of the formerly dreaded infectious scourges. In 2008 noncommunicable diseases were responsible for 36 million deaths, 63% of the total deaths occurred in the world. The noncommunicable disease deaths are projected to increase by 15% between 2010 and 2020 (to 44 million deaths) [52]. The increase of such noncommunicable diseases offers a challenge not only to medicine, but to exercise as well

[23]. It seems that as improvements in medical science allow us to escape decimation by such communicable diseases, we live longer only to fall prey to the noncommunicable diseases at a slightly later date.

Regular daily physical activity is defined as exercise, the value of which as a prophylactic and therapeutic measure has been proved for the past five decades by much evidence [76] [23]. Although the available evidence indicates that exercise maintains optimum levels of health and fitness, we do not yet have all the answers as to how and why. It may not be unrealistic to have further scientific investigation for the ultimate development of a 'pharmacopoeia of exercise'. One of the relevant interests in the next five decades is to combine designs and problem solving skills of engineering with purposes of such 'pharmacopoeia of exercise' arising from medical and biological sciences. The exercise influences the CR system [118] [23] [130]. Due to conditions such as the CR system can result in faster physiological response, non-invasive diagnostic strategies, low risk of depression in sufferers, the motivation of this research comes from the unsolved issues surrounding human CR responses to exercise, and tends to develop an innovative method for cardiovascular disease detection and diagnosis, home based rehabilitation monitoring, and exercise strength regulation under free living conditions.

> Within a second after muscular contraction, there is a withdrawal of vagal outflow to the heart, which is followed by an increase in sympathetic stimulation of the heart. This results in an increase in cardiac output to ensure that blood flow to the muscle is matched to the metabolic needs. [78]

The CR system involves the cardiovascular system (e.g., heart, arteries and veins) and the respiratory system (e.g., mouth, nose and lungs). In most cases, as the body is exposed to exercise, the cardiovascular system immediately responds to changes in cardiac output (Q), blood flow, and blood pressure, while the respiratory system triggers

an acceleration of your normal breathing rate [76].

> The cardiorespiratory response to dynamic exercise displays a well-defined pattern in normal human subjects. Dynamic exercise is accompanied by an increase in pulmonary ventilation, a rise in cardiac output, caused by an increase both in heart rate and stroke volume, and a redistribution of blood flow towards active muscles, mainly owing to a strong decrease in their vascular resistance. As a consequence of skeletal muscle vasodilation, total peripheral resistance falls, and systemic arterial pressure only rises modestly [114] [42] [92].

Since most of dynamics occurred in both cardiovascular and respiratory systems (CR systems) are nonlinear in fact, and this makes our study very interesting and challenging.

> In the second half of the 20th century, developments in mathematical modeling were limited to basic paradigms, such as flow in morphologically simple regions (e.g., Poiseuille or Womersley solutions) [123], or to models based on electric network analogies. Exact solutions are very difficult to obtain in more general situations, because of the strong nonlinear interactions among different parts of the system and the geometric complexities of individual vascular morphologies. [123]

With all essential dynamical characteristics of the CR kinetics taken into account, this PhD dissertation includes the use of application engineering principles (such as data acquisition, signal processing and modeling, and control theory) and computer simulation techniques for a better choice of the monitoring, modeling, and control of human CR responses to exercise, which features a small, portable, non-invasive, and reliable automated exercise assistance system provided for more efficient and safe exercises. As such,

it particularly concerns about the response relationship between exercise and human CR system from control engineering practice and aims to develop a set of methodologies to the monitoring, modeling, and control of human CR responses to exercise under a portable and non-invasive manner.

1.2 Aims

Currently, both invasive and non-invasive biomedical measurements are rapidly developed. However, an invasive device is usually considered to have higher potential hazard than an equivalent non-invasive device [38]. In human exercise responses and relative areas, the approach to non-invasive measurement is more considered than the one to invasive measurement, due to its specific circumstances where the users will only compromise the non-invasive conditions for their daily exercises meaning that no break in the skin is created, and there is no contact with the mucosa, or skin break, or internal body cavity beyond a natural or artificial body orifice.

Another important performance taken into account is portability. Continuous measurement of key CR responses, such as heart rate (HR), oxygen consumption (VO_2), cardiac output (Q), and stroke volume (SV), for outdoor exercise is an important and very challenging problem, as most existing equipment for measuring CR variables is only suitable for indoor exercise monitoring because of its size, weight, and mobility limitations. We aim to develop a sophisticated body-worn portable sensor network, which can wirelessly monitor the key CR variables to both indoor and outdoor exercise under free living conditions.

In addition, the fundamental difficulty of this study is the modeling and control of CR responses from non-invasive measured parameters. The qualitative methodology is commonly a fashionable branch of research in the area of the biomedical system mod-

eling and control. However, the reliability of such approaches is weakened by the fact that the plant is under-standardized and depends on the insights and the abilities of the observer, thus making an assessment of reliability difficult [50]. To this end, we emphasize a quantitative approach for this study, as it eliminates extraneous variables within the internal structure of systems, and can directly assess the experimental data by a standardized test [50]. Following this idea, our studies develop model-based control systems in terms of both single-input single-output (SISO) and multiple-input single-output (MISO) frameworks. First, within the SISO closed-loop control framework a control oriented modeling approach using support vector regression (SVR) is presented. Based on that, a novel model predictive control (MPC) algorithm is developed for the regulation of exercise intensity. Moreover, in order to achieve a more reliable control performance for exercisers, a fault tolerant control design with MISO processes is introduced. The multi-loop integral controllability (MIC) analysis for MISO processes is proposed.

Describing in more details the purpose of this study, there are a number of aims as follows:

1. **Develop a switching model for human CR responses to the onset and offset of exercise.** This approach investigates the modeling of human CR responses to both the onset and offset of exercise. Twenty subjects performed standardized square-wave exercise bouts on a treadmill. During exercise, HR and VO_2 were monitored and recorded by a portable gas analyzer (K4b^2, Cosmed). Experimental results confirm that the dynamical characteristics at the onset and offset of exercise are distinctively different. In order to fully justify the variations of system dynamics, an innovative switching Resistance-Capacitor (RC) model is proposed. This model can not only explicitly depict the dynamical characteristics at the onset/offset of exercise and the transition in between but also attempt to quantify

lactate metabolism following the term 'oxygen debt'. The proposed model is simulated by using Matlab/Simulink, which shows that this single switching model can estimate human CR responses well in the sense that the simulated model output fits well with the experimental observations at the onset and offset of exercise.

2. **Develop a control oriented modeling methodology to depict nonlinear behaviour of CR dynamics to exercise by using support vector regression (SVR).** In order to effectively regulate CR responses to exercise, a SISO closed-loop control framework is proposed. Within this framework, the nonlinear behaviour of CR dynamic response at the onset and offset of treadmill exercise is investigated. A well designed exercise protocol is applied for capturing nonlinear dynamic behaviours, and a healthy male subject has been invited to participate in the test. Non-invasively measured variables, such as ECG, body movements, and oxygen saturation (S_pO_2), have been reliably monitored and recorded. Based on three sets of experimental data, both steady state gain and time constant of HR response are identified. We established nonlinear models for steady state gain and time constant vs walking speed based on SVR. By using the established SVR models, the nonlinear behaviours for both onset and offset of exercises have been well described.

3. **Develop a model-based control methodology for the regulation of exercise strength at the onset and offset of exercise.** In this regard, the study explores control methodologies to handle time variant behavior for HR dynamics at the onset and offset of exercises. To achieve this goal, a novel switching Model Predictive Control (MPC) algorithm is presented to optimize the exercise strength at both onset and offset of exercises. Specifically, Dynamic Matrix Control (DMC), one of the most popular MPC control algorithms, has been employed as the essential of the optimization of process regulation while switching strategy

has been adopted during the transfer between the onset and offset of exercises. The parameters of the DMC/MPC controller have been well tuned based on a previously established SVM based regression model relating to both onset and offset of treadmill walking exercises. The effectiveness of the proposed modeling and control approach has been shown from the regulation of dynamical HR response to exercise through simulation using MATLAB.

4. **Develop a Multi-loop Integral Controllability (MIC) analysis method for nonlinear 2ISO and MISO processes.** Although the performance of the SISO models is adequate, we believe that a special non-square model, unitizing the fault-tolerant scheme that adds multiple redundant input data, would be achieve a better estimate of each of the desired CR variables. Multi-loop integral control is still one of the most popular control strategies in industry due to its simplicity, efficiency, offset free tracking, and capability for fault tolerance. Skogestad and Morari introduced Decentralized Integral Controllability (DIC) to investigate the decentralized unconditional stability under multi-loop integral control for square systems. However, in engineering practice, some multivariable processes may not be square, which often utilize multiple redundant control inputs for the regulation of only one single output. This study extends the concept of Decentralized Integral Controllability to non-square systems, and presents sufficient conditions for MISO nonlinear processes based on singular perturbation analysis.

   For HR regulation during treadmill exercises, simultaneously adjusting both treadmill speed and gradient is able to handle system failures and improve the reliability of treadmill based exercise rehabilitation. By using the MIC analysis method, this study provides sufficient conditions for HR tracking under multi-loop integral control. Simulation results indicate that simultaneously manipulating gradient and speed can significantly achieve better tracking performance.

5. **Develop an Android application for monitoring and regulation of outdoor exercise.** This study develops an Android application to estimate human CR towards the predefined exercise protocol and assist people to regulate exercise strength under the outdoor exercise environment. During exercise, a portable HxMBT Bluetooth HR chest strap is unitized to monitor the HR dynamics. In order to obtain the real-time HR data, the developed Android application is paired and connected with the HxMBT HR sensor via Bluetooth, while developing a boundary control method for regulations of exercise strength following the predefined exercise protocol, and an auditory system for exercise guidance (this technique has been applied, until now, to a boundary control algorithm, and is compatible with HR signals (Zephyr®) only. The results obtained, however, are encouraged enough to, in a near future, develop more portable Bluetooth instruments and sensors such as ECG (electrocardiogram), respiration rate, body temperature, tri-axial accelerometery).

1.3 Background

> Mathematical and numerical investigations of the cardiovascular system, although a relatively new research area, will give rise to some of the major mathematical challenges of the coming decades. - Alfio Quarteroni

The physiology of the cardiovascular system has been elucidated only gradually over many centuries. Among the major actors in the lengthy process have been some of the central characters in human history.

Aristotle (384 - 322 B.C.), for example, identified the role of blood vessels in transferring "animal heat" from the heart to the periphery of the body (although he ignored blood

circulation). In the third century B.C., Praxagoras realized that arteries and veins have different roles (believing that arteries transported air while veins transported blood). Galen (c. 130 - 200 A.D.) was the first to observe the presence of blood in arteries. [123]

Much later, in the 17th century, Sir William Harvey inaugurated modern cardiovascular research with his *De Motu Cardis and Sanguinis Amimalibus*, in which he wrote, "When I turned to vivisection I found the task so hard I was about to think that only God could understand the heart motion." His plaintive moment notwithstanding. Harvey observed that the morphology of valves in veins is such that they are effective only if blood is flowing toward the heart. His conclusion: "I began privately to consider if it (the blood) had a movement, as it is, it would be in a circle." [123]

In the 18th century, the Reverend S. Hales introduced quantitative studies of blood pressure (Hemostatics, 1773). Later, Euler and D. Bernoulli both made great contributions to fluid dynamics research. In particular, Bernoulli, investigating the laws governing blood pressure as a professor of anatomy at the University of Basel in Switzerland, formulated his famous law relating pressure, density, and velocity: $p + 1/2\rho|\mu|^2$ =const (vis viva equation, 1730). [123]

In the 19th century, J.P. Poiseuille, a medical doctor and a physicist, was studying the flow of blood in arteries when he derived the first simplified mathematical model of flow in a cylindrical pipe, a model that still bears his name today. T. Young later made fundamental contributions to research on elastic properties of arterial tissues and on the propagation of pressure: "The inquiry in which manner and at what degree the circulation of the blood depends on the muscular and the elastic powers of the heart and of the arteries, supposing the nature of these powers to be known, must become simply a question belonging to the most renowned departments of the theory of hydraulics" (from a lesson given by Young at the Royal Society of London in 1809). [123]

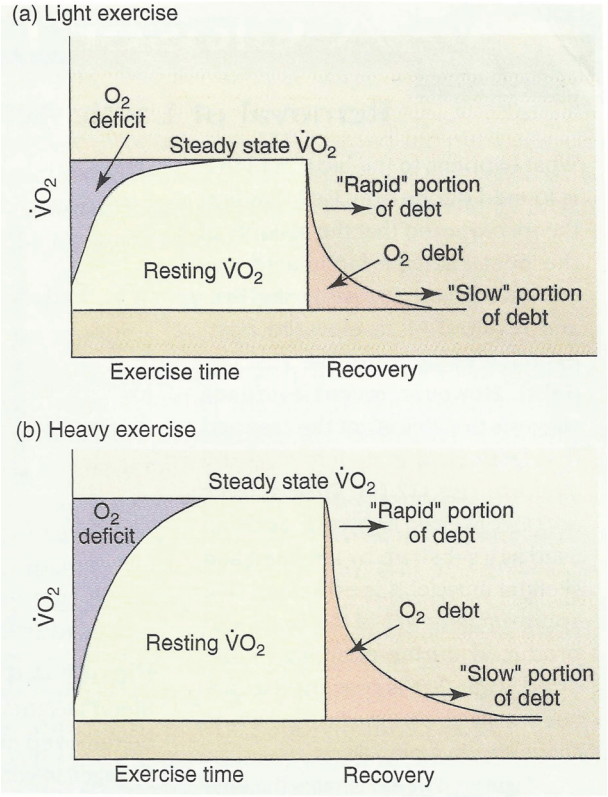

Fig. 1.1: A. V. Hill's hypothesis for energy metabolism during light to moderate exercise and recovery.

At the beginning of the 20th century, the increase of degenerative diseases (such as cardiovascular diseases and obesity) results to developments in exercise physiology. In 1922, A. V. Hill et al. introduced the idea that the exercise energy metabolism during exercise can be described using financial-accounting terms. The concept of 'oxygen debt' was first coined in the analysis of exercise energy metabolism, see Fig. 1.1. The body's carbohydrate stores are linked to energy 'credits'. If these stored credits are expended during exercise bouts, then a 'debt' is occurred. The greater energy 'deficit', or use of available stored energy credits, the larger energy 'debt' occurs [101]. The ongoing oxygen uptake after exercise workouts is thought to represent the metabolic cost of repaying this debt.

Since the second half of the 20th century, numerous linear and nonlinear mathematical

models were developed. In 1979, Magosso et al. established input design for model discrimination problem arising from respiratory control during exercise [51]. In 1980, Hajek et al. developed a model of the heart rate regulation during exercise and recovery, by measuring the reflex vagal under different exercise intensity [74]. In 2002, Magosso and Ursino introduced a mathematical model for cardiovascular response to dynamic exercise based on electric network analogies [97], in which they stated, "The model is used to simulate the steady state response of the main cardiovascular hemodynamic quantities (systemic arterial pressure, and blood flow in working muscle) to various intensity levels of two-legs dynamic exercise." In 2005, Meste et al. used a frequency analysis method to extract the heart period series under graded exercise conditions [102]. In 2008, Cheng et al. proposed a nonlinear model for the HR response to treadmill walking exercise, describing the central and peripheral local responses to walking exercise and their interactions [39]. In 2009, Cabasson et al. introduced a analysis method for time delay estimation of electrocardiographic signal processing from exercise and recovery, with an enhancement of PR interval estimation (index of the atrioventricular conduction time) by limiting the distortion effect of the T wave overlapping the P wave at high heart rates [28]. In 2011, Mesto et al. established a specific heart rate variability analysis during exercise stress testing based on the integral pulse frequency modulation model, where a time-varying threshold is included to account for the non-stationary mean heart rate [14]. Based on developments in mathematical modeling, control techniques also were applied to developed models before. Su et al., for example, successfully identified the heart rate dynamic responses during treadmill exercise by using Hammerstein models in 2007 [148]. Stefano et al. following this study, introduced nonlinear control techniques. They concluded, "An non-local and non-switching control guarantees heart rate regulation with no exact knowledge of model parameters and nonlinearities: It simply generalizes to the nonlinear framework the classical proportional-integral control design

for linear models of HR response during treadmill exercises. [134]"

Recently developments in mathematical modeling in terms of the exercise physiology of the cardiovascular system are limited to basic paradigms, such as models based on electric network analogies. Exact solutions are very difficult to obtain in more general situations, because of the strong nonlinear interactions among different parts of the system.

1.4 Thesis contributions

The aim of our studies is to research and develop new methods and devices to monitor, evaluate, and control of human CR system for safe and effective exercise and rehabilitation under free-living conditions.

During medical diagnosis and analysis of CR kinetics, transient response of HR/VO_2 is important as it contains indicators of current disease or warnings about impending cardiac diseases [4]. Although both linear and nonlinear modeling approaches [134] [74] [28] [39] [102] [14] [71] [15] [27] have been applied to explore dynamic characteristics of HR/VO_2 response to exercise, few papers explore variation of dynamic characteristics under different exercise intensities at the both onset and offset of exercises. For moderate exercise, literatures often assume HR/VO_2 dynamics can be described by linear time invariant models. In the previous study [151], it was observed that time constant of HR response to exercise is influenced by the load of exercise, as well as by self conditions. If the model contains less uncertainty, higher control performance can be expected. Therefore, it is worthwhile to establish a more accurate dynamical model to enhance the control performance of HR regulation.

The first attempt to describe the physiological variation in dynamics of the oxygen

uptake response during exercise and recovery (also called the onset and offset of exercise) perhaps was proposed by A.V. Hill and others in 1922 [53], who used financial-accounting philosophies to analyze this behavior. According to their hypothesis, the concept of 'oxygen debt' was first coined in the analysis of exercise energy metabolism, see Fig. 1.1. The body's carbohydrate stores are linked to energy 'credits'. If these stored credits are expended during exercise bouts, then a 'debt' is occurred. The greater energy 'deficit', or use of available stored energy credits, the larger energy 'debt' occurs [101]. The ongoing oxygen uptake after exercise workouts is thought to represent the metabolic cost of repaying this debt. Their studies employed financial-accounting terms to qualitatively depict energy metabolism during exercise and recovery.

The first contribution in this thesis is a *switching Resistance-Capacitor (RC) model* provided whose dynamics, which can closely describe human CR responses during exercise and recovery, not only numerically verify the physiological phenomena reported by A.V. Hill and others but also quantify energy 'credits', 'debt', and the whole energy process during exercise and recovery. The previous modeling approaches (apart from a preliminary version of our proposed modeling methodology [169]) utilize only a single non-switching model for either the onset or offset of exercise. Though it can accurately describe the dynamical characteristics at the onset and/or offset of exercise, the transient behavior during switching has previously been overlooked. A natural solution for the limitations of previous methods without description of a switching transient is to utilize a model inclusive of a switching mechanism. In order to be consistent with experimental observations, the switching model should guarantee the continuity of model output during model switching. In addition, it is also desired that the switching model can provide physiological explanations for variations of the dynamic characteristics at the onset and offset of exercise. My supervisors introduced to use the traditional series Resistance-Capacitor (RC) circuit for modeling of dynamic variations at a non-switching

single onset or single offset of exercise. Following their idea, in this study, an innovative *switching Resistance-Capacitor (RC) model* in terms of the traditional series RC circuit was proposed, which uses electronic terms to quantify human CR responses at the onset, offset, and transition between exercise. Based on the RC model, a possible physiological explanation for the process of body energy storage and dissipation at the onset and offset of exercise is also provided.

Another contribution in this thesis is that an nonlinear control approach, namely *machine learning based model predictive control*, is presented in order to describe nonlinearities found by the experimental observation, showing that the time constant of HR/VO_2 response to exercise is influenced by the load of exercise, as well as by self conditions (e.g., during a constant exercise intensity such as step response, steady state gain and time constant of HR/VO_2 response to exercise were found to mostly still be varying in every single moment). This approach is a modeling and control integrated method including a support vector machine regression (SVR) and a model predictive control (MPC). In addition, the model based switching control strategy is also adopted dealing with the transfer between the onset and offset of exercise, in that the dynamics in between are dramatically different, and should be described separately.

Moreover, the previous monitoring methods in terms of management of CR responses to exercise are only suitable for indoor exercise monitoring because of the size, weight and mobility limitations of equipments [101] [44] [25]. Fig. 1.2 shows an exercise monitoring equipment. The current method developed in this PhD thesis has been successfully implemented for outdoor exercise, which includes a portable Bluetooth heart rate sensor and a smart phone (the HxMBT HR sensor (Zephyr®) and Sumsang Galaxy mobile phone (Sumsang®) in our experiments), referred to as *Smartphone-based portable exercise monitoring and regulation system*. In this regard, an Android software is developed in order to implement the wireless communication amongst hardwares, including an

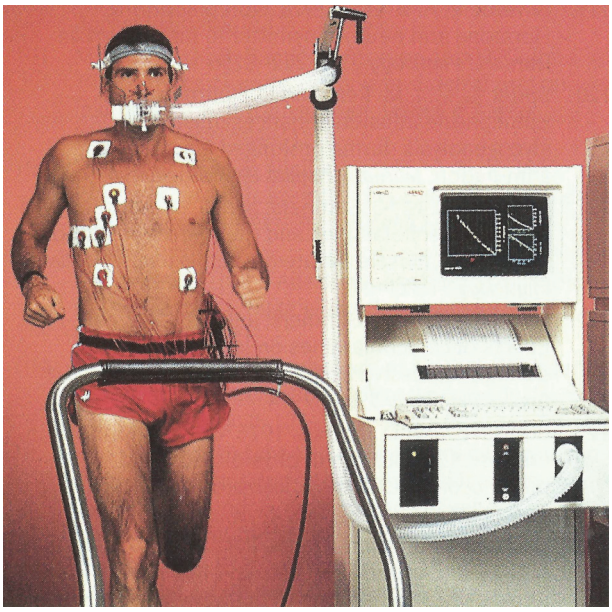

Fig. 1.2: Monitoring equipment for ECG and VO_2 during treadmill exercise. [118]

easy-to-use interface and a supervision system. Until now, we have developed a boundary control algorithm to manage or assist people to do exercise. However, the main contribution of this study is to provide a platform in which the exercise intensity and duration in outdoor exercises can be well regulated by configuring audible and/or visible reminder features of mobile phones.

Except for issues on SISO feedback control for human CR responses to exercise, some problems in MISO feedback system in terms of fault tolerant scheme are also discussed in this thesis. This study discusses the system fault tolerant ability in 2ISO and MISO plants in terms of the nonlinear multi-loop integral controllability (MIC) analysis, and provides sufficient conditions which ensure plants for 2ISO and MISO are MIC respectively. The multi-loop integral controller design for both 2ISO and MISO is such that the control performance can satisfy the free offset tracking results of the closed loop system under faulty conditions.

1.5 Publications

1.5.1 Book chapters

- W. Chen, Steven W. Su, Yi Zhang, Ying Guo, N. Nguyen, Branko G. Celler, and Hung T. Nguyen, " Nonlinear modeling using support vector machine for heart rate response to exercise", In: Computational Intelligence and its Applications: Evolutionary Computation, Fuzzy Logic, Neural Network and Support Vector Machine Techniques, World Scientific, 2010.

- Yi Zhang, Steven W. Su, Hung T. Nguyen, and Branko G. Celler, "Machine learning based nonlinear model predictive control for heart rate response to exercise", In: Computational Intelligence and its Applications: Evolutionary Computation, Fuzzy Logic, Neural Network and Support Vector Machine Techniques, World Scientific, 2010.

1.5.2 Journal articles

- Azzam Haddad, Yi Zhang, Steven Su, Branko Celler and Hung Nguyen, "Modelling and Regulating of Cardio-Respiratory Response for the Enhancement of Interval Training", BioMedical Engineering OnLine, 2014. -accepted

- Yi Zhang, Azzam Haddad, Steven W. Su, Branko G. Celler, Aaron Coutts, Rob Duffield, Cheyne Donges, and Hung T. Nguyen, "A switching model for human cardiorespiratory responses to the onset and offset of exercise", IEEE Transactions on Biomedical Engineering, 2013. - submitted

- Lu Wang, Yi Zhang, Ying Guo, N. Nguyen, D.M. Zhang, and Branko G. Celler, " A mathematical model of cardiovascular system under graded exercise levels", International Journal of Bioinformatics Research and Applications, vol. 8, No. 5/6, pp.455-473,

2012.

- Yi Zhang, W. Chen, Steven W. Su, and Branko G. Celler, "Nonlinear modelling and control for heart rate response to exercise", International Journal of Bioinformatics Research and Applications, 2011.

1.5.3 Conference papers

- Yi Zhang, Steven W. Su, Andrey V. Savkin, Branko G. Celler, and Hung T. Nguyen, "Multi-loop integral controllability analysis for nonlinear multiple-input single-output processes", Proceedings of Australian Control Conference (AUCC), Sydney, Australia, pp. 82-92, November 15-16, 2012.

- Yi Zhang, Steven W. Su, Azzam Haddad, Branko G. Celler, and Hung T. Nguyen, "Onset and offset exercise response model in electronic terms", Proceedings of the 9th IASTED International Conference on Biomedical Engineering, Innsbruck, Austria, February 15-17, 2012.

- Kevin Weng, Yi Zhang, T.N. Nguyen, Azzam Haddad, Branko G. Celler, Steven W. Su, Ying Guo, and Hung T. Nguyen, "Multi-loop integral control by using redundant control inputs for passive fault tolerant implementation", The 2011 International Conference on Measurement and Control Engineering (ICMCE2011), Puerto Rico, USA, pp. 7-12, October 21-23, 2011.

- Yi Zhang, Niu Wang, Azzam Haddad, "Control system design and implementation by using a 32-bit system-on-chip (I) software design", The 2010 International Conference on Management Science and Engineering, vol. 2, pp. 34-37, 2010.

- Yi Zhang, "Control system design and implementation by using a 32-bit system-on-chip (II) hardware implementation", The 2010 International Conference on Management

Science and Engineering, vol. 2, pp. 38-41, 2010.

- Yi Zhang, Nadarajah Veluppillai, Steven W. Su, and Jordan Nguyen, "Model predictive controller design for static var compensator", Proceedings of the 8th Asia-Pacific Conference on Control & Measurement, vol. 3, pp. 100-104, 2008.

1.6 Structure of the thesis

This thesis is structured in 9 chapters. The brief overview of CR system and exercise in biomedical applications is presented in Chapter 2, providing an insight into the background used to this study for dealing with the problems inherent in the exercise-related biomedical engineering field, such as metabolic energy process, CR fitness, measurement of work and energy expenditure, treadmill, exercise protocols, exercise and diseases. In Chapter 3, the detailed quantitative modeling methodology that we proposed for human CR responses to the onset and offset of exercise, as it is originally devised, is presented. The next chapters 4 and 5 are centered on the control approach of human CR responses to exercise, starting with Chapter 4 where considering the nonlinear time-varying of dynamics of CR exercise responses a qualitative modeling and simulation methodology called *Support Vector Machine* is proposed to deal with such dynamics. As this control oriented modeling approach can describe the nonlinear time-variance, Chapter 5 focuses on a novel model-based control algorithm, called *switching Model Predictive Control (MPC)*, which has been proposed for the optimization of exercise efforts. Chapter 6 describes an enhancement of control methodology for dealing with system fault tolerance inherited to the development of exercise-related biomedical devices, the fault tolerant control scheme that applies redundant actuators to handle potential system failures. To this end, a special non-square 2ISO systems, adjusting both treadmill speed and gradient simultaneously for the control of single output variable (such as HR or

VO_2), is proposed. In Chapter 7, it extends the multi-loop integral control analysis of 2ISO systems, described already in Chapter 6, and tackles a theoretical problem namely the controllability analysis of MISO systems. Chapter 8 depicts a portable noninvasive exercise monitoring methodology for measuring CR variables in the both indoor and outdoor environments, using the developed smartphone application. Finally, Chapter 9 provides a summary of the applicability of this study, lists the major contribution of the dissertation, and presents an outlook of open problems and possible future research efforts extending the work presented in this thesis.

Chapter 2

Literature review in exercise biomedicine

2.1 Exercise metabolism

There are three metabolic energy pathways existing in the human body: the phosphagen system, glycolytic system and the aerobic system [86]. The phosphagen system (also called the adenosine triphosphate (ATP)-creatine phosphate (CP) system) provides the fastest pathway to resynthesize ATP. CP, stored in skeletal muscles, is catabolised to allow the phosphate to combine with ADP to produce ATP. No carbohydrate or fat is used in this process and the regeneration of ATP is resultant solely from CP. As this process does not require the presence of oxygen to resynthesize ATP, it is anaerobic in nature. The phosphagen system is the predominant energy system used for all-out exercise lasting up to about 10 seconds.

Glycolysis is the second-fastest way to resynthesize ATP and is the dominant system for exercise lasting from 30 seconds to about 2 minutes. During glycolysis, carbohydrate, in the form of either blood glucose (sugar) or glycogen (the stored form of glucose in muscles and the liver), is degraded through a series of chemical reactions to form pyruvate (glycogen is first converted into glucose through a process called glycogenolysis). For every glucose molecule converted to pyruvate through glycolysis, two molecules of usable ATP are produced [56][86]. Thus, only small volumes of energy are produced via this pathway. Once pyruvate is formed, it has two fates: conversion to lactate or

conversion to a metabolic intermediary molecule called acetyl coenzyme A (acetyl-CoA), which enters the mitochondria for oxidation and the production of more ATP [128][86]. Conversion to lactate occurs when the demand for oxygen is greater than the supply (i.e., during anaerobic exercise). Conversely, when there is enough oxygen available to meet the muscles' needs (i.e., during aerobic exercise), pyruvate (via acetyl-CoA) enters the mitochondria and goes through the aerobic system.

The aerobic system, which is dependent on the sufficient presence of oxygen in the mitochondria, is the slowest pathway to resynthesize ATP. The aerobic system, including the Krebs cycle and the Electron Transport Chain, uses blood glucose, glycogen and fat as fuels to resynthesize ATP in the mitochondria of muscle cells. Carbohydrate, glucose and glycogen are first metabolized through glycolysis, with the resulting pyruvate (via acetyl-CoA), entering the Krebs cycle. The electrons removed from the fuel sources in the Krebs cycle are then transported through the Electron Transport Chain, where ATP and water are produced. Complete oxidation of glucose via glycolysis, the Krebs cycle and the electron transport chain produces 36 molecules of ATP for every molecule of glucose broken down. Thus, the aerobic system produces 18 times more ATP than does anaerobic glycolysis (via lactate) from each glucose molecule.

Fat, which is stored as triglyceride in adipose tissue underneath the skin and within skeletal muscles (called intramuscular triglyceride), is the other major fuel for the aerobic system, and is the largest store of energy in the body. When using fat, triglycerides are first broken down into free fatty acids and glycerol (a process called lipolysis). The free fatty acids, which are composed of a long chain of carbon atoms, are transported to the muscle mitochondria, where the carbon atoms are used to produce acetyl-CoA (a process called beta-oxidation).

Following acetyl-CoA formation, fat metabolism is identical to carbohydrate metabolism, with acetyl-CoA entering the Krebs cycle and electrons being transported to the elec-

tron transport chain to form ATP and water. The oxidation of free fatty acids yields many more ATP molecules than the oxidation of glucose or glycogen. For example, the oxidation of the fatty acid palmitate produces 129 molecules of ATP [128][56].

2.2 Human cardiorespiratory responses to exercise

CR fitness is the ability of human body's cardiovascular and respiratory systems to supply oxygen to skeletal muscles during physical activity. Regular exercise makes these systems more efficient by enlarging the heart muscle, enabling more blood to be pumped with each stroke, and increasing the number of small arteries in skeletal muscles, which supply more blood to working muscles. Exercise improves the respiratory system by increasing the amount of oxygen that is inhaled and distributed to body tissue [46].

2.2.1 Indicators of cardiorespiratory fitness

There are numerous variables in terms of indicating the cardiovascular fitness during exercise, such as electrocardiogram (ECG), blood pressure, cardiac output (Q), respiration rate, body temperature, and plasma glucose concentration, etc.

2.2.1.1 Electrocardiogram

An ECG is used to measure the rate and regularity of heartbeats, as well as size and position of the chambers, the presence of any damage to the heart, and the effects of drugs or devices used to regulate the heart, such as a pacemaker. Electrocardiography is a transthoracic (across the thorax or chest) interpretation of the electrical activity of the heart over a period of time, as detected by electrodes attached to the surface of the skin and recorded by a device external to the body.

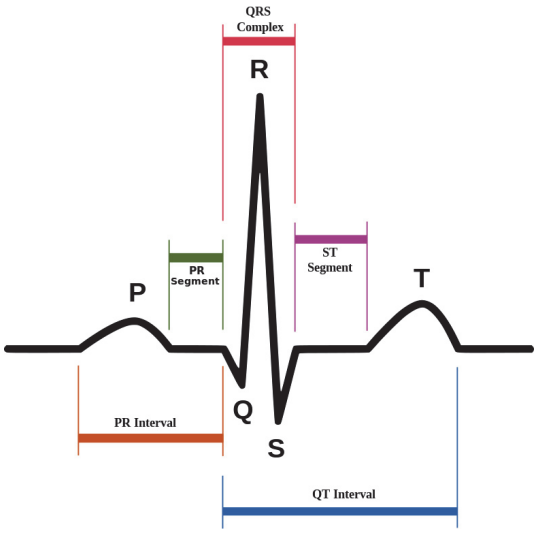

Fig. 2.1: The normal ECG during rest.

Fig. 2.1 illustrates a normal ECG pattern. Each of these distinct waveforms is identified by different letters. The P wave results from the depolarization of the atria, the QRS complex results from ventricular depolarization, and the T wave is due to ventricular repolarization.

Analysis of the ECG during exercise is often used in the diagnosis of coronary artery disease. The most common cause of heart disease is the collection of fatty plaque (also called atherosclerosis) inside coronary vessels. This collection of plaque reduces blood flow to the myocardium. The adequacy of blood flow to the heart is relative - it depends on the metabolic demand placed on the heart. An obstruction to a coronary artery, for example, may allow sufficient blood flow at rest, but may be inadequate during exercise due to increased metabolic demand placed on the heart. Therefore, a graded exercise test may serve as a 'stress test' to evaluate cardiac function. [118]

An example of an abnormal exercise ECG is shown in Fig. 2.2, the depressed ST segment in the picture on the right when compared to the normal ECG on the left. Myocardial ischemia (reduced blood flow) may be detected by changes in the ST segment of the ECG.

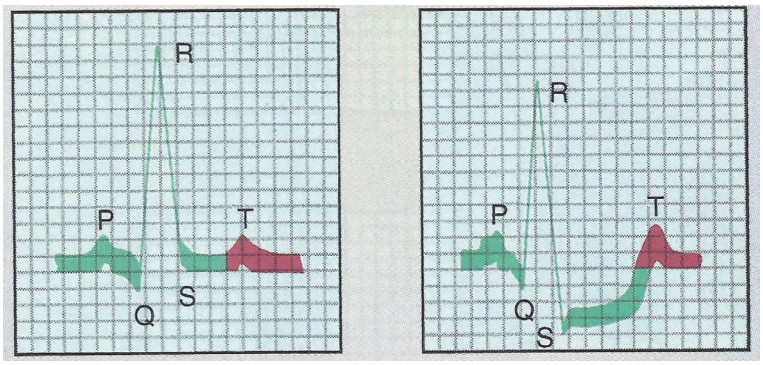

Fig. 2.2: Depression of the ST segment of the electrocardiogram as a result of myocardial ischemia (left: normal right: ischemia). [118]

2.2.1.2 Blood pressure

Blood pressure, sometimes referred to as arterial blood pressure, is the force exerted by blood against the arterial walls and is determined by how much blood is pumped and the resistance to blood flow. Arterial blood pressure can be estimated by the use of a sphygmonanometer. The normal blood pressure of an adult male is 120/80, while that of adult females tends to be lower (110/70). The larger number in the expression of blood pressure is the systolic pressure expressed in millimeters of mercury ($mm\ Hg$); the lower number in the blood pressure ratio is the diastolic pressure, again expressed in ($mm\ Hg$). Systolic blood pressure is the pressure generated as blood is ejected from the heart during ventricular systole. During ventricular relaxation (diastole), the arterial blood pressure decreases and represents diastolic blood pressure.

In the body, the arterial blood pressure depends on a variety of physiological factors, including cardiac output, blood volume, resistance to flow, and blood viscosity. An increase in any of these variables results in an increase in arterial blood pressure. Conversely, a decrease in any of these variables causes a decrease in blood pressure. Acute (short-term) regulation is achieved by the sympathetic nervous system, while long-term regulation of blood pressure is primarily a function of kidneys. [43]

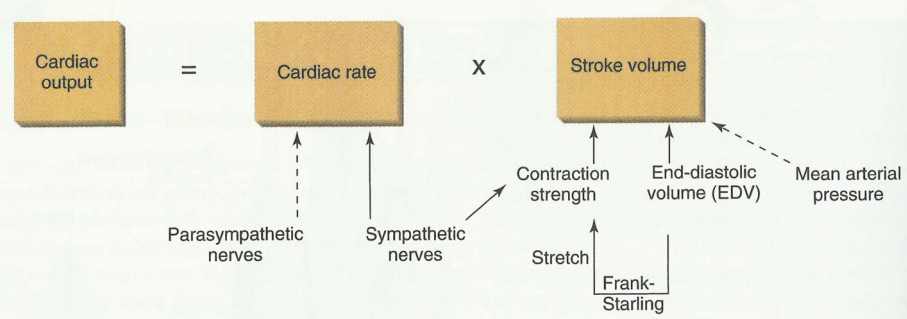

Fig. 2.3: Factors that regulate Q (variables that stimulate Q are shown by solid arrows, while factors that reduce Q are shown by dotted arrows). [118]

2.2.1.3 Cardiac output

Cardiac output (Q) is the product of the HR and SV (amount of blood pumped per heartbeat):

$$Q = HR \times SV. \tag{2.1}$$

Thus, Q can be increased due to a rise in either HR or SV. During exercise, the increase in Q is due to an increase in both HR and SV. Fig. 2.3 summarizes those variables that influence Q during exercise.

HR is the number of heartbeats per unit of time, typically expressed as beats per minute (bpm) [138]. During exercise the quantity of blood pumped by the heart must change in accordance with the elevated skeletal muscle oxygen demand. Since the SA node controls HR, changes in HR often involve factors that influence the SA node. The two most prominent factors that influence HR are the parasympathetic and sympathetic nervous systems [132] [158]. The parasympathetic nervous system acts as a braking system to slow down heart rate. Conversely, stimulation of the sinoatrial node (SA node) and atrioventricular node (AV node) by the sympathetic nervous system is responsible for increases in heart rate [85].

SV is the volume of blood pumped from one ventricle of the heart with each beat. SV, at

rest or during exercise, is regulated by three variables: the end-diastolic volume (the volume of blood in the ventricles at the end of diastole); the average aortic blood pressure; and the strength of ventricular contraction. The end-diastolic volume influences SV in the following way. Two physiologists, Frank and Starling, demonstrated that stretch of the ventricles increased with an enlargement of the end-diastolic volume. This relationship has become known as the Frank-Starling law of the heart. The increase in the end-diastolic volume results in a lengthening of cardiac fibers, which improves the force of contraction. A rise in cardiac contractility results in an increase in the rate of venous return to the heart.

2.2.1.4 Respiration rate

VO_2, oxygen consumption, is the amount of oxygen taken up and utilized by the body per minute. Oxygen extraction considers the amount of oxygen in arterial blood that is sent to metabolically active tissue, and the amount of oxygen in venous blood being returned to the heart. The difference in arterial oxygen content and venous oxygen content determines the amount of oxygen that was used by the tissue. Oxygen delivery, on the other hand, is a measure of cardiac function, specifically of Q. Accurately measuring oxygen uptake or consumption can be evaluated directly in a clinical setting. It typically uses a treadmill or stationary bike as an ergometer to measure control exercise intensity. The subject wears a mask with a breathing tube connect to oxygen and carbon dioxide analyzers to measure consumption and outputs.

VO_2max is most closely linked to the functional capacity of the cardiovascular system to deliver blood to the working muscles during maximal and supramaximal ($>100\%VO_2max$) work, while maintaining mean arterial blood pressure. It has the form of

$$VO_{2max} = Q \times (C_aO_2 - C_vO_2), \tag{2.2}$$

where Q is the cardiac output of the heart, C_aO_2 is the arterial oxygen content, and C_vO_2 is the venous oxygen content. $(C_aO_2 - C_vO_2)$ is also known as the arteriovenous oxygen difference (systemic oxygen extraction).

Endurance training programs that increase VO_{2max} involve a large muscle mass in dynamic exercise (e.g., running, cycling, swimming, or cross-country skiing) for twenty to sixty minutes per session, three to five times per week at an intensity of about 50% to 85% VO_{2max} [43].

2.2.1.5 Body temperature

Skin temperature of human body can be measured by placing temperature sensors (such as thermistors) on the skin at various locations. The mean skin temperature can be calculated by assigning certain factors to each individual skin measurement in proportion to the fraction of the body's total surface area that each measurement represents. For example, mean skin temperature (T_s) can be estimated by the following formula:

$$T_s = (T_{forehead} + T_{chest} + T_{forearm} + T_{thigh} + T_{calf} + T_{abdomen} + T_{back})/7, \tag{2.3}$$

where $T_{forehead}$, T_{chest}, $T_{forearm}$, T_{thigh}, T_{calf}, $T_{abdomen}$, and T_{back} represent skin temperatures measured on the forehead, chest, forearm, thigh, calf, abdomen and back, respectively.

Heat production increases during exercise due to muscular contraction and is directly proportional to the exercise intensity. Fig. 2.4 illustrates the roles of evaporation, convection, and radiation in heat loss during constant-load exercise in a moderate environment. [105]

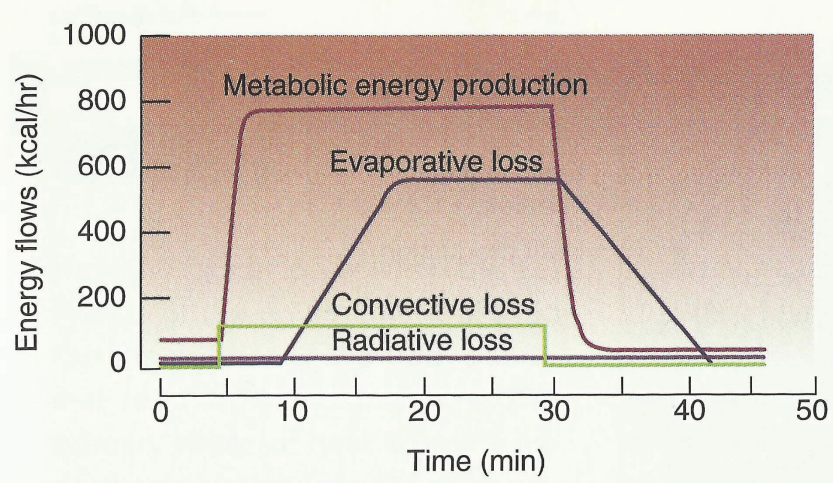

Fig. 2.4: Changes in metabolic energy production, evaporative heat loss, convective heat loss, and radiative heat loss during 25 minutes of submaximal exercise in a cool environment. [118]

2.2.1.6 Plasma glucose concentration

Plasma glucose is the amount of glucose present in the blood [40] [54] [68] [79] [146] [101]. It is maintained by a rate of glucose appearance (entry into the blood) and glucose disposal (removal from the blood). In the healthy individual, rate of appearance and disposal are essentially equal during activity of moderate intensity and duration; however, sufficiently exercise intense (such as the onset exercise in our experiment) can result in an imbalance leaning towards a higher rate of disposal than appearance, at which point glucose levels fall. Rate of glucose appearance is dictated by the amount of glucose being absorbed at the gut as well as hepatic glucose output. Although glucose absorption from the gut is not typically a source of glucose appearance during exercise, the liver is capable of catabolising stored glycogen (glycogenolysis) as well as synthesizing new glycogen (gluconeogenesis). When a subject exercises initially, the body responds to the activity by releasing hormones that cause it to increase rate of glucose appearance. This occurs primarily through glycogenolysis. However, along with continued exertion of the workout, rate of glucose appearance is dropping down as glucose

units are quickly used up. Thereby onset of exercise can induce a tendency of decreasing the blood glucose level, because the rate of consumed energy within muscle cells is gradually larger than that supplied through glucongeogenesis or muscle glycogen [101]. Following the workout of exercise, firstly rate of glucose appearance remains high as the demanded energy from muscle cells sharply reduces. This imbalanced plasma glucose concentration triggers the gluconeogenesis process in the liver. Then the blood glucose level, for a healthy individual, can drop down to its pre-exercise equilibrium at which one starts exercising.

2.2.2 Measurement of work and energy expenditure

2.2.3 Treadmill

Treadmill is a device for walking or running while staying in the same place. Work usually can be calculated for a participant moving on a treadmill by knowing the participant's body weight, and the gradient and speed at which the participant is moving.

Medical treadmills are class IIb active therapeutic devices and also active devices for diagnosis. They measure the HR of the subject. When connected through interface with ECG or ergospirometry or blood pressure monitor they become a new medical system (e.g., stress test system or cardiopulmonary rehab system) and measure also the ECG, VO_2max, breath volumes, blood pressure, muscle activity and various other vital functions.

2.2.4 Exercise protocol

The onset and offset of exercise (also namely exercise and recovery) is a test that evaluates an individual's physiological response (e.g., HR and VO_2) to exercise, the intensity

of which is increased in stages.This kind of test can be performed using bench (for step-ups), a cycle ergometer, or a treadmill. A typical test has three stages: warm-up, the onset of exercise (also called exercise), and the offset of exercise (also called recovery). The warm-up stage aims to minimize effects of the anaerobic system for the onset and offset of exercise, including the phosphagen and glycolytic systems with respect to the metabolic energy pathways introduced in section 2. Moreover, the exercise duration and intensity for the onset and offset of exercise in experiments are followed by [16], in which the VO_2max was estimated in people of different ages. For example, the horizontal axis in Fig. 2.5 demonstrates the warm-up (before 0), exercise (0 - 10 min), and recovery (10 - 20 min), respectively. The test starts with a subject walking gently on a treadmill for warm-up, whose intensity will then be accelerated in the onset of exercise stage at the predefined time interval. After the onset of exercise workout the subject is followed by the offset of exercise stage, which usually has a same exercise intensity with the one in the warm-up stage. HR and VO_2 are monitored continuously. The onset and offset of exercise provides estimates of the ability of the lungs, heart, and blood vessels to deliver oxygen to respiring tissue; therefore they are measurements of aerobic or CR fitness.

2.2.4.1 Transition from rest to exercise

At the beginning of exercise there is a rapid increase in Q. It has been shown that Q begins to increase within the first second after muscular contraction begins, see Fig. 2.5. If the work rate is constant and below the lactate threshold, a steady state plateau in HR, SV and Q is reached within two to three minutes. This response is similar to that observed in oxygen uptake at the beginning of exercise. [118]

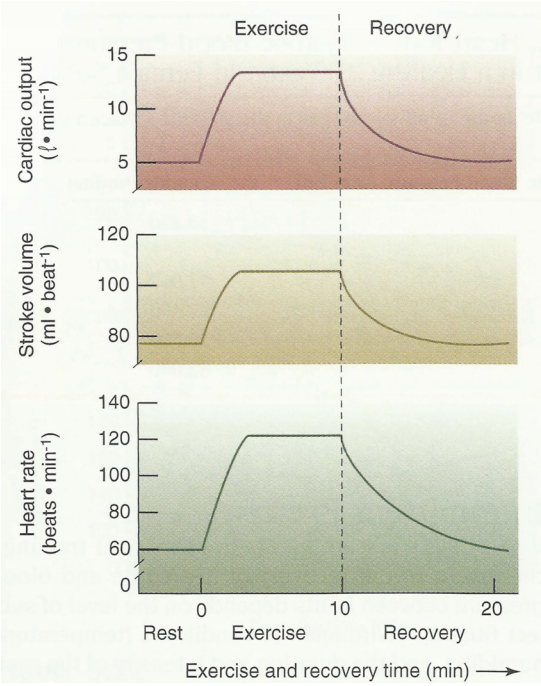

Fig. 2.5: Changes in Q, SV, and HR during the transition from rest to submaximal constant intensity exercise and during recovery. [118]

2.2.4.2 Transition from exercise to recovery

Recovery from short-term, low exercise intensity is generally rapid. Fig. 2.5 shows that HR, SV, and Q all decrease rapidly back toward resting levels following this exercise protocol. Recovery speed varies from individual to individual, with well-conditioned subjects demonstrating better recuperative powers than untrained subjects. In regard to recovery HRs, the slopes of HR decay following exercise protocol are generally the same for trained and untrained subjects. However, trained subjects recover faster since they do not achieve as a high HR as untrained subjects during a particular exercise protocol. [131]

Recovery from long-term exercise is much slower than the response depicted in Fig. 2.5. This is particularly true when the exercise is performed in hot/humid conditions, since an elevated body temperature delays the fall in HR during recovery from exercise. [131]

2.2.4.3 Energy expenditure

In biology, energy balance is the biological homeostasis of energy in living systems. It is measured with the following equation [157]:

$$Energy\ intake = internal\ heat\ produced + external\ work + energy\ stored. \quad (2.4)$$

In the US, it is generally measured using the energy unit calorie (i.e., kilogram calorie), which equals the energy needed to increase the temperature of 1 kg of water by 1 °C. This is about 4.184 kJ.

Energy expenditure is mainly a sum of internal heat produced and external work. In general, there are two techniques employed in the measurement of human energy expenditure: direct calorimetry and indirect calorimetry. Direct calorimetry is the process that measures a body's metabolic rate via the measurement of heat production. The general process can be drawn schematically as [26]:

$$Foodstuff + O_2 \rightarrow ATP + Heat. \quad (2.5)$$

Although directly calorimetry is considered to be a precise technique for the measurement of metabolic rate, equipment for measurement of heat production is very expensive and the measuring process during exercise is complicated. Fortunately, the term called indirect calorimetry can be used to measure metabolic rate, which can be explained by the following relationship:

$$Foodstuff + O_2 \rightarrow Heat + CO_2 + H_2O. \quad (2.6)$$

Since a direct relationship exists between O_2 consumed and the amount of heat produc-

tion in the body, measuring O_2 consumption (VO_2) provides an estimate of metabolic rate [60].

2.3 Exercise and diseases

The nature of the illness that beset the whole world population in recent years has undergone a transition from a predominance of infectious disease (e.g. tuberculosis and pneumnia) to the present predominance of degenerative diseases (e.g. cancer and cardiovascular diseases) [76]. This change represents the contribution of the medical profession, both in research and clinical practice, toward the virtual control and the imminent eradication of a large portion of the formerly dreaded infectious scourges. For example, in 1996 cardiovascular diseases and cancers were responsible for 1.5 million deaths, greatly overshadowing all other causes of death [7].

The increase of such degenerative diseases such as cardiovascular and coronary heart diseases, stroke, cancer, diabetes mellitus, osteoporosis, and osteoarthritis offers a challenge not only to medicine, but to exercise as well [23]. It seems that as improvements in medical science allow us to escape decimation by such infectious diseases as tuberculosis, diphtheria, and poliomyelitis, we live longer only to fall prey to the degenerative diseases at a slightly later date. Because degenerative diseases will represent the majority of the whole illness of human beings, and because the major degenerative diseases occur later in life (after 25 years of age), as explained latter in the section 2.3, it is not uncommon to see such individuals in adult fitness programs, where the research for biomedical devices in terms of the secretion of exercise has been explored by engineers.

Exercise was used as a primary nonpharmacological intervention for a variety of problems, and as a normal part of therapy for the treatment of coronary heart disease and diabetes. This section 2.3 will discuss the special concerns that must be addressed when

exercise is used for people with specific diseases.

2.3.1 Cardiac diseases

2.3.1.1 Risk factors

Coronary heart disease involves degenerative changes in the intima, or inner lining, of the larger arteries that supply the myocardium. The problem of establishing the cause of cardiovascular diseases and coronary heart diseases is much more difficult, because genetic, environmental, and behavioral factors are involved in a very complex manner. The difficulty of establishing 'cause' in cardiovascular diseases and coronary heart diseases is best described by the model called the web of causation [96] [130] [118]. Fig. 2.6 shows how a combination of genetic (heredity), environmental (stress) and behavioral (diet, smoking, physical activity) factors interact to cause cardiovascular disease [130] [145]. These risk factors play a major role in prevention programs aimed at reducing disease and premature death associated with degenerative diseases [21] [84].

The process, atherosclerosis, is the leading contributor to heart attack and stroke deaths [7] [45]. Fig. 2.7(a) shows the progressive occlusion of an artery from a buildup of calcified fatty substances in atherosclerosis. The first overt sign of atherosclerotic change occurs when lipid-laden macrophage cells cluster under endothelial lining in the artery to form bulge (fatty streak). Over time, proliferating smooth muscle cells migrate to the inner endothelial layer and accumulate to narrow the lumen of the artery. A thrombus forms and plugs the artery, depriving the myocardium of normal blood flow and oxygen supply. When the thrombus blocks one of the smaller coronary vessels, a portion of the heart muscle dies (necrosis) and person suffers a heart attack or myocardial infarction (MI) [118].

The early classic epidemiological studies related to atherosclerotic disease and physical

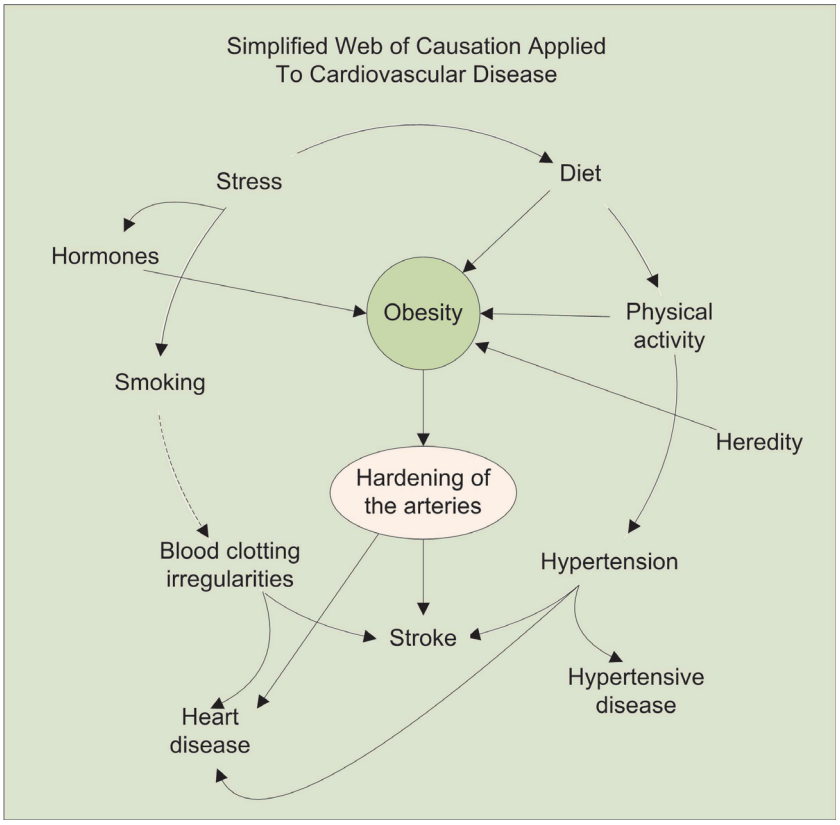

Fig. 2.6: Web of causation: an epidemiologic model showing the complex interaction of risk factors associated with development of chronic degenerative disease such as cardiovascular disease.

activity is based primarily on the epidemiological investigation conducted in Framingham, Massachusetts [45]. When this study began in 1949, cardiovascular disease already accounted for 50 percent of all deaths in the United States. The Framingham study is an observational prospective study designed to determine how those who develop cardiovascular disease differ from those who do not. Approximately 5000 men and women were examined every year, and measures such as blood pressure, electrocardiographic abnormalities, serum cholesterol, smoking, and body weight were obtained. The investigators were then able to relate the different measures to the progression of coronary heart diseases [45].

The Framingham Study found that the risk of coronary heart diseases increases with the

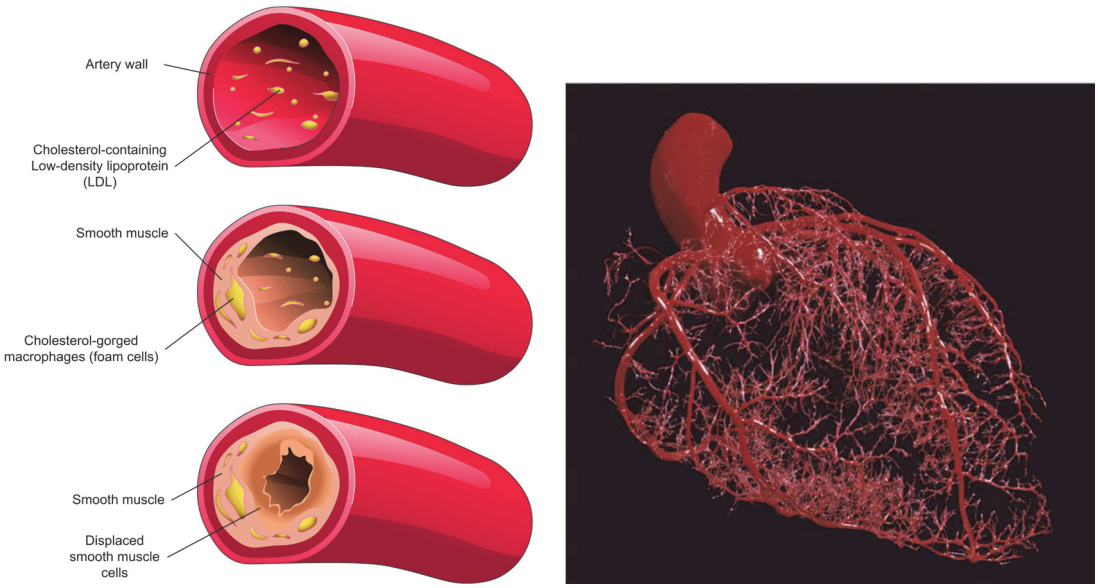

(a) Deterioration of a coronary artery.

(b) Cast of coronary artery vasculature.

Fig. 2.7: Coronary atherosclerosis disease. A coronary artery bypass graft (CABG) creates a new 'transportation route' around the blocked region to allow the required blood flow to deliver oxygen and nutrients to the previously 'starved' surrounding heart muscle. The saphenous vein from the leg is the most commonly used bypass vessel. CABG involves sewing the graft vessels to the coronary arteries beyond the narrowing or blockage, with the other end of the vein attached to the aorta. Medications (statins) lower total and LDL-cholesterol, and daily low-dose aspirin (81 mg) reduces post-CABG artery narrowing beyond the insertion site of the graft. Repeat CABG surgical mortality averages 5 to 10%.

number of cigarettes smoked, the degree to which the blood pressure is elevated, and the quantity of cholesterol in the blood [84]. In addition, the overall risk of coronary heart diseases increases with the number of risk factors; that is, a person who has a systolic blood pressure of 160 mm Hg, a serum cholesterol of 250 mg/dl, and smokes more than a pack of cigarettes a day has about six times the risk of coronary heart disease as a person who has only one of these risk factors (see Fig. 2.6). It is important to remember that risk factors interact with each other to increase the overall risk of coronary heart diseases. This has implications for prevention as well as treatment. In this regard, getting a hypertensive patient to quit smoking confers more immediate benefit than any anti-hypertensive drug [84]. Furthermore, regular physical activity reduces the risk of

coronary heart diseases, even in those who smoke and are hypertensive. The concern about whether a risk factor is related to cardiovascular disease has special significance for physical activity. For many years physical inactivity was believed to be only weakly associated with heart disease and was not given much attention as a public health concern. However, in the late 1980s and early 1990s that changed rather dramatically. In 1987, Powell et al. [57] did a systematic review of the literature dealing with the role of physical activity in the primary prevention of coronary heart diseases. The review found the association to be plausible given the role of physical activity in improving glucose tolerance, increasing fibrinolysis (breaking of clots), and reducing blood pressure. They also investigated the percentages of U.S. population at risk for recognized risk factors related to coronary heart diseases and risk ratio for each risk factor (see Fig. 2.8). The investigators calculated the relative risk of coronary heart diseases due to inactivity to be about 1.9, meaning that sedentary people had about twice the chance of experiencing cardiovascular diseases that physically active people had. The relative risk was similar to smoking (2.5), high serum cholesterol (2.4), and high blood pressure (2.1). See Fig. 2.6 for more on risk factors.

It should be noted that when the authors controlled for smoking, blood pressure, cholesterol, age, and sex (all of which are linked with coronary heart disease), the association of physical activity and coronary heart disease remained, indicating that physical activity was an independent risk factor for coronary heart diseases [11]. Obviously, this conclusion is contradictory to the historical study [33]. It used to classify risk factors for coronary heart diseases into primary and secondary. Primary meant that a factor in and of itself increased the risk of coronary heart diseases, and secondary meant that a certain factor increased the risk of coronary heart diseases only if one of primary factors was already present. Of course, Powell et al. were not the only investigators in this issue [111] [57] [142].

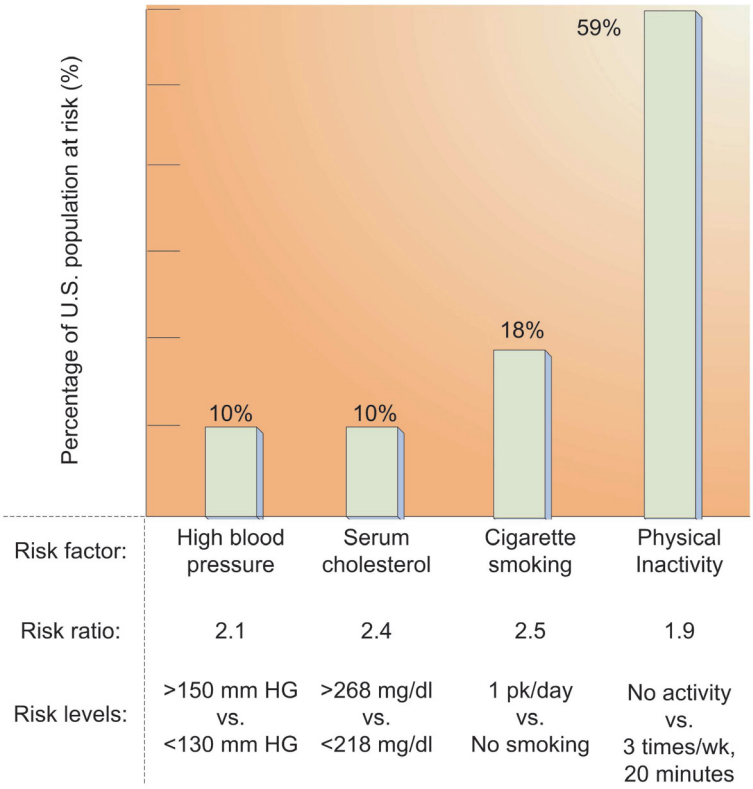

Fig. 2.8: Percentage of U.S. population at risk for recognized risk factors related to coronary heart disease and risk ratio for each risk factor.

2.3.1.2 Cardiac patient

The persons served by exercise rehabilitation programs include those who have experienced angina pectoris, myocardial infarctions (MI), coronary artery bypass graft (CABG) surgery, and angioplasty [55]. Angina pectoris is the chest pain related to ischemia of the ventricle due to occlusion of one or more of the coronary arteries. The symptoms occur when the work of the heart (estimated by the double product: systolic blood pressure $\times$ HR) exceeds a certain value. Nitroglycerin is used to prevent an attack and/or relieve the pain by relaxing the smooth muscle in veins to reduce venous return and the work of the heart [99]. Angina patients may also be treated with a β-blocker like propranolol (Inderal®). Exercise training supports this drug effect: as the person becomes trained, the HR response at any work rate is reduced. This allows

the individual to take on more tasks without experiencing the chest pain.

Myocardial infarction (MI) patients have actual heart damage (loss of ventricular muscle) due to a prolonged occlusion of one or more of the coronary arteries. The degree to which left ventricular function is compromised is dependent on the mass of the ventricle permanently damaged. These patients are usually on medications to reduce the work of the heart (β-blocker), and control the irritability to the heart tissue so that dangerous arrhythmias (irregular heart rhythms) do not occur. Generally, these patients experience a training effect similar to those who do not have a MI [55].

Coronary artery bypass graft (CABG) surgery patients have had surgery to bypass one of more blocked coronary arteries. In this procedure, a blood vessel from the patient is sutured onto the existing coronary arteries above and below the blockage. The success of the surgery is dependent on the amount of heart damage that existed prior to surgery, as well as the success of the revascularization itself. In those who had chronic angina pectoris prior to CABG, most find a relief symptoms, with 50 to 70% having no more pain [167]. These patients benefit from systematic exercise training because most are deconditioned prior to surgery as a result of activity restrictions related to chest pain. In addition, exercise improves the chance that the blood vessel graft will remain open [122] and helps the patient to differentiate angina pain from chest wall pain related to the surgery.

Some coronary heart disease patients undergo percutaneous transluminal coronary angioplasty (PTCA) to open occluded arteries. In this procedure the chest is not opened; instead, a balloon-tipped catheter (a long slender tube) is inserted into the coronary artery, where the balloon is inflated to push the plaque back toward the arterial wall [159]. 'Stents' may be used in the PTCA procedure to help keep the artery open. These do not appear to affect exercise test results in predicting closure of the artery [93].

2.3.1.3 Cardiac rehabilitation

Exercise program is now an accepted part of the therapy used to treat an individual who has some form of coronary heart diseases. The details of how to structure such programs, from the first steps taken after being confined to a bed to the time of returning to work and beyond, are described clearly in books such as Guidelines for Exercise Testing and Prescription by American College of Sports Medicine (ACSM) [17], Wenger and Hellerstein's Rehabilitation of the Coronary Patient [166], ACSM's Exercise Management for Persons with Chronic Diseases and Disabilities [106], and ACSM's Resource Manual for Guidelines for Exercise Testing and Prescription [107].

Cardiac rehabilitation includes a 'Phase I' inpatient exercise program that is used to help the patients make the transition from the cardiovascular event (e.g., a myocardial infarction that put them in the hospital) to the time of discharge from the hospital. The specific signs and symptoms exhibited by the patient are used to determine whether the patient should be placed in an exercise program, and if so, when to terminate the exercise session [17]. Once the patient is discharged from the hospital, a 'Phase II' program can be started. This program includes warm-up, the onset of an exercise session (strengthening exercises), and the offset of an exercise session (cool-down activities: slow walking and stretching exercises). However, the coronary heart disease patients, who are generally very deconditioned (VO_2max of 20 ml $\cdot$ kg$^{-1}\cdot$min^{-1}), require only light exercise to achieve their target heart rate (THR), whose range describes the optimum intensity of exercise consistent with making gains in maximal aerobic power and equals to 70-85% HR max. In addition, because these patients are on a wide variety of medications that may decrease maximal HR, the THR zone is determined from their graded exercise test (GXT) results; the 220-age formula cannot be used. The patients usually begin with intermittent low-intensity exercise (e.g., one minute on and one minute off) using a variety of exercises to distribute the total work output over a larger muscle mass.

In time the patient increases the duration of the work period for each exercise. The onset of exercises emphasize a low resistance and high repetition format to involve the major muscle groups. Given that CABG and post-MI patients have had direct damage to their hearts, the exercise should facilitate, not interfere with, the healing process. At the end of the exercise sessions, the offset of exercises is recommended to gradually return HR toward normal. This part of the exercise session is viewed as important in reducing the chance of a cardiovascular episode after the exercise session [77]. After a patient completes probably 8 to 12 week 'Phase II' program, the person may continue in a 'Phase III' program away from the hospital where a portable noninvasive automated exercise assisted device is urgently required.

2.3.1.4 Cardiac rehabilitation in biomedical applications

There is no question that cardiac patients have improved cardiovascular functions as a result of an exercise program. Recent clinical results show in higher VO_2max values, higher work rates are achieved without ischemia [117] [166]. The exercise program improves lipid profile (lower total cholesterol and higher HDL cholesterol), and the saturated fat content of the diet can modify these variables [115]. However, a proposed exercise program that doctors made as a prescription for their cardiac patients is only available in the medical system, until a reliable, portable, and noninvasive automated exercise assistance application is developed, and that is a part of our studies.

2.3.2 Diabetes

Diabetes is a major health problem in the world. More than 366 million people worldwide, or 8.3% of adults, have the diabetes in 2011. If these trends continue, by 2030, about 552 million people, or one adult in 10, will have diabetes (see Fig. 2.9). Diabetes

kills or injures people indirectly by resulting in blindness, kidney disease, stroke, and heart disease [10]. The major types of diabetes are Type 1 diabetics (lack of insulin) and Type 2 (resistance to insulin). Type 2 diabetics makes up about 85 to 95% of all diabetes in high-income countries and may account for an even higher percentage in low- and middle-income countries [109]. Type 1, insulin-dependent diabetes, is caused by destruction of the β cells that produce insulin in the pancreas. As insulin deficiency influences the rate of glucose uptake in the blood, the disease is controlled through regular insulin injections. The treatment of Type 1 primarily includes diet and insulin to achieve control of the blood glucose concentration (BGL). An exercise program may complicate matters. Richter at al. [127] and Kemmer et al. [87] point out the difficulties a Type 1 has starting an exercise program: the person must maintain a regular exercise schedule, as well as altering diet and insulin. Such behaviors are difficult for some to follow on a day-to-day basis, and the use of exercise in maintaining the metabolic control has been diminished. Because metabolic control can be achieved by insulin and daily diet based on self-monitored blood glucose, exercise makes it complicated. Type 2 is caused by a reduced sensitivity of the target cells for insulin, against influencing glucose regulation. It is mainly linked to obesity. The increased mass of fat tissue results in a resistance to insulin, and thus this disease is often managed via diet and exercise to reduce body weight and to help control plasma glucose. Table 2.1 summarizes the difference between Type 1 and Type 2 diabetics [22] [31].

2.3.2.1 Exercise and the type 2 diabetic

There is some epidemiological evidence that Type 2 diabetes is linked to a lack of physical activity and low fitness [89]. In addition, current research supports the benefits of exercise training in the prevention and treatment of insulin resistance and Type 2 diabetes [81]. However, an inadequate physical activity may result in the occurrence

Fig. 2.9: Percentage (%) of diabetes (20-79 years) by IDF region, 2011 and 2030.

Table 2.1: Summary of the differences between Type 1 and Type 2 diabetes.

Characteristics	Type 1 Insulin-Dependent	Type 2 Noninsulin-Dependent
Another name	Juvenile-onset	Adult-onset
Age at onset	<20	>40
Development of disease	Rapid	Slow
Family history	Uncommon	Common
Insulin required	Always	Common, but not always
Pancreatic insulin	None, or very little	Normal or higher
Katoacidosis	Common	Rare
Body fatness	Normal/lean	Generally obese

of a hypoglycemic response [1]. The exercise increases the rate at which glucose leaves blood. In this way, exercise has been regarded as a useful part of the treatment to regulate blood glucose in the diabetic. The beneficial effect of exercise however, is

dependent on whether or not the diabetic has sufficient insulin prior to and during exercise. The controlled diabetic has sufficient insulin such that glucose can be taken up into muscle during exercise and can catabolise stored glycogens in the normal increase from the liver due to the action of glycogenolysis [118]. In contrast, the diabetic with inadequate insulin experiences only a small increase in glucose utilization by muscle, but has the normal increase in glucose release from the liver. This leads to an elevation of the plasma glucose, resulting in hyperglycemia [1].

The exercise prescription for the Type 2 diabetic aims to improve HRmax or VO_2max. The exercise program for general Type 2 diabetic patients includes 20 - 60 minutes of a continuous aerobic exercise, at 70% - 85% HRmax, 3 to 5 times per week [108] [29] [19]. Strength training with light weights is also recommended [29] [144].

As for deconditioned individuals with exercise programs, the combination of frequency, intensity, and duration of each exercise session must be carefully managed, so as to directly benefit those with borderline hypertension, high cholesterol, obesity, conditions often related to Type 2 diabetes. Because for those, it is even more difficult to carry along an exercise program with clear identification and controlled BGC. Thus, it would be much safer if the exercise session for a diabetic can be supervised by someone or some smart devices which could provide suggestions and assistance if a problem is occurred.

The American Diabetes Association states that exercise is only one part of the treatment in terms of therapy for the diabetic; diet is the other [2]. The type 2 diabetic secures numbers of benefits from proper exercise and dietary practices: lower body fat and weight, increased HDL cholesterol, increased sensitivity to insulin, improved capacity for work [90] [163]. These changes should not only improve the prognosis of the Type 2 diabetic as far as control of blood glucose is concerned, but should also reduce the overall risk of coronary heart diseases [127].

2.3.2.2 Diabetics in biomedical applications

As mentioned earlier, the patients have a variety of risk factors in addition to their diabetes such as hypertension, high cholesterol, and hyperglycemia. In order to reduce the chance of a 'surprise' hypoglycemic or hypertensive responses to exercise, it is important for clear communication to exist between the participant and the exercise leader, the latter supervising and managing the overall exercise session that the participant carries (in most cases, nowadays it is represented by nurses or doctors in the hospital). However, there are limitations in that it is not reasonable for every diabetic individual to have their daily exercise activity in hospitals. Our studies concern about this problem from the view of control and biomedical engineering. Instead of the duty of 'exercise leader', a reliable, portable, and noninvasive automated exercise assistance application is proposed to help every diabetics control BGC, as well as enjoy the joy of exercise.

2.3.3 Hypertension

Today, approximately 1 billion people worldwide have high blood pressure (BP) above the recommended level of <120 systolic and <80 diastolic (Table 2.2), and this number is expected to increase to 1.56 billion people by the year 2025 [91]. Raised BP is a high-risk condition that causes about 51% of deaths from stroke and 45% from coronary heart diseases [110]. For this reason, non-pharmacological approaches, including diet and physical activity, are first line interventions for high BP management, even when medication therapy is implemented [59] [83].

2.3.3.1 Exercise and hypertension

Generally, the person with prehypertension (systolic BP 120 - 139 mmHg and/or diastolic BP 80 - 89 mmHg) should use exercise to control BP and establish behaviours

Table 2.2: Definition and classification of BP levels (mmHg) [59].

Category	Systolic	Diastolic
Normal	<120	<80
High normal*	120-139	80-89
Grade 1 (mild)	140-159	90-99
Grade 2 (moderate)	160-179	100-109
Grade 3 (severe)	⩾180	⩾110
Isolated systolic hypertension	⩾140	≤90
* High-normal has been labeled as prehypertension[83].		

that favorably influence other aspects of health. Baster and Baster-Brooks [20] indicate that the relationship between sedentary behaviour and hypertension is so strong that the National Heart Foundation [59], the World Health Organisation and International Society of Hypertension [110], the Unite States Joint National Committee on Detection, Evaluation and Treatment of High Blood Pressure [83], and the American College of Sports Medicine (ACSM) [106] have all recommended increased physical activity as a first line intervention for preventing and treating patients with prehypertension. Such organisations also suggest exercise as a non-pharmacological intervention program for patients with grade 1 (140 - 159/80 - 90 mmHg), or grade 2 (160 - 179/100 - 109 mmHg) hypertension (Table 2.2). Physical activity is significant for most of hypertensive individuals because it is a low cost intervention with a reducing effect on BP, and a non-pharmacological prescription for cardiac diseases (such as coronary heart diseases and cardiovascular diseases, see section 2.3.1).

Current physiological studies have identified the following physiological benefits of exercise for hypertensive-related diseases. Physical activity improves endothelial function. The endothelium lining of blood vessel walls maintains normal vasomotor tone, enhances fluidity of blood, and regulates vascular growth [139]. There are also vascular structural changes such as increased length, cross sectional area, and diameter of existing arteries

and veins in addition to new vessel growth [106]. According to ACSM [106], physical activity may also reduce the elevated sympathetic nerve activity that is common in postexercise hypertension (PEH). The exact mechanism for PEH remains unclear, but appears to involve the arteries and cardiopulmonary baroreflexes. Studies suggest that the operating point of the arterial baroreflex is set to a lower BP after an acute bout of exercise [75].

2.3.3.2 Exercise prescription for hypertensive patients

ACSM suggests endurance exercise at low intensities (40% to 70% VO_2max) is effective in reducing BP . Lower-intensity exercise should be done frequently and for durations long enough to result in the expenditure of a large number of calories. Gordon et al. [70] proposes a goal of 14 to 20 kcal/kg per week (about 980 to 1440 kcal for a 70 kg person). Based on the literature review, Baster and Baster-Brooks [20] summarize a more detailed exercise prescription, including patient category, exercise testing and monitoring, exercise type, frequency, intensity, and duration (Table 2.3). To prescribe the appropriate column in Table 2.3 to each hypertensive individual, patient's age, BP and overall cardiovascular disease risk need to be considered. They also agree that a variety of rhythmical and aerobic exercise, under indoor or outdoor environments, is the preferred treatment strategy (walking, running, cycling, swimming) for all hypertensive patients. More specifically, however, patients over 50 years of age will require additional evaluation followed by a designed and monitored exercise program. This is because at least half will be overweight, and/or will have high cholesterol; 40 - 50% will have heart, stroke and/or vascular conditions [20]. In addition, β-blockers that most patients with suspected cardiovascular diseases take diminish the HR response to exercise, therefore medical supervision in dedicated rehabilitation centres is necessary.

Table 2.3: Exercise prescription to hypertensive patients based on health status and age [106].

Category	Column A	Column B	Column C
	• Prehypertensives with no suspected CVD <50 years • Grade 1 hypertensives <50 years	• Prehypertensives with suspected CVD • Prehypertensives >50 years • Grade 2 hypertensives with no suspected CVD <50 years	• Hypertensives with no suspected CVD >50 years • Hypertensives with suspected CVD
Exercise monitoring	Not necessary	Recommended	Recommended
Exercise type	Aerobic activities (monitoring not necessary, but suggest they seek advice from a clinical exercise physiologist for a conditioning and aerobic based training program)	Walking, cycling, swimming until medically evaluated (periodic monitoring may be necessary)	Walking, cycling, swimming until medically evaluated (periodic monitoring may be necessary)
Frequency	6-7 days/week	5-7 days/week	5-7 days/week
Intensity	Start with 20-30 minutes continuous aerobic activity at comfortable pace (50-65%) of maximum HR for 3-4 weeks for general conditioning, then exercise at up to 85% of HR_{max}	Work at light-moderate intensity until evaluated and conditioned, then undertake a maintenance aerobic program at up to 85% HR_{max}	Light-moderate lower intensity can start with 20-30 mins/day of continuous activity, then build to 45-60 mins/day
Duration	Minimum 150 mins/week of aerobic activity	Start with 20-30 mins/day of continuous activity, then build to 30-60 mins/day	Start with 20-30 mins/day of continuous activity, then build to 30-60 mins/day

2.3.3.3 Hypertension in Biomedical Applications

A reliable, portable, and noninvasive way for the monitoring and regulation of the human CR response to exercise is also tightly related to the treatment of hypertension.

As mentioned earlier, some hypertensive individuals should be placed under medical supervision in dedicated rehabilitation centres, where an aerobic based training program predefined for each patient will be monitored by a certified clinical exercise physiologist. However, dedicated rehabilitation centres are generally only available in major cities. They are usually used for post cardiac event patients and not readily accessible to other patient populations. An alternative is to develop a reliable portable noninvasive automated exercise assistance application, not only monitoring the overall exercise session, but also regulating their metabolic dynamics.

2.4 Conclusion

This chapter introduces the exercise-related biomedicine background for known medical knowledge in literatures about patient behaviors for some popular CR diseases, and how exercise plays a primary role to prescribe these diseases by applying biomedical techniques and devices.

One of most important issues found in biomedical engineering area is to develop an exercise assistance application for improving CR fitness. HR and VO_2 are commonly considered as the major indicators of CR responses to exercise. The concept and definition of those variables are presented in this chapter. More importantly, a predefined exercise protocol including warm-up, the onset of exercise, and the offset of exercise is a necessary standard for estimation and regulation of CR systems in response of specific-exercise.

In this chapter, the relationship between CR system and exercise based on our literature investigations also is outlined from the exercise physiological view. In particular, the metabolic energy process under exercise conditions are clearly explained. It would be beneficial for understanding of the mathematic model we discussed in Chapter 3.

The medical background for exercise and its relevant diseases in clinical medicines is introduced in this chapter. It has been reported that exercise and relevant biomedical devices play a primary role to prescribe CR diseases, such as cardiac diseases, diabetes, and hypertension. The details of diseases and exercise prescriptions are presented that would enable us to have a deep understanding of our study, if necessary.

Chapter 3

A single-input single-output switching model for human cardiorespiratory responses to the onset and offset of exercise

3.1 Introduction

One of the greatest public health challenges confronting many industrialized countries is the obesity epidemic. Low-to-moderate intensity exercise, suitable for every fitness level, remains one of the healthiest and risk averse methods for reducing body fat [147] [66] [63]. As HR and oxygen uptake (VO_2) are the key indicators of exercise intensity [62] [12] [153] [35] [113] [9] [18], this study explores the modeling of both HR and VO_2 responses in order to facilitate the assessment of human CR responses at the onset and offset of exercise (also called exercise and recovery). For this purpose, twenty subjects performed standardized square-wave exercise bouts on a treadmill following predefined protocols. During exercise and recovery, HR and VO_2 were monitored and recorded by a portable gas analyzer (Cosmed®) . The experimental results are consistent with the observations reported in existing literature [134] [151] [169] [101] [51]; in that the dynamics of the HR/VO_2 response vary at onset and offset of exercise.

There are both linear and nonlinear [134] [74] [28] [39] [102] [14] [71] [15] [27] modeling approaches for the estimation of HR and/or VO_2 responses to exercise. However, to the

best of our knowledge, almost all the existing modeling approaches (apart from a preliminary version of this study [169]) utilize only a single non-switching model for either the onset or offset of exercise. Although it can accurately describe the dynamical characteristics at the onset and/or offset of exercise, the transient behavior during switching has previously been overlooked. A natural solution for the limitations of previous methods without a description of a switching transient is to utilize a model inclusive of a switching mechanism. In order to be consistent with experimental observations, the switching model should guarantee the continuity of model output during model switching. In addition, it is also desired that the switching model can provide physiological explanations for the variations of the dynamic characteristics at the onset and offset of exercise. In this paper, we propose an innovative switching Resistance-Capacitor (RC) model , which uses electronic terms to quantitatively describe human CR responses at the onset, offset, and transition between exercise. Based on the RC model, a possible physiological explanation for the process of body energy storage and dissipation at the onset and offset of exercise is also provided.

The physiological mechanisms for the variation in the dynamics of the HR/VO_2 response at the onset and offset of exercise may be associated with the concept of 'oxygen debt', as first proposed by Archibald Vivian Hill and others [53]. According to A. V. Hill [53], the body's carbohydrate stores are linked to energy 'credits'. If these stored credits are expended during onset of exercise, then a 'debt' is occurred. The greater energy 'deficit', or use of available stored energy credits, the larger energy 'debt' occurs [101]. The ongoing oxygen uptake after onset of exercise is thought to represent the metabolic cost of repaying this debt. Their studies [53] used financial-accounting terms to qualitatively describe the process of energy storage and dissipation at the onset and offset of exercise. However, a quantitative description for this process, e.g., the amount of energy 'credits' and 'debt', has to date not been addressed. The proposed switching RC model can be

regarded as an extension of these studies [53]. Indeed, it is proposed this model can not only numerically verify these reported physiological phenomena, but also provide a quantitative description for energy 'credits', 'debt', and the whole energy process during the onset and offset of exercise.

The remaining of the paper is organized as follows. Section 3.2 presents experimental details including experimental equipments and protocols. Section 3.3 introduces the proposed switching RC model as well as model analysis and verification, and Section 3.4 concludes the paper.

3.2 Experiment

In order to investigate HR and VO_2 responses to the onset and offset of exercise, twenty healthy untrained males participated in this study. The University of Technology, Sydney (UTS) approved this study and an informed consent was obtained from all participants before commencement of data collection.

The participants were divided into two groups. As shown in Table 3.1, subjects in the group A have a mean age of 30.63 years (range, 26 - 42 years), a mean weight of 74.63 kg (range, 55 - 90 kg), and a mean height of 173.38 cm (range, 164 -180 cm). Different with the group A, the larger mean values of age, 45.4 years (range, 36 - 53 years), and weight, 91.9 kg (range, 71.2 - 102.3 kg), are in the group B. Due to this difference, the exercise protocols of groups A and B are defined separately, in order to reach as close as to 80% of HR $_{max}$ and VO_{2max} in exercise [16]. The protocol has three stages: warm up, onset of exercise, and offset of exercise. Fig. 3.1 shows the protocols served for the two groups; group A involving 4-minute walking at 5 km/h followed by 6-minute running at 9 km/h and 5-minute recovery period at 5 km/h and group B involving 4 minutes warm up at 3 km/h with 8 minutes onset period at 8 km/h and 8 minutes offset period at 3

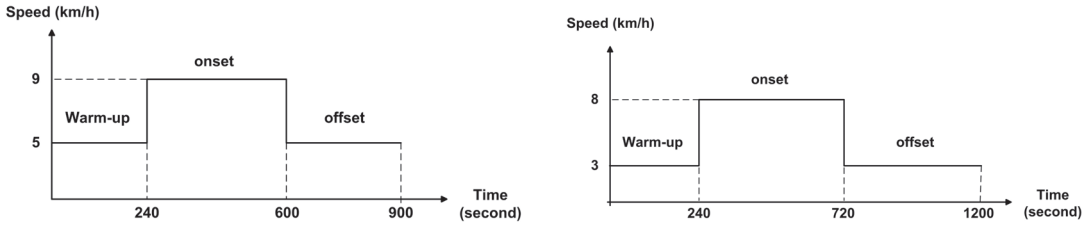

Fig. 3.1: The exercise protocols for group A (left) and group B (right).

km/h.

As prior nutritional intake, physical activity and environment conditions were standardized for all participants. The participants consumed a standardized light meal at least 2 hours before the experiment and not to engage in any exercises for 24 hours prior to each experiment [44][25]. The temperature and humidity of the laboratory were set at 20 - 25 °C and 50% relative humidity, respectively. To avoid random errors and improve the accuracy of the recorded data, the protocol was repeated twice by subjects and the obtained data are interpolated, averaged and filtered.

Table 3.1: Subject physical characteristics.

Group A				**Group B**			
ID	**Age**	**Height**	**Mass**	**ID**	**Age**	**Height**	**Mass**
ANDW	27	175	55	ANEL	40	173	102.3
AHMD	32	170	87	BIKE	45	179	97.1
ISSA	29	176	90	BRRU	45	173	100.8
YASA	29	187	100	CHRI	37	170	71.2
ARDI	42	175	80	DACR	53	183	99.2
RAMI	29	164	64	GAHI	45	182	98.4
SATM	31	169	67	MABR	36	186	92.1
OMAR	26	180	77	MACU	53	175	88.8
				MAYE	45	180	94.0
				RABL	43	178	99.6
				ROMU	50	182	86.1
				WADO	53	173	72.9
MEAN	30.63	173.38	74.63	**MEAN**	45.4	178	91.9
STD	4.66	4.95	11.10	**STD**	5.9	5	10.5

All physiological measurements in this study were collected by a COSMED portable gas

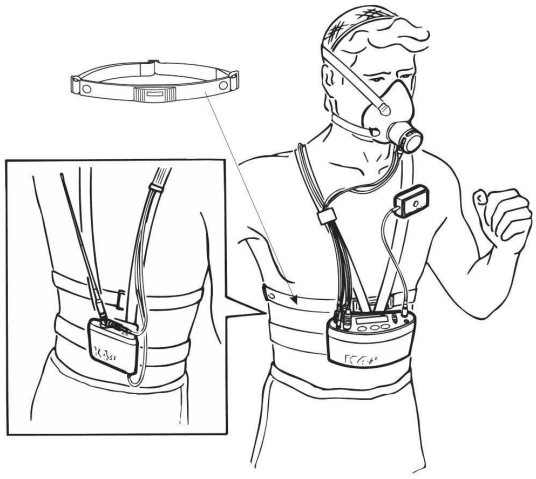

Fig. 3.2: The wearable K4b^2 Gas analyzer equipment for indoor and outdoor exercises.

analyzer (Cosmed®), see Fig. 3.2. The COSMED system includes a compatible HR monitor which consists of one transmitter in the elastic belt and one receiver. The two parts are assembled as close as possible for capturing the most effective communication signals. K4b^2 gas analyzer and its compatible products are chosen because it has been reported to be valid, accurate and reliable [5][116][49]. The data of HR and VO_2 of all subjects in groups A and B are shown in Fig. 3.3.

It has been widely accepted that the step response of HR/VO_2 can be approximated as a first-order process [134][155], $\frac{K}{Ts+1}$, where K is the steady state gain and T is the time constant. Based on the data sets in Fig. 3.3, Matlab System Identification Toolbox was used to establish the first-order process for both HR and VO_2 responses in two groups. The coefficients (K and T) for each set of data are identified, and the calculated mean and standard deviation (STD) are shown in Table 3.2. The results indicate that the steady state gain (K) at offset of exercise is obviously smaller than that at onset of exercise for both HR and VO_2. Moreover, the mean values of time constant (T) at offset of exercise is notably larger than that at onset for both HR and VO_2.

There are similar results reported by previous literature [151] [169] [101], which has identified the differences of the onset and offset dynamics. However, most of the studies

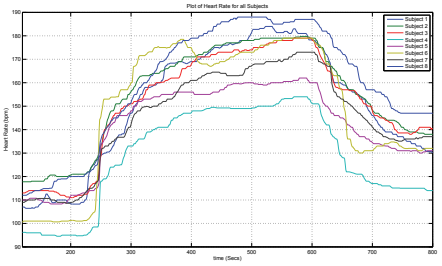

(a) The HR signals for group A

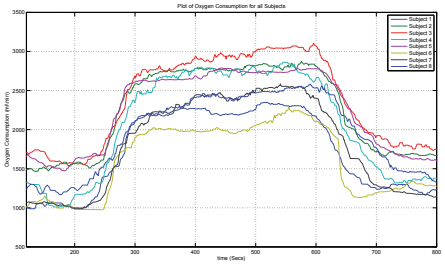

(b) The VO_2 signals for group A

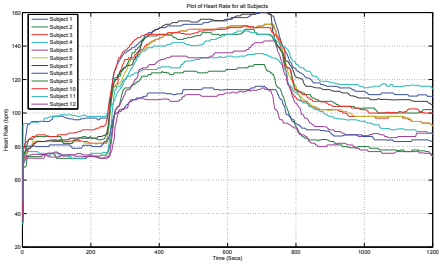

(c) The HR signals for group B

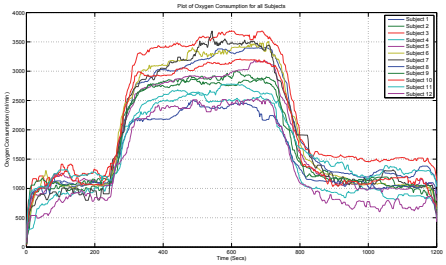

(d) The VO_2 signals for group B

Fig. 3.3: The measured experimental data for HR and VO_2 responses for both groups of A and B.

separate the onset and offset as two stages, and build a single model for each stage respectively. Some studies just construct an average model for both onset and offset of the exercise response. In contrast with existing studies, in the next section, however, we will introduce a switching RC circuit model. This single switching model can quantitatively depict the two different dynamical responses by properly setting the values of the circuit components (resistors and capacitors).

Table 3.2: The mean and STD results of T and K of the experiment results for the HR and VO_2 responses at onset and offset of exercise.

		Group A		Group B	
		Mean	STD	Mean	STD
HR Response at Onset of Exercise	T	64.8763	20.1383	56.3168	14.9114
	K	15.3587	2.1107	11.3341	2.4178
HR Response at Offset of Exercise	T	94.8688	28.3923	83.1042	10.6905
	K	11.28	2.0237	9.0163	1.7090
VO_2 Response at Onset of Exercise	T	47.5963	12.7307	62.3447	8.8390
	K	326.3613	45.3776	386.4850	74.8645
VO_2 Response at Offset of Exercise	T	63.6250	18.1615	68.1723	8.6944
	K	311.0388	49.2890	369.5700	66.5761

3.3 Mathematic model for body's cardiorespiratory responses to exercise

3.3.1 Metabolic energy process

The following description about metabolic energy process (mainly from [86] [128] [56]) is a necessary background for the analysis of human CR responses during the onset and offset exercises.

There are three metabolic energy pathways existing in the human body: the phosphagen system, glycolytic system and the aerobic system [86]. The phosphagen system (also called the adenosine triphosphate (ATP)-creatine phosphate (CP) system) provides the fastest pathway to resynthesize ATP. CP, stored in skeletal muscles, is catabolised to allow the phosphate to combine with ADP to produce ATP. No carbohydrate or fat is used in this process and the regeneration of ATP is resultant solely from CP. As this process does not require the presence of oxygen to resynthesize ATP, it is anaerobic in nature. The phosphagen system is the predominant energy system used for all-out exercise lasting up to about 10 seconds.

Glycolysis is the second-fastest way to resynthesize ATP and is the dominant system for exercise lasting from 30 seconds to about 2 minutes. During glycolysis, carbohydrate, in the form of either blood glucose (sugar) or glycogen (the stored form of glucose in muscles and the liver), is degraded through a series of chemical reactions to form pyruvate (glycogen is first converted into glucose through a process called glycogenolysis). For every glucose molecule converted to pyruvate through glycolysis, two molecules of usable ATP are produced [56] [86]. Thus, only small volumes of energy are produced via this pathway. Once pyruvate is formed, it has two fates: conversion to lactate or conversion to a metabolic intermediary molecule called acetyl coenzyme A (acetyl-CoA), which enters the mitochondria for oxidation and the production of more ATP [128] [86]. Conversion to lactate occurs when the demand for oxygen is greater than the supply (i.e., during anaerobic exercise). Conversely, when there is enough oxygen available to meet the muscles' needs (i.e., during aerobic exercise), pyruvate (via acetyl-CoA) enters the mitochondria and goes through the aerobic system.

The aerobic system, which is dependent on the sufficient presence of oxygen in the mitochondria, is the slowest pathway to resynthesize ATP. The aerobic system, including the Krebs cycle and the Electron Transport Chain, uses blood glucose, glycogen and fat as fuels to resynthesize ATP in the mitochondria of muscle cells. Carbohydrate, glucose and glycogen are first metabolized through glycolysis, with the resulting pyruvate (via acetyl-CoA), entering the Krebs cycle. The electrons removed from the fuel sources in the Krebs cycle are then transported through the Electron Transport Chain, where ATP and water are produced. Complete oxidation of glucose via glycolysis, the Krebs cycle and the electron transport chain produces 36 molecules of ATP for every molecule of glucose broken down. Thus, the aerobic system produces 18 times more ATP than does anaerobic glycolysis (via lactate) from each glucose molecule. Of course, fat is also a major fuel for the aerobic activities [128] [56].

3.3.2 The proposed switching RC model

The proposed switching model (an electronic circuit) is shown in Fig. 3.4. By analyzing the model, this section gives a possible physiological explanation of the process of energy storage and dissipation at the onset and offset of exercise. Although, in the following, the proposed circuit is applied to explain the observed exercise characteristics of HR only, it can also account for that of VO_2 in a similar way.

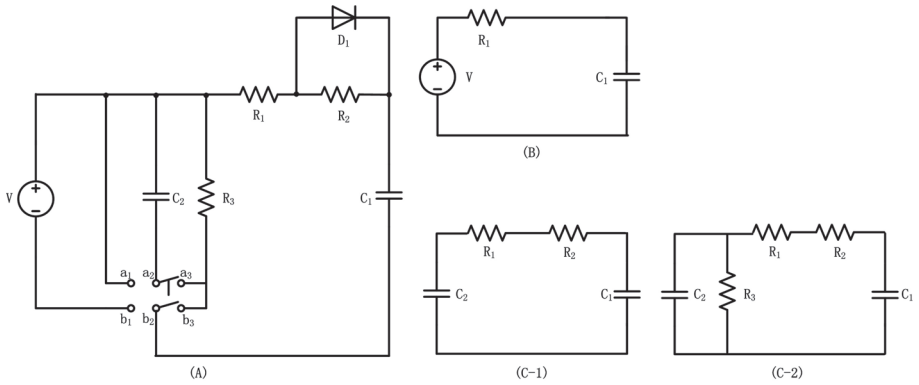

Fig. 3.4: (A). The mathematic model for the HR response at onset and offset of exercise; (B). the onset circuit; (C-1). the offset circuit C-1; (C-2). the offset circuit C-2 (C_1: HR indication, C_2: non-exercise energy compensation index, R_1: exercise resistance for onset of exercise, R_2: exercise resistance related to offset of exercise, and R_3: exercise resistance related to long-term recovery exercise).

In Fig. 3.4(A), the voltage of DC power supply, V, stands for the power required for the body to maintain the exercise intensity. The integral of V with respect to time is therefore regarded as the total energy required for the onset of exercise. According to the discussions in section 3.3.1, the energy required for exercise is generated through the metabolic energy pathways [86]. In Fig. 3.4, the capacitor C_1 is utilized to depict cardiac response. Specifically, its voltage, $V_{c_1}(t)$, represents the HR response to exercise. The capacitor C_2 is related to the process of glycogen regeneration. Particularly, the integral of its voltage ($\int V_{c_2}(t)dt$) stands for the amount of energy for the regeneration of glycogen (e.g., when the supply for glucose is greater than the demand, glucose is resynthesized to glycogen through a process called gluconeogenesis), and it only occurs

in the periods of offset (or long-term recovery) of exercise. The resistors R_1, R_2 and R_3 are associated with the energy dissipation of human body during exercises. We have termed them exercise resistances and intuitively, their reciprocals characterize the ability of overcoming exercise resistance of human body. In particular, R_1 is mainly related to the response for the onset of exercise, R_2 for the offset of exercise and R_3 for long-term recovery exercise.

As shown in Fig. 3.4(A), two circuits are separated by a double-pole double-throw (DPDT) switch. At first, the DPDT connects to a_1 and b_1 poles, and the onset circuit is triggered as shown in Fig. 3.4(B). The function of the dioxide D_1 is to short the R_2 out. When the connector is switched from poles of a_1 and b_1 to the other pair of poles a_3 and b_3, the offset circuit will be run afterwards as shown in Fig. 3.4(C-1)/Fig. 3.4(C-2). In the following analysis, we will derive the dynamics of the onset (Fig. 3.4(B)) and offset circuits (Fig. 3.4(C-1)/(C-2)) to show how the two different dynamic characteristics are implemented in the single switching RC model.

In the onset period (between t_0 and t_1 in Fig. 3.5(A)), the DC power supply V charges the capacitor C_1, up to V_1 at time t_1 that approximately equals the DC power supply V. The voltage of capacitor C_1 (which represents the HR response to onset of exercise) can be calculated by using the following equation:

$$V_{c_1}(t) = V(1 - e^{-\frac{t}{R_1 C_1}}) \quad (t_0 \leq t \leq t_1) \tag{3.1}$$

It can be seen that the steady state value of $\mathrm{V}_{c_1}(t)$ is V.

Remark 1 The onset circuit can well support the hypothesis made by A. V. Hill and others [53]. In the onset period, $V_{c_1}(t)$ exponentially grows that implies an increase of HR. Since Q can be expressed as Q = SV $\times$ HR, if we assume SV remains constant during moderate exercise, HR should be proportional to Q that represents the power

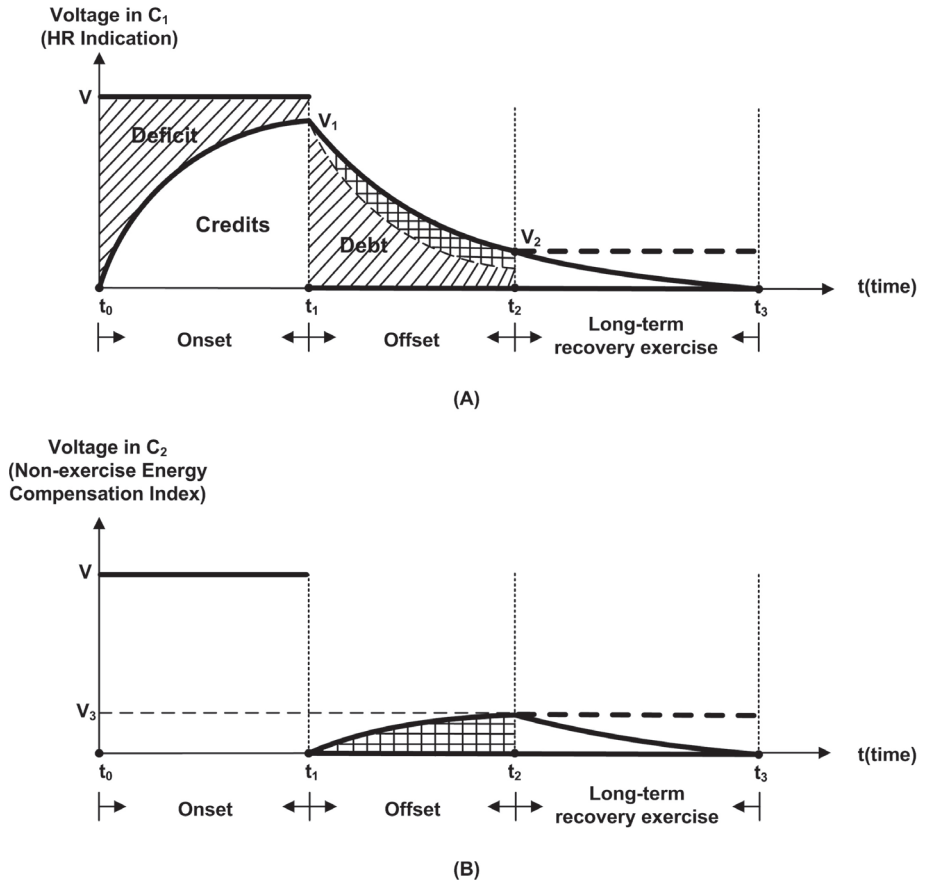

Fig. 3.5: (A). Voltage variations in C_1; (B). voltage variations in C_2.

generated by the heart. In this regard, the amount of energy generated by the heart in the onset period would also be proportional to the integral of Eq. (3.1), which is just the white area in the onset period. However, the actual energy required is not totally proportional to this white area. According to the hypothesis made by A. V. Hill and others [53], the white area is thought as energy 'credits', and the line shadowed area is energy 'deficit' representing those ATP that cannot be pumped out by heart beat as quickly as possible to satisfy tissue's urgent needs. Within the circuit, the step response of HR is approximated as a first order process [155] and its time constant (T) is impossible to be 0. Therefore, HR cannot instantaneously reach to the steady state level (V) at the beginning of exercise. Then, energy 'deficit' occurs.

In the offset period (between t_1 and t_2 in Fig. 3.5), the offset circuit is taking place. Both circuits C-1 and C-2 in Fig. 3.4 are applicable for the analysis of this period. If assume R_3 is sufficiently big, the current passing through R_3 is negligible. Thus, the two circuits (C-1 and C-2) are approximately equivalent when R_3 is sufficiently big.

During the offset period, the capacitor C_1 is discharging and its voltage follows an exponential decay down to V_2 at time t_2. Conversely, the capacitor C_2 is charging, which results to an exponential growth of its voltage from 0 at time t_1 to V_3 at time t_2. It is assumed that $V_2 \approx V_3 \approx \frac{C_1 V_1}{C_1+C_2}$ at time t_2. The voltage variations of C_1 (HR indication) and C_2 (Non-exercise Energy Consumption Index) in this period can be respectively described as:

$$V_{c_1}(t) = \frac{C_1}{C_1+C_2}V_1 + \frac{C_2 V_1}{C_1+C_2}e^{-\frac{(C_1+C_2)t}{C_1C_2(R_1+R_2)}} \quad (t_1 \le t \le t_2), \tag{3.2}$$

$$V_{c_2}(t) = \frac{C_1}{C_1+C_2}V_1 - \frac{C_1 V_1}{C_1+C_2}e^{-\frac{(C_1+C_2)t}{C_1C_2(R_1+R_2)}} \quad (t_1 \le t \le t_2). \tag{3.3}$$

Remark 2 The precise biochemical explanation for the offset of exercise is not possible, because the specific chemical dynamics are still unclear [101]. The offset circuit, however, provides a possible physiological explanation from the view of the body's energy storage and dissipation process. The experimental observation (see section 3.2) shows that the time constant at offset of exercise is larger than that at onset of exercise, meaning that the line shadowed area plus cross line shadowed area in this period is greater than the area of energy 'deficit' in the onset period. If the two line shadowed areas (the areas of energy 'deficit' and 'debt' in Fig. 3.5) would equal each other (i.e., the energy 'debt' equals to the energy 'deficit'), a question is raised: what does the extra area (the cross line shadowed area in Fig. 3.5(A)) represent? According to mass-energy equivalence relation ($E = MC^2$), any change in the energy of an object causes a change in the mass of that object [86]. Thus, the extra cross line shadowed area implies there must exist an energy storage process, which converts the energy into 'molecules', and causes a change in the body's mass. It is well believed that any physiological process which contributes to the recovery of the body to its pre-exercise condition may result in the appearance of the extra area, e.g., glycogenesis (a process of glycogen synthesis). For this reason, the capacitor C_2 is going to store this kind of energy, like the liver stores glycogens. Thus, the cross line shadowed area in Fig. 3.5(B) is presumably proportional to the one with the same mark in Fig. 3.5(A). However, there still has been a controversial issue in A. V. Hill's hypothesis. In his hypothesis, the line shadowed areas plus the cross line shadowed area between t_1 and t_2 in Fig. 3.5(A) are thought to represent the metabolic cost of repaying energy 'debt' [53]. However, in this study, energy 'debt' is only a part of that. Instead, glycogenesis and all others for the recovery of the body to its pre-exercise condition also take place in the offset period.

Based on Eq. (3.1) - Eq. (3.3), time constants and steady state gains for the onset and offset of exercise are derived as follows:

$$\begin{cases} \tilde{K}_{on} = \frac{K_{on}}{K_{on}} = 1, \\ T_{on} = R_1 C_1, \\ \tilde{K}_{off} = \frac{K_{off}}{K_{on}} = \frac{C_2}{C_1 + C_2}, \\ T_{off} = (R_1 + R_2)\frac{C_1 C_2}{C_1 + C_2}, \end{cases} \tag{3.4}$$

where K_{on} (K_{off}) and T_{on} (T_{off}) represent the steady state gains and the time constants of onset (offset) exercise respectively. New defined parameters $\tilde{K}_{on}$ and $\tilde{K}_{off}$ are normalized steady state gains. If K_{on}, K_{off}, T_{on}, and T_{off} are given and assume R_2 is a predefined free parameter, the values of capacitors and resistor (C_1, C_2, and R_1) can be calculated by the following equations:

$$\begin{cases} C_1 = \frac{T_{off} - T_{on}\tilde{K}_{off}}{R_2 \tilde{K}_{off}}, \\ C_2 = \frac{T_{off} - Ton\tilde{K}_{off}}{R_2(1 - \tilde{K}_{off})}, \\ R_1 = \frac{T_{on} R_2 \tilde{K}_{off}}{T_{off} - T_{on}\tilde{K}_{off}}. \end{cases} \tag{3.5}$$

Remark 3 There are two divergent behaviors after the offset period. See Fig. 3.4, the dash and solid lines in the period between t_2 and t_3 show the two possible consequent behaviors, which are depicted by the offset circuit C-1 (see Fig. 3.4(C-1)) and the offset circuit C-2 (see Fig. 3.4(C-2)) respectively. The offset circuit C-1 enables the shift of equilibrium point, as the equilibrium is 0 at time t_0 and then becomes $V_2 \approx V_3 \approx \frac{C_1 V_1}{C_1 + C_2}$ at time t_3. Alternatively, in circuit C-2, there is no shift of equilibrium, i.e., the equilibrium remains at 0 around time t_3. The circuit C-1 is applicable to the repetitive switching of training behaviors (e.g., interval training), and the circuit C-2 is fitting for the single switching behaviors (e.g., single combination of onset and offset training).

3.3.3 Model verification

This section verifies the proposed model for both HR and VO_2 by using the experimental data of groups A and B respectively. In section 3.2, we have already calculated the time constants and steady state gains of HR and VO_2 for both two groups (see Table 3.2). Based on these results, we can identify all parameters (the values of resistors and capacitors) of four switching RC models according to Eq. (3.5). The identified parameters of the four models are summarized in Table 3.3. These four models are implemented by using Matlab/Simulink (see Fig. 3.6). The simulated model outputs are compared with their corresponding experimental data as shown in Fig. 3.7. In Fig. 3.7, the dash curves represent the model outputs, and the solid lines stands for the experimental results. This figure clearly indicates that the model outputs fit well with the experimental data at the onset/offset of exercise and the transition in between for both two groups.

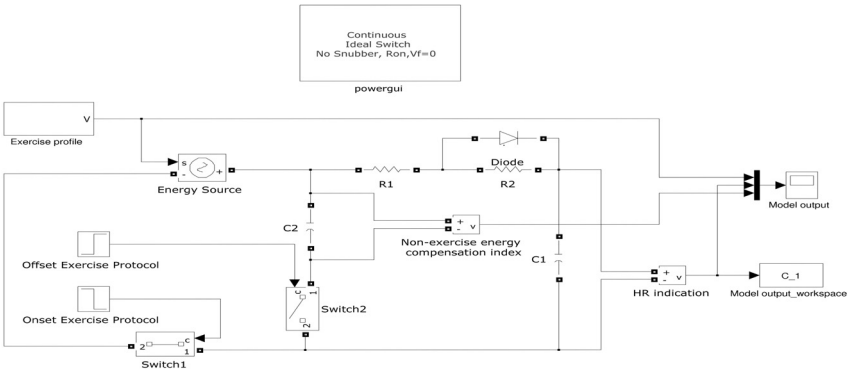

Fig. 3.6: The simulated schematic diagram.

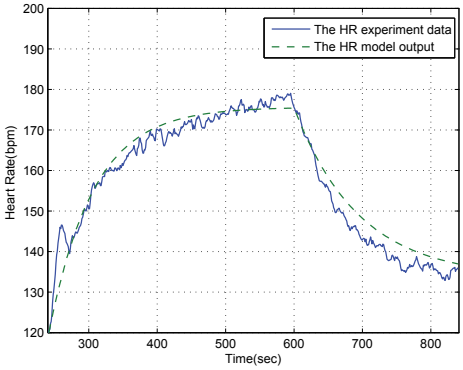

(a) HR for group A

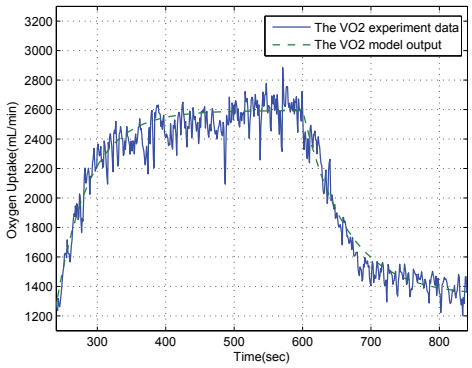

(b) VO_2 for group A

(c) HR for group B

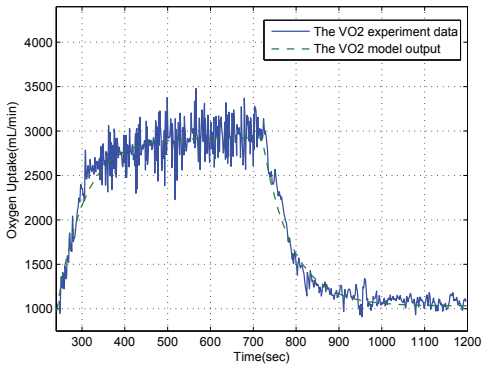

(d) VO_2 for group B

Fig. 3.7: The model outputs vs. the experiment results for both HR and VO_2 responses at onset and offset of exercise for subjects in group A and B.

Table 3.3: Tuning parameters for switching RC model for both HR and VO_2 responses at onset and offset of exercise for subjects in group A and B.

Model Parameters	Physiological Significance	Group A		Group B	
		HR	VO_2	HR	VO_2
R_1 (Ω)	Capacity of exercise resistance at the onset of exercise	100.9028	248.3758	116.9592	696.7596
R_2 (Ω)	Capacity of exercise resistance at the offset of exercise	100	100	100	100
C_1 (F)	Heart rate response at both onset and offset of exercise	0.6430	0.1916	0.4815	0.0895
C_2 (F)	The process of glycogen regeneration	1.7782	3.8900	1.8731	1.9550
V (V)	The total energy required for the onset of exercise	55.1	1319	59.58	1945.6

3.4 Conclusion

Two slightly different exercise protocols were used for two different groups of subjects to investigate the dynamic characteristics of the HR and VO_2 responses to onset and offset of treadmill exercise. The portable gas analyzer K4b^2 was used to measure breath-by-breath VO_2 and beat-by-beat HR values. It was concluded that the dynamic characteristics of human CR responses at the onset and offset of exercise are distinctively different. Based on the experimental observations, we developed a switching RC model that can explicitly depict the dynamical characteristics of human CR responses at the onset/offset of exercise and the transition in between. In addition, the developed model provides the quantitative analyses for the terms of energy 'credit', 'deficit', and 'debt'. The validity of the proposed switching model is confirmed by comparing the simulated model outputs with the experimental results. In the next step, we will develop a general framework for the implementation of bump-less switching between two or more higher dimensional systems based on multi-realization theory [8] [149].

Chapter 4

An nonlinear modeling method using support vector machine for cardiorespiratory responses to exercise

Although considered as an experimentally validated mathematic model of the human CR responses to the onset and offset of exercise, the proposed switching model in Chapter 3 has not been identified the time-varying nonlinear dynamics of CR responses during exercises (i.e., as early stated that the HR response to the onset and offset of exercise can be approximated as the first order process, we observed that time constant and steady state gain is influenced not only by exercise intensity, but also by self-conditions), whose time-varying dynamics are a challenge for control engineers. In order to accurately regulate nonlinear time-variate dynamics of cardiovascular responses to exercise for individual exercisers, we proposed another modeling approach, a control oriented modeling approach, to depict nonlinear behavior of HR responses at both the onset and offset of treadmill exercises. In the following, this model will be built up based on support vector machine regression (SVR). The nonlinear behaviors at both the onset and offset of exercises have been well described by using the established SVR models. The model provides the fundamentals for the optimization of exercise efforts by using model based optimal control approaches, which will be covered in the next Chapter 5.

4.1 Introduction

Exercise and regular daily physical activity are of vital importance for general well being and in the management of obesity and diabetes. Obesity and diabetes are now worldwide public health issues. They lead to increased morbidity and mortality from a range of associated diseases including heart disease, stroke and kidney failure. The global health care expenditure attributable to diabetes has been estimated in 2003 and 2006 by the International Diabetes Federation (IDF) and reported in the second and third editions of the Diabetes Atlas. Recent major randomized clinical trials [160] [112] internationally have demonstrated safe exercise as the best means for the prevention of type 2 diabetes in individuals.

We seek to develop a control oriented modeling approach to proficiently estimate CR response to exercise for individuals, by non-invasive means. HR, as we know, has been extensively applied to evaluate CR response [153] [154] [58] [12] [62] to exercise as it can be easily measured by cheap wireless portable noninvasive sensors. In this sense, therefore, developing nonlinear models with respect to the analysis of dynamic characteristics of HR response is the starting point of this project. Based on the model, a nonlinear *switching Model Predictive Control (MPC)* approach will be developed to optimize exercise effects while keeping level of exercise intensity within the safe range .

There are plenty of papers [136] [37] about the analysis of steady state characteristics of HR response. Nonlinear behavior has been detected and nonlinear models have been established for response analysis when response entering steady state. During medical diagnosis and analysis of CR kinetics, however, transient response of HR is more valuable as it contains indicators of current disease or warnings about impending cardiac diseases [4]. Although both linear and nonlinear modeling approaches [74] [39] have been applied to explore dynamic characteristics of heart response to exercise, few papers

focus on the variation of dynamic characteristics under different exercise intensities for both the onset and offset of exercises. For moderate exercise, literatures often assume HR dynamics can be described by linear time invariant models. In this study, it was observed time constant of heart response to exercise is influenced by the load of exercise, as well as by self conditions (e.g., during a constant exercise intensity, steady state gain and time constant of HR/VO_2 response to exercise were found to mostly still be varying in every single moment). Papers [41] [41] prove that exercise effects can be optimized by regulating heart rate following a predefined exercise protocol. It is well known that higher control performance can be obtained if the model contains less uncertainty. Therefore, it is worthwhile to establish a more accurate dynamical model to enhance the controller design of heart rate regulation. In this study, we designed a treadmill walking exercise protocol to analyze step response of heart rate. During experiments, ECG, body movement, and oxygen saturation were recorded by using portable non-invasive sensors: Alive ECG monitor, Micro Inertial Measurement Unit (IMU), and Alive Pulse Oximeter. It was confirmed that time constant are not invariant especially when walking speed is faster than 3 miles/hour. Time constant for offset exercise is normally bigger than that of onset exercises. Steady state gain variation under different exercise intensity has also been visibly observed. Furthermore, the experiment results indicate that it is difficult to describe the variation of the transient parameters (such as, time constant) by using a simple linear model. We applied the novel machine learning method, support vector machine (SVM), to depict the nonlinear relationship .

SVM is a new promising non-linear, non-parametric classification technique, which already showed good results in the medical diagnostics. The main advantages in this study is to offer a regularization parameter, which can avoid over-fitting of the HR/VO_2 response during exercise, guarantee the continuity during model switching, and achieve

good tracking for nonlinear systems at onset and offset of exercise. Support vector machine based regression [48] (Support Vector Regression (SVR)) has been successfully applied to nonlinear function estimation [67] [156]. Vapnik et al. established the foundation of SVM [161] [162]. The formulation of SVM embodies the structure of the risk minimization principle, which has been shown to be superior to other traditional empirical risk minimization principles [72]. SVR applies the kernel methods implicitly to transform data into a feature space (this is known as a kernel trick [135]), and uses linear regression to get a nonlinear function approximation in the feature space. SVR is extremely efficient in terms of speed and complexity, and successfully solves the over-fitting problem [73] by introducing regularization techniques. By using radial basis function (RBF) kernel, this study efficiently established the nonlinear relationship between time constant and exercise intensity for both onset and offset exercises.

This section is organized as follows. Section 4.2 provides preliminary knowledge of SVM based regression. Section 4.3 describes the experimental equipments and exercise protocol. Data analysis and modeling results are given in section 4.4. Eventually, section 4.5 gives conclusions.

4.2 SVM Regression

Let $\{u_i, y_i\}_{i=1}^{N}$ be a set of inputs and outputs data points ($u_i \in U \subseteq R^d, y_i \in Y \subseteq R$, N is the number of points). The goal of the support vector regression is to find a function $f(u)$ which has the following form

$$f(u) = w \cdot \phi(u) + b, \tag{4.1}$$

Where $\phi(u)$ is equivalent to mapping the input space U into the new high-dimensional feature spaces induced by a kernel $F = \{\phi(u) \mid u \in U\}$, which are nonlinearly transformed from u. The weight vector w and bias b are defined as the hyperplane by the equation $\langle w \cdot \phi(u) \rangle + b = 0$. The hyperplane is estimated by minimizing the regularized risk function:

$$\frac{1}{2}\|w\|^2 + C\frac{1}{N}\sum_{i=1}^{N} L_\varepsilon(y_i, f(u_i)), \tag{4.2}$$

The first term is called the regularized term. The second term is the empirical error measured by ε-insensitivity loss function which is defined as:

$$L_\varepsilon(y_i, f(u_i)) = \begin{cases} \mid y_i - f(u_i) \mid -\varepsilon, \mid y_i - f(u_i) \mid > \varepsilon \\ 0, \qquad \mid y_i - f(u_i) \mid \leq \varepsilon \end{cases} \tag{4.3}$$

This defines an ε tube. The loss is equal to zero if the difference between the predicted $f(u_i)$ and the measured value is less than ε (see Fig. 4.1). For all other predicted points outside the tube, the loss is equal to magnitude of the difference between the predicted value and the radius of the tube. The radius ε of the tube and the regularization constant C are both determined by user.

The selection of parameter C depends on application knowledge of the domain. Theoretically, a small value of C will under-fit the training data because the weight placed on the training data is too small, thus resulting in large values of mean square error (MSE) on the test sets. However, when C is too large, SVR will over-fit the training set so that $\frac{1}{2}\|w\|^2$ will lose its meaning and the objective goes back to minimize the empirical risk only. Parameter ε controls the width of the ε-insensitive zone. Generally, the larger the ε the fewer number of support vectors and thus the sparser the representation of the solution. However, if the ε is too large, it can deteriorate the accuracy on the training data.

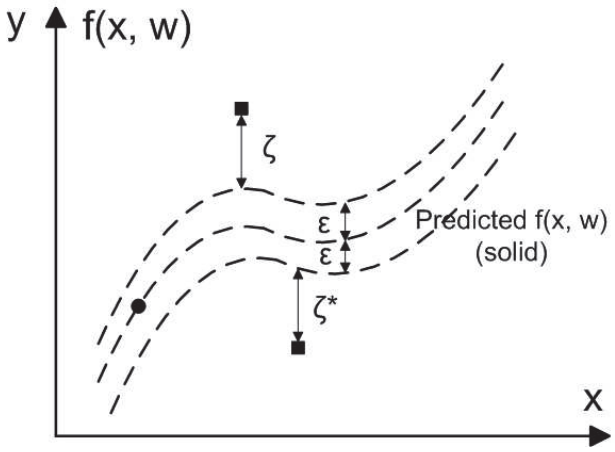

Fig. 4.1: The parameters used in (one-dimension) Support Vector Regression.

By solving the above constrained optimization problem, we have

$$f(u) = \sum_{i=1}^{N} \beta_i \phi(u_i) \cdot \phi(u_i) + b, \tag{4.4}$$

As mentioned above, by the use of kernels, all necessary computations can be performed directly in the input space, without having to compute the map $\phi(u)$ explicitly. After introducing kernel function $k(u_i, u_j)$, the above equation can be rewritten as follows.

$$f(u) = \sum_{i=1}^{N} \beta_i k(u_i, u) + b, \tag{4.5}$$

Where the coefficients β_i corresponding to each (u_i, y_i). The support vectors are the input vectors u_j whose corresponding coefficients $\beta_j \neq 0$. For linear support regression, the kernel function is thus the inner product in the input space:

$$f(u) = \sum_{i=1}^{N} \beta_i \langle u_i, u \rangle + b, \tag{4.6}$$

For nonlinear SVR, there are a number of kernel functions which have been found to provide good generalization capabilities, such as polynomials, radial basis function

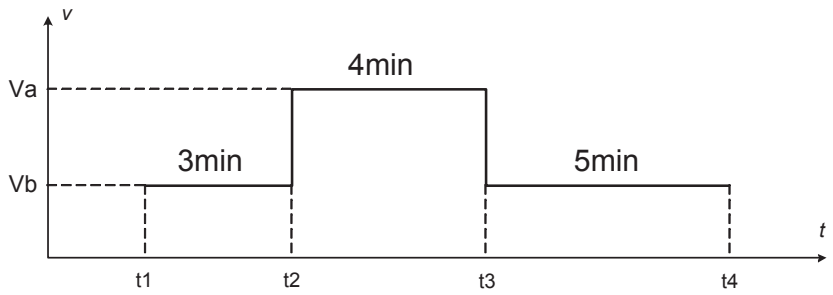

Fig. 4.2: Experiment protocol.

(RBF), sigmod. Here we present the polynomials and RBF kernel functions as follows:

Polynomial kernel: $k(u, u') = ((u \cdot u') + h)^p$.

RBF Kernel: $k(u, u') = exp(-\frac{\|u - u'\|^2}{2\sigma^2})$.

Details about SVR, such as the selection of radius ε of the tube, kernel function, and the regularization constant C, can be found in [135] [95].

4.3 Experiment

A 41 years old healthy male joined the study. He is 178 cm high and 79 kg heavy.

Table 4.1: The Values of Walking Speed V_a and V_b.

	Set 1	Set 2	Set 3	Set 4	Set 5	Set 6
Va (m/h)	0.5	1.5	2	2.5	3	3.5
Vb (m/h)	1.5	2.5	3	3.5	4	4.5

Experiments were performed in the afternoon, and the subject was allowed to have a light meal one hour before the measurements. After walked for about 10 minutes on the treadmill to get acquainted with this kind of exercise, the subject walked at six sets of exercise protocol (see Fig. 4.2) to test step response. The values of walking speed V_a and V_b were designed to vary exercise intensity and are listed in Table I. To

properly identify time constants for onset and offset exercises, the recorded data should be precisely synchronized. Therefore, time instants t_1, t_2, t_3, and t_4 should be identified and marked accurately. In this study, we applied a Micro Inertial Measurement Unit (Xsens MTi-G IMU) to fulfill this requirement. We compared both attitudes information (roll, pitch, and yaw angles) and acceleration information provided by the Micro-IMU. It was observed that acceleration information alone is sufficient to identify these time instants (see Fig. 4.3 and Fig. 4.4).

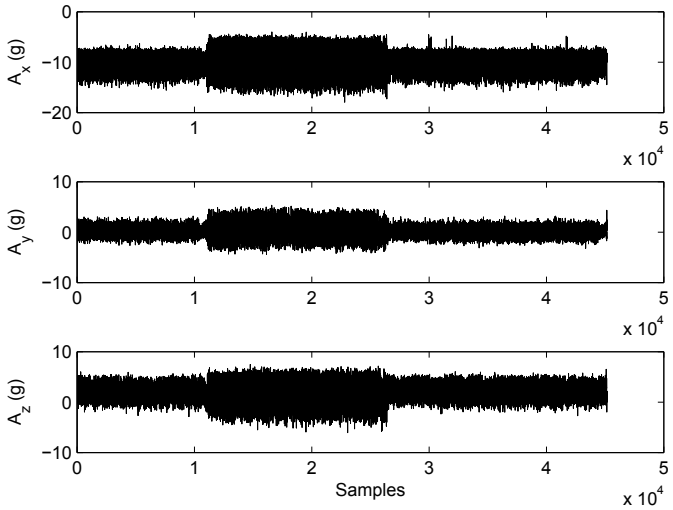

Fig. 4.3: Accelerations of three axes provided by the Micro IMU.

During experiments, continuous measurements of ECG, body movement, and S_pO_2 (oxygen saturation) were made by using portable non-invasive sensors. Specifically, ECG was recorded by using Alive ECG Monitor. Body movement was measured by using the Xsens MTi-G IMU. S_pO_2 was monitored by using Alive Pulse Oximeter to guarantee the safety of the subject. The experimental scenario is shown in Fig. 4.5.

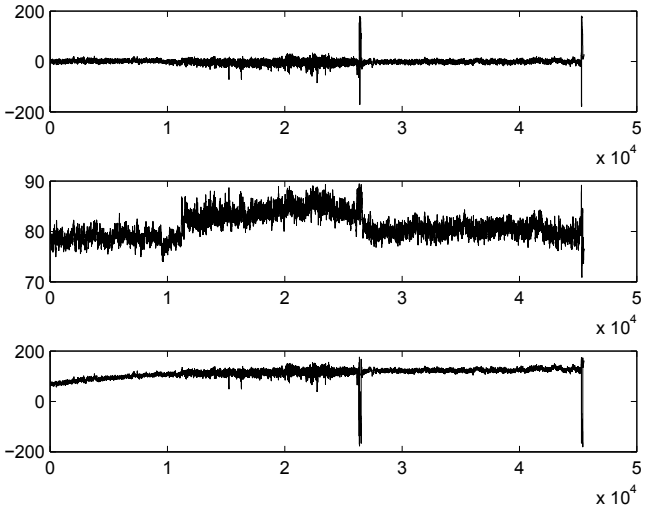

Fig. 4.4: Roll, pitch and yaw angles provided by the Micro IMU.

4.4 Data analysis and discussion

Original signals of IMU, ECG, and S_pO_2 are shown in Fig. 4.4, Fig. 4.6, and Fig. 4.7 respectively. It is well known that even in the absence of external interference the heart rate can vary substantially over time under the influence of various internal or external factors [155]. As mentioned before, in order to reduce the variance, designed experimental protocol has been repeated three times. Experimental data of these repeated experiments has been synchronized and averaged.

A typical measured heart rate response is shown in Fig. 4.8. Paper [155] found that HR response to exercise can be approximated as first order process from a control application point of view. Therefore we established first order model for six averaged step response data by using Matlab System Identification Toolbox.

Table 4.2 shows the identified steady state gain (K) and time constant (T) by using averaged data of three sets of experimental data. A typical Curve fitting result is shown in Fig. 4.9. From Table 4.2, we can clearly see that both steady state gain and time

Fig. 4.5: Experimental scenario.

constant vary when walking speed V_a and V_b change. Furthermore, time constant of offset exercise are noticeably bigger than those of onset exercises. However, it should be pointed out the variant of time constant is not distinctly dependent on walking speed when walking speed is less than 3 miles/hour. Overall, experimental results indicate that HR dynamics at onset and offset exercise exhibited highly nonlinearity when walking speed is higher than 3 miles/hour.

Table 4.2: The identified time constants and steady state gains by using averaged data.

Sets	Onset		Offset	
	DC gain	Time constant	DC gain	Time constant
1	9.2583	9.4818	7.9297	27.358
2	11.264	10.193	9.8561	27.365
3	10.006	13.659	8.9772	26.741
4	12.807	18.618	12.087	30.865
5	17.753	38.192	17.953	48.114
6	32.911	55.974	25.733	81.693

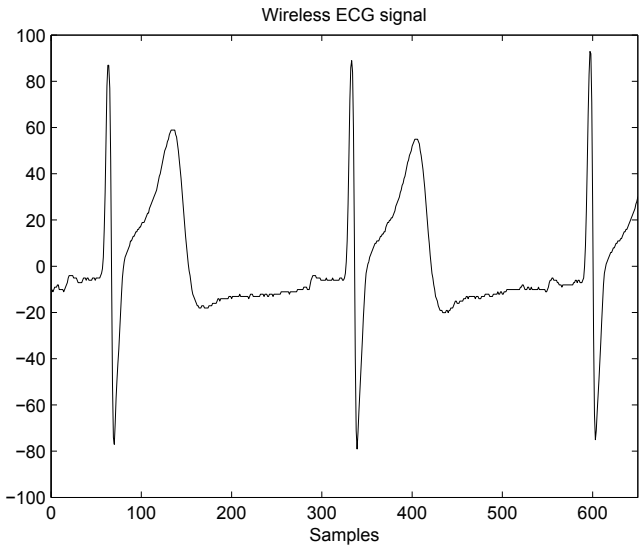

Fig. 4.6: Original ECG signal.

In order to quantitatively describe the detected nonlinear behavior, we employed the novel machine learning modeling method, support vector machine regression, to model time constant and DC gain of HR dynamics.

The time constant regression results at onset and offset exercises are shown in Fig. 4.10 and Fig. 4.11 respectively. In these figures, the continuous curve stands for the estimated input output steady state relationship. The dotted lines indicate the ε-insensitivity tube. The plus markers are the points of input and output data. The circled plus markers are the support points. It should be emphasized that ε-insensitive SVR just uses less than 30 percent of total points to sparsely describe the nonlinear relationship efficiently.

It can be seen that time constant at offset exercise is bigger than that at onset exercise. It can be also observed the time constant at onset exercise is more accurately identified than that at offset exercise. This is indicated by the ε tube (or the width of the ε-nsensitive zone). It is probability that the recovery stage can be influenced by more other exercise unrelated factors than those at the onset exercise.

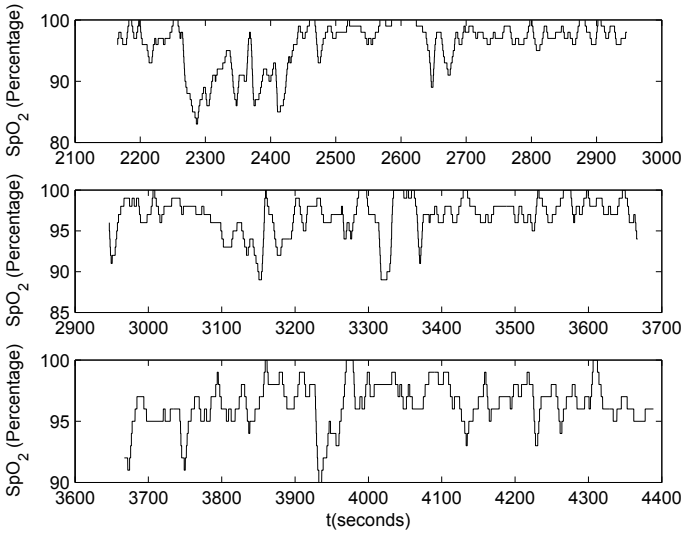

Fig. 4.7: The recording of SpO_2.

The SVM regression results for DC gain at onset and offset exercises are shown in Fig. 4.12 and Fig. 4.13. It can be observed the DC gain for recovery stage is less than that at onset exercise. Especially, when walking speed is greater than 3 miles per hour.

4.5 Conclusion

This study aims to capture nonlinear behavior of HR response to treadmill walking exercises by using support vector machine based analysis. We identified both steady state gain and the time constant under different walking speeds by using the data from a healthy middle aged male subject. Both steady state gain and the time constant are not invariant under different walking speeds. The time constant for recovery stage is longer than that at onset of exercise as predicted. In this study, these nonlinear behaviors have been quantitatively described by using an effective machine learning based approach, named SVM regression. Based on the established model, we have already developed a new switching control approach which will be reported somewhere else. We believe this

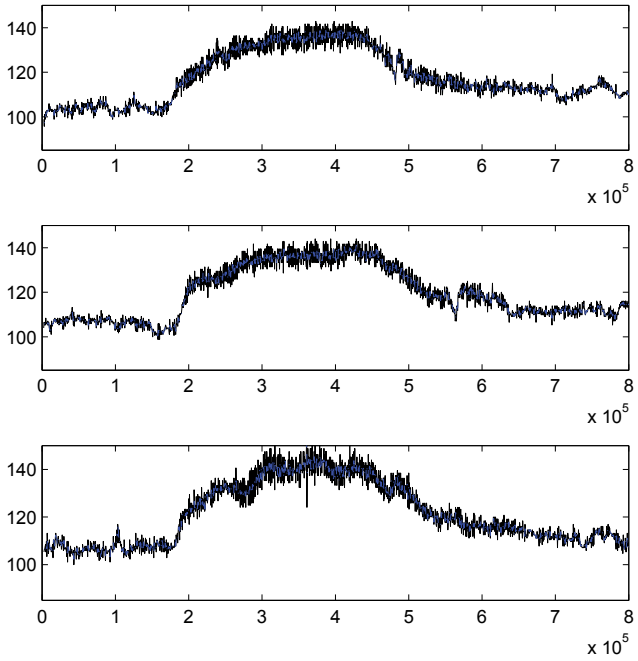

Fig. 4.8: A measured HR step response signal.

integrated modeling and control approach can be utilized to a broad range of process control. In the next step of this study, we are planning to recruit more subjects to test the established nonlinear modeling and control approach further.

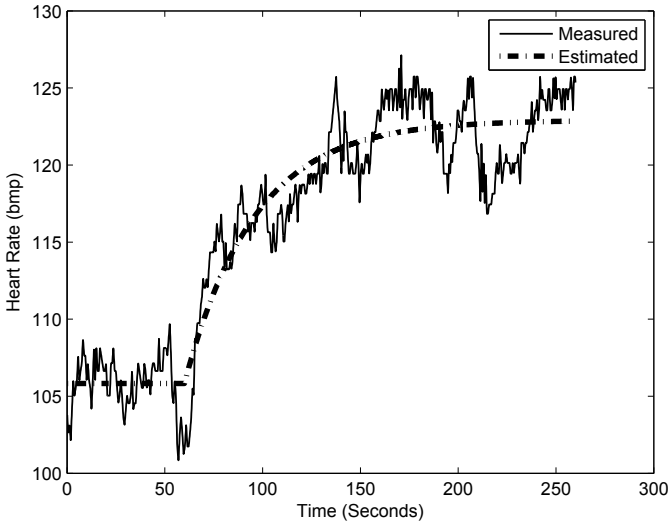

Fig. 4.9: A typical curve fitting result.

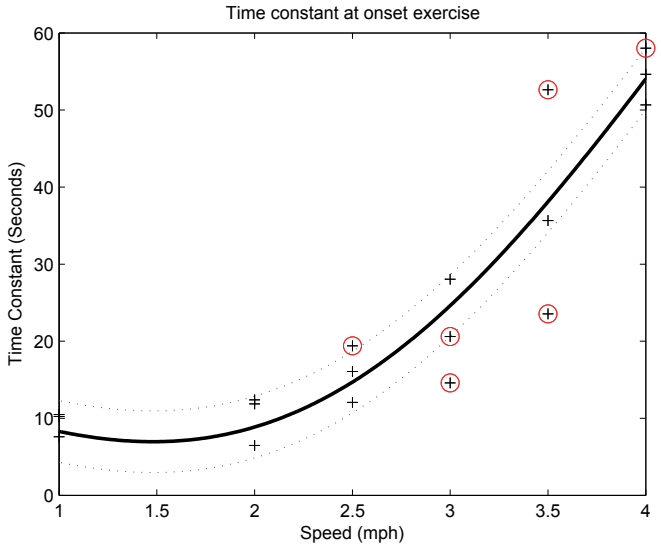

Fig. 4.10: SVM regression results for time constant at the onset of exercise.

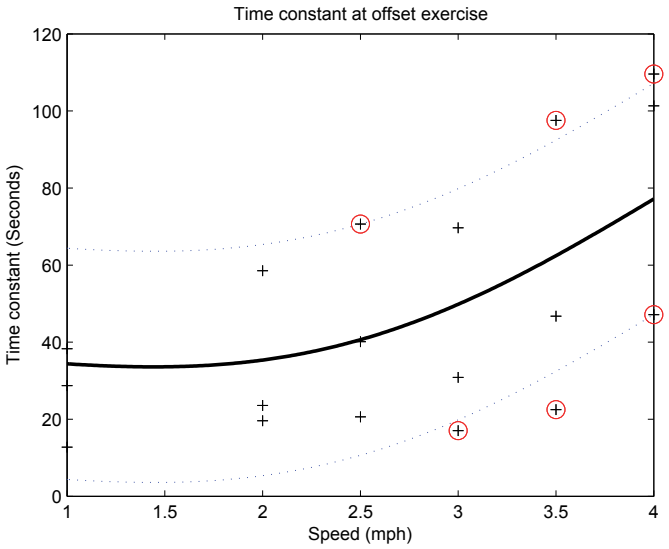

Fig. 4.11: SVM regression results for time constant at the offset of exercise.

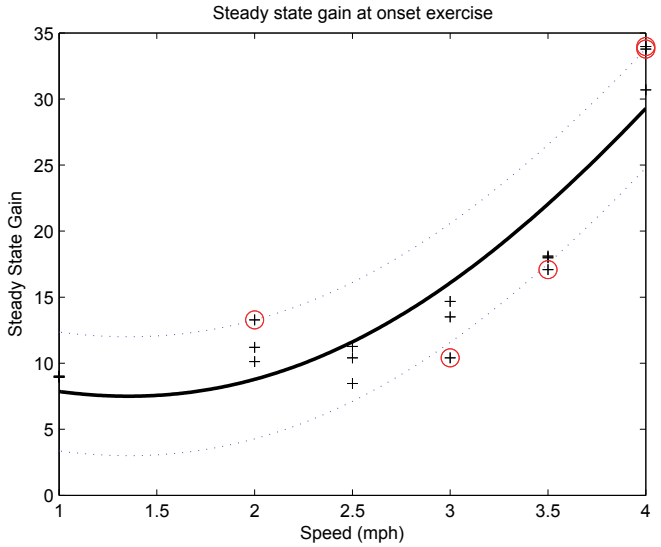

Fig. 4.12: SVM regression results for DC gain at the onset of exercise.

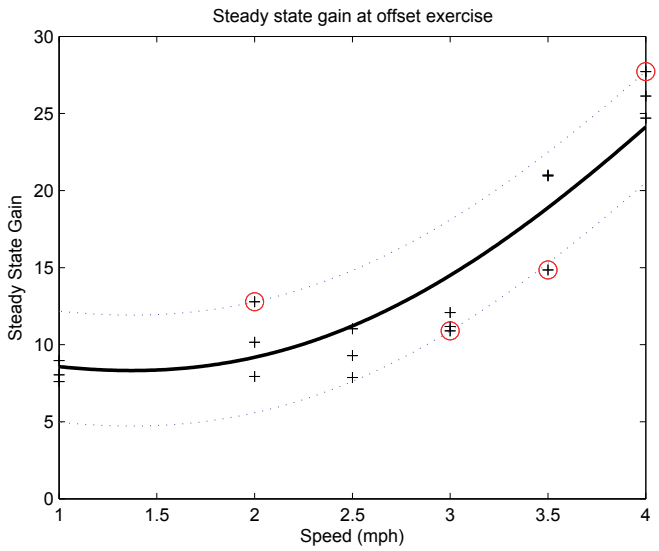

Fig. 4.13: SVM regression results for DC gain at the offet of exercise.

Chapter 5

A machine learning based control method for human cardiorespiratory responses to exercise

5.1 Introduction

As HR was found to be a predictor of major ischemic heart disease events, cardiovascular mortality, and sudden cardiac death [6] [4], many scholars have been interested in monitoring it to evaluate the cardiovascular fitness[153] [154] [58] [12] [62]. HR is determined by the number of heartbeats per unit of time, it can vary with as the body's need for oxygen changes during exercise.

SVM regression offers a solution for nonlinear behavior description of HR response to moderate exercises as shown in Chapter 4. This SVM based model for HR estimation can be used to implicitly indicate some key cardio-respiratory response to exercise, such as oxygen uptake as discussed in [153] and [164]. In our previous study [36], it is shown that time constant of HR response are not invariant. It is often bigger at offset of exercise than that for onset of exercise. The captured difference leads to setting up two nonlinear models separately to present the dynamic characteristics of HR at onset and offset of exercise.

One process possessing two or more quite different characteristics is quite common not only for human body responses but also for some industrial processes. For instance, the

boiler is widely used in live stream sector which is a closed vessel where water or other liquid is heated. It may only takes a few minutes to heat the water (or other liquid) up to 100 °C, but may spend several hours to cool down in general. Although it is evident that using different model for different stage (as shown in section 4) may provide more precise description of the process, it requires more advanced control strategy to handle this complicate mechanism.

MPC is a family of control algorithms that employ an explicit model to predict the future behavior of the process over a prediction horizon. The controller output is calculated by minimizing a predefined objective function over a control horizon. Fig. 5.1 illustrates the 'moving horizon' technique used in MPC. Recently, MPC has established itself in industry as an important form of advance control [125] due to its advantages over traditional controllers [65] [104]. MPC displays improved performance because the process model allows current computations to consider future dynamic events. This provides benefit when controlling processes with large dead times or non-minimum phase behavior. MPC also allows for the incorporation of hard and soft constraints directly in the objective function. In addition, the algorithm provides a convenient architecture for handling multi-variable control due to the superposition of linear models within the controller.

In this study, one of the most popular MPC algorithms, Dynamic Matrix Control (DMC), is selected to control the HR responses based on previously established SVM based nonlinear time variant model. The major benefit of using a DMC controller is its simplicity and efficiency for the computation of optimal control action, which is essentially a least-square optimization problem.

To well handle different dynamic characteristics at onset and offset of exercises, the switching control strategy has been implemented during the transmission between onset and offset of treadmill exercises. By integrating the proposed modeling and control

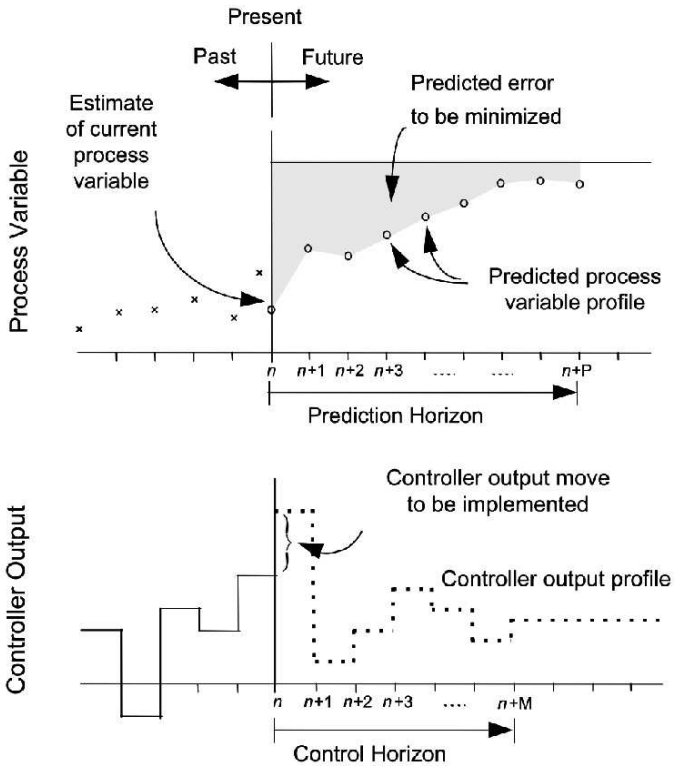

Fig. 5.1: The 'moving horizon' concept of model predictive control [47].

methods, HR response to exercise has been optimally regulated at both onset and offset of exercises.

The organization of this chapter is as follows. The preliminaries of DMC/MPC are clarified in section 5.2. The proposed switching DMC control approach is discussed in section 5.3, which is followed by simulation results. Conclusions are given in section 5.4.

5.2 Background

5.2.1 Model-based predictive control (MPC)

5.2.1.1 Brief introduction for MPC

The development of MPC began in the late seventies after the publication of the paper by Richalet et al in 1978 [126] and has considerably developed both within the research control community and industry. Initially, it was developed to meet the specialized control needs of petroleum refineries. Currently, the MPC technology is used in a wide variety of application areas including chemical, food processing, automotive, aerospace, metallurgy, and pulp and paper [24].

The MPC controller has proved that it delivers significant financial benefits to industries, compared to other advance control methods. A survey conducted by Qin and Badgwell in 2003 [121] identifies that there are more than 4600 industrial applications of MPC. This varies from SISO to very complex multiply-input multiply-output (MIMO) with over 600 variables. The MPC has become a very powerful and attractive strategy as it has many advantages.

In relation to the MPC controller, the systems constraints are very systematically added into the controller design, in order to handle the constraints effectively. In addition, the

handling features of MIMO delivers the capacity to perform all multivariable processing in a single loop hence eliminating the need of a cascading process. This significantly increases the performance of the controller. In addition, the MPC technology can be applied to linear and non-linear systems, and the concept is equally applicable to SISO and MIMO models.

Another advantage of MPC is measured disturbance can be added into the system dynamic to compensate the disturbance in the controller optimization process. Furthermore, the ability explicitly of the system model and ability to predict the system behavior helps engineers to learn the system performance in advance [94].

One of its drawbacks is that it requires more computational power when calculating the online control optimization and plant linearization. However, this problem can be overcome with the latest high speed microprocessor computers [24].

5.2.1.2 MPC structure

The basic structure of the MPC controller consists of two main elements as depicted in Fig. 5.2. The first element is the predicted model of the process to be controlled. Further, if any measurable disturbance or noise exists in the process it can be added to the model of the system for compensation. The second element is the optimizer that calculates the future control action to be executed in the next step while taking into account the cost function and constraints [24].

As it can be seen in the Fig. 5.2, the set point is corrected for any model error or disturbance through the feedback loop. While the basic structure of the MPC remains the same, the control algorithms vary with the predicted model used to represent the processes and the noises, and cost function to minimize the error. Some of the most popular algorithms are:

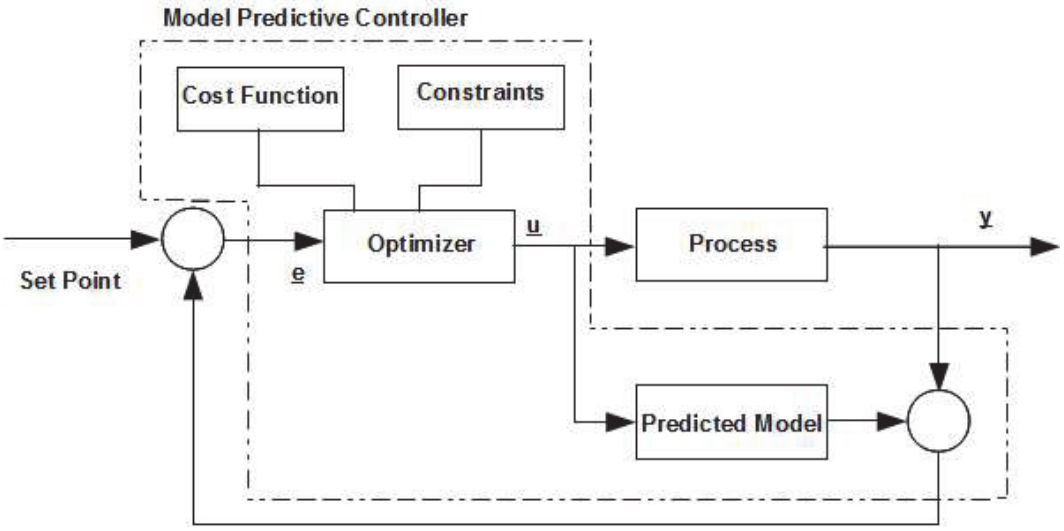

Fig. 5.2: Structure of Model Predictive Control.

1. Dynamic matrix control (DMC)

The DMC uses a step response to model the process dynamic. This method was initially introduced in Shell Oil in the early period of 1973 [129]. One of the main popular characteristics of this method is handling the constraints using the quadratic programming (QP) method. A general discrete state-space model can also use this method in the controller design [24].

2. Model algorithmic control (MAC)

It was initially called as model predictive heuristic control (MPHC). This method is the same as the previous DMC method except for a few differences. Firstly, it uses an impulse response to model the system whereas the DMC uses step response. Furthermore, it does not follow the concept of control horizon and introduces a reference trajectory as a first order system which is computed to minimize the error between output and reference trajectory [24].

3. Predictive functional control (PFC)

Richalet developed this controlled method to achieve a fast process. This method uses

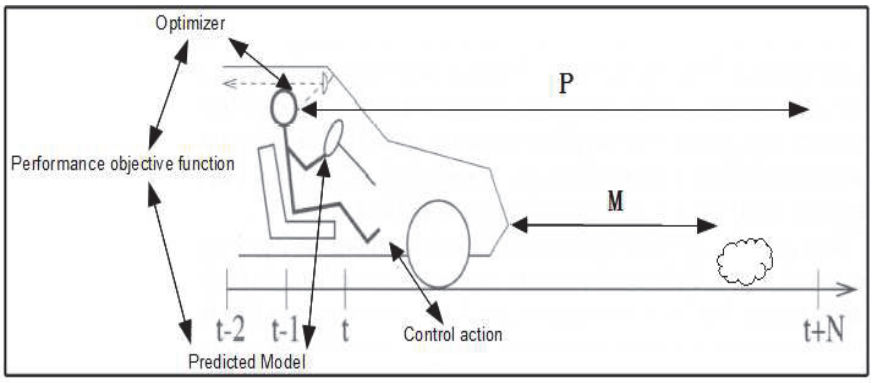

Fig. 5.3: Structure of Model Predictive Control.

the state space model of the process and handles non-linear and unstable space model [124].

4. Extended prediction self adaptive control (EPSAC)

Discrete transfer function (z-transform) is used to model the process. Its control method is very simple. It assumes the control signal stays constant from instant t. The disturbance model can also be included in the model [129].

5. Generalized predictive control (GPC)

A controlled autoregressive integrated moving average (CARIMA) model is used to predict the output of the system. The GPC uses quadratic cost function with weighting of control effort. An analytic solution of optimal control can be given in the absence of constraints [129].

5.2.1.3 MPC control strategy

The MPC control strategy can be explained by comparing the behavior of human beings when driving a car, as shown in Fig. 5.3.

The prediction horizon (P) is how far the driver can see in front of the car. The moving horizon (M) is how far the driver can take actions to control. The predicted model is the

trained driving skills of human beings. For example, if there is an emergency situation ahead and the driver takes the emergency stop immediately, the distance between the location where one began one's actions and the point where the car actually is stopped, is called by moving horizon. The drive adjusts the control actions such as accelerator, brake, and steering by looking long ahead of the desired trajectory. The control decision can be changed with the conditions ahead such as a signal light, traffic, road type etc. Hence the driver only executes the first control action for the decision of that instance and continually adjusts the control action for the changes ahead.

The optimizer setting of the accelerator or brake depends on driver optimization criteria and reaction. By combining the optimization criteria and driving skills, one can drive one's car for different purposes, similar to real MPC. For example, if the driver wants to minimize the traveling time, the driver will accelerate more and if he/she wants to save the fuel they drive at a constant speed [170].

5.2.2 Dynamic matrix control (DMC)

DMC uses a linear finite step response model of the process to predict the process variable profile, $\hat{y}(k+j)$ over j sampling instants ahead of the current time, k:

$$\hat{y}(k+j) = y_0 + \underbrace{\sum_{i=1}^{j} A_i \triangle u(k+j-i)}_{\text{Effect of current and future moves}} + \underbrace{\sum_{i=j+1}^{N-1} P_i \triangle u(k+j-i)}_{\text{Effect of past moves}}$$
$$j = 1, 2 \cdots P; N : ModelHorizon. \quad (5.1)$$

where P is the prediction horizon and represents the number of sampling intervals into the future over which DMC predicts the future process variable [47]. In Eq. (5.1), y_0 is the initial condition of the process variable, $\triangle u_i = u_i - u_{i-1}$ is the change in the

controller output at the ith sampling instant, A_i and P_i are composed by the ith unit step response coefficient of the process, and N is the model horizon and represents the number of sampling intervals of past controller output moves used by DMC to predict the future process variable profile.

The current and future controller output moves have not been determined and cannot be used in the computation of the predicted process variable profile. Therefore, Eq. (5.1) reduces to

$$\hat{y}(k+j) = y_0 + \sum_{i=j+1}^{N-1} (P_i \triangle u(k+j-i)) + d(k+j), \tag{5.2}$$

where the term $d(k+j)$ combines the unmeasured disturbances and the inaccuracies due to plant-model mismatch. Since future values of the disturbances are not available, $d(k+j)$ over future sampling instants is assumed to be equal to the current value of the disturbance, or

$$d(k+j) = d(k) = y(k) - y_0 - \sum_{i=1}^{N-1} (H_i \triangle u(k-j)), \tag{5.3}$$

where $y(k)$ is the current process variable measurement.

The goal is to compute a series of controller output moves such that

$$R_{sp}(k+j) - \hat{y}(k+j) = 0, \tag{5.4}$$

Substituting Eq. (5.1) in Eq. (5.4) gives

$$\underbrace{R_{sp}(k+j) - y_0 - \sum_{i=j+1}^{N-1} P_i \triangle u(k+j-i) - d(k+j)}_{\text{Predicted error based on past moves, e(k+j)}} = \underbrace{\sum_{i=1}^{j} A_i \triangle u(k+j-i)}_{\text{Effect of current and future moves to be determined}} \tag{5.5}$$

Eq. (5.5) is a system of linear equations that can be represented as a matrix equation of the form

$$\begin{bmatrix} e(k+1) \\ e(k+2) \\ e(k+3) \\ \vdots \\ e(k+M) \\ \vdots \\ e(k+P) \end{bmatrix}_{P\times 1} = \begin{bmatrix} a_1 & 0 & 0 & \dots & 0 \\ a_2 & a_1 & 0 & \dots & 0 \\ a_3 & a_2 & a_1 & \dots & 0 \\ \vdots & \vdots & \vdots & \ddots & \vdots \\ a_M & a_{M-1} & a_{M-2} & & a_1 \\ \vdots & \vdots & \vdots & \ddots & \vdots \\ a_P & a_{P-1} & a_{P-2} & \dots & a_{P-M+1} \end{bmatrix}_{P\times M} \times \begin{bmatrix} \triangle u(k) \\ \triangle u(k+1) \\ \triangle u(k+2) \\ \vdots \\ \triangle u(k+M-1) \end{bmatrix}_{M\times 1} \tag{5.6}$$

or in a compact matrix notation as18

$$\bar{e} = A \triangle \bar{u}, \tag{5.7}$$

where $\bar{e}$ is the vector of predicted errors over the next P sampling instants, A is the dynamic matrix, and $\triangle\bar{u}$ is the vector of controller output moves to be determined.

An exact solution to Eq. (5.7) is not possible since the number of equations exceeds the degrees of freedom ($P > M$). Hence, the control objective is posed as a least squares optimization problem with a quadratic performance objective function of the form determined.

$$\min_{\triangle\bar{u}} J = [\bar{e} - A \triangle \bar{u}]^T [\bar{e} - A \triangle \bar{u}], \tag{5.8}$$

The DMC control law of this minimization problem:

$$\triangle \bar{u} = (A^T A)^{-1} A^T \bar{e}, \tag{5.9}$$

Implementation of DMC with the control law in Eq. (5.9) results in excessive control action, especially when the control horizon is greater than one. Therefore, a quadratic penalty on the size of controller output moves is introduced into the DMC performance objective function. The modified objective function has the form

$$\min_{\triangle\bar{u}} J = [\bar{e} - A \triangle \bar{u}]^T [\bar{e} - A \triangle \bar{u}] + [\triangle\bar{u}]^T \lambda [\triangle\bar{u}], \tag{5.10}$$

where λ is the move suppression coefficient (controller output weight). This weighting factor plays a crucial role on the optimizer of DMC. If the value of λ is enough large, the optimizer attaches more importance to the effects of $\triangle u$, so that the robustness of output moves of the process is straightly improved, but the accuracy of output moves along with reference profile might be sacrificed. In the same way to reduce the value of λ, to optimize the effect of $\bar{e}$ has higher priority than that of $\triangle u$. Accuracy of system becomes more significant than robustness.

In the unconstrained case, the modified objective function has a closed form solution of (e.g., Marchetti, Mellichamp, & Seborg, 1983; Ogunnaike, 1986) [98] [120]

$$\triangle \bar{u} = (A^T A + \lambda I)^{-1} A^T \bar{e}, \tag{5.11}$$

Adding constraints to the classical formulation given in Eq. (5.10) produces the quadratic dynamic matrix control (QDMC) [103] [64] algorithm. The constraints considered in this work include:

$$\hat{y}_{min} \leq \hat{y} \leq \hat{y}_{max} \tag{5.12a}$$

$$\triangle \bar{u}_{min} \leq \triangle \bar{u} \leq \triangle \bar{u}_{max} \tag{5.12b}$$

$$\bar{u}_{min} \leq \bar{u} \leq \bar{u}_{max} \tag{5.12c}$$

5.2.3 Programming approach in C language for DMC

The whole follow-up steps for DMC implementation in C language are listed in Table 5.1. The DMC control system similar with PID control is a closed loop system. At the beginning of loop, DMC parameters (such as P, M, N and λ), initial value of input, and set point array R should be defined by developers. More details will be found about tuning DMC parameters in section 5.2.4. After initializations, the process output $y(k)(k = 1)$ is calculated and recorded for further steps.

Table 5.1: The identified time constants and steady state gains by using averaged data.

Dynamic Matrix Control (DMC) Algorithm Implementation using C Language Programming	
Steps	Actions
1	Initialize prediction horizon (P), moving horizon (M), move suppression coefficient (λ), model horizon (N), input value $u(k-1)$, set point R and the process output, $y(k)$, is measured.
2	Compute free response of the system by using F matrix and measured $y(k)$, and calculate error vector $e(k+j) = R_{sp}(k+j) - [\hat{y}(k+j) + d(k+j)]$ $(j = 1, 2 \ldots P)$.
3	Compute $u(k) = K \times e(k+j)$ by using performance objective function (optimizer) : $K = (A^T A + \lambda I)^{-1} A^T$
4	$u(k)$ is added to controller output
5	Shift the value of $p.v$ matrix and update the first element with $u(k)$
6	$k = k + 1$
7	Repeat step 1—6

The error vector $e(k+j)$ can be rewritten by extending $\hat{y}(k+j)$ according to Eq. (5.1)

$$e(k+j) = R_{sp}(k+j) - [y_0 + \underbrace{\sum_{i=1}^{j} A_i \triangle u(k+j-i)}_{\text{Effect of current and future moves}} + \underbrace{\sum_{i=j+1}^{N-1} P_i \triangle u(k+j-i)}_{\text{Effect of past moves}} + d(k+j)], \tag{5.13}$$

A and P matrix in Eq. (5.13) both are composed of elements of unit step response under the selected length of model horizon (N) in different ways, based on superposition principle [69].

$$\sum_{i=1}^{j} A_i \quad (j = 1, 2, \cdots P)$$

for current and future effects is represented by

$$\begin{bmatrix} a_1 & 0 & 0 & \dots & 0 \\ a_2 & a_1 & 0 & \dots & 0 \\ a_3 & a_2 & a_1 & \dots & 0 \\ \vdots & \vdots & \vdots & \ddots & \vdots \\ a_M & a_{M-1} & a_{M-2} & & a_1 \\ \vdots & \vdots & \vdots & \ddots & \vdots \\ a_P & a_{P-1} & a_{P-2} & \dots & a_{P-M+1} \end{bmatrix}_{P\times M} ;$$

$$\sum_{i=j+1}^{N-1} P_i \quad (j = 1, 2, \cdots P)$$

for past moves is expressed as

$$\begin{bmatrix} a_2 & a_3 & a_4 & \dots & a_N \\ a_3 & a_4 & a_5 & \dots & a_{N+1} \\ a_4 & a_5 & a_6 & \dots & a_{N+2} \\ \vdots & \vdots & \vdots & \ddots & \vdots \\ a_M & a_{M+1} & a_{M+2} & & a_{N+M-2} \\ \vdots & \vdots & \vdots & \ddots & \vdots \\ a_{P+1} & a_{P+2} & a_{P+3} & \dots & a_{P+N-1} \end{bmatrix}_{P\times N-1} .$$

As noted in Eq. (5.4), the ideal control goal assumes $e(k + j) = 0$, which directly generates the representations of Eq. (5.5). Importantly, it vividly tells us that the effects of current and future moves could be completely re-described by calculating the

effects of past moves. Along with this result, we can safely write error vector as

$$e(k+j) = R_{sp}(k+j) - y_0 - \sum_{i=j+1}^{N-1} P_i \triangle u(k+j-i) - d(k+j), \tag{5.14}$$

replacing $d(k+j)$ with Eq. (5.3), $e(k+j)$ can be revised by

$$e(k+j) = R_{sp}(k+j) - y(k) + \underbrace{[\sum_{i=1}^{N-1} H_i \triangle u(k+j-i) - \sum_{i=j+1}^{N-1} P_i \triangle u(k+j-i)]}_{\text{F Matrix}}, \tag{5.15}$$

As for minimizing the combination of set point tracking (e) and control effect ($\triangle u$), the modified objective function has been proposed in Eq. (5.10). By a series of mathematical manipulations, Eq. (5.16) is obtained:

$$\triangle \hat{u} = \underbrace{A^T A + \lambda I)^{-1} A^T}_{\text{K}} e, \tag{5.16}$$

5.2.4 Formulation of tuning DMC parameters

The foundation of DMC lies with the formal tuning rules [140] [141] based on fitting the controller output to measured process variable dynamics at one level of operation with a FOPDT model approximation. A FOPDT model has the form

$$\tau_p \frac{dy(t)}{dt} + y(t) = K_p u(t-\theta_p) \quad or \quad \frac{y(s)}{u(s)} = \frac{K_p e^{-\theta_p s}}{\tau_p s + 1}, \tag{5.17}$$

where K_p is the process gain, τ_p is the overall time constant and θ_p is the effective dead time. Specifically, K_p indicates the size and direction of the process variable response to a control move, τ_p describes the speed of the response, and θ_p tells the delay prior to

when the response begins.

The tuning parameters for single-loop DMC include the sample time (T_s), prediction horizon (P), moving horizon (M), model horizon (N) and move suppression coefficient (λ).

The tuning parameters are calculated offline prior to the start-up of the DMC controller. Following this previous work, the sample time, Ts, is computed as

$$T_s = Max(0.1\tau_p, 0.5\theta_p), \tag{5.18}$$

This value of sample time balances the desire for a low computation load (a large T_s) with the need to properly track the evolving dynamic behavior (a small T_s). Many control computers restrict the choice of T_s [61] [13]. Recognizing this, the remaining tuning rules permit values of T_s other than that computed by Eq. (5.18) to be used.

The sample time and the effective dead time are used to compute the discrete dead time in integer samples as

$$k = Int(\frac{\theta_p}{T_s}) + 1, \tag{5.19}$$

The prediction horizon, P, and the model horizon, N, are computed as the process settling time in samples as

$$P = N = Int(\frac{5\tau_p}{T_s}) + k, \tag{5.20}$$

Note that both N and P cannot be selected independent of the sample time.

A larger P improves the nominal stability of the closed loop. For this reason, P is selected such that it includes the steady-state effect of all past controller output moves,

i.e., it is calculated as the open loop settling time of the FOPDT model approximation.

The control horizon, M, must be long enough such that the results of the control actions are clearly evident in the response of the measured process variable. The tuning rule thus chooses M as one dead time plus one time constant, or

$$M = Int(\frac{\tau_p}{T_s}) + k, \tag{5.21}$$

This equation calculates M such that $M \times T$ is larger than the time required for the FOPDT model approximation to reach 60% of the steady state.

The final step is the calculation of the move suppression coefficient, λ. Its primary role in DMC is to suppress aggressive controller actions. Shridhar and Cooper [140] [141] (1997, 1998) derived the move suppression coefficient based on a FOPDT model fit as

$$\lambda = \frac{M}{10}(\frac{3.5\tau_p}{T} + 2 - \frac{M-1}{2})K_p^2, \tag{5.22}$$

Eq. (5.22) is valid for a control horizon greater than 1 ($M > 1$). When the control horizon is 1 ($M = 1$), no move suppression coefficient should be used ($\lambda = 0$).

5.3 Control methodologies design

5.3.1 Discrete Time Model

From the previous studies, HR response to exercise can be approximated as first order process, which is expressed in S-domain as Eq. (5.23).

$$H(s) = \frac{Y(s)}{U(s)} = \frac{K}{Ts+1}, \tag{5.23}$$

For obtaining the discrete time model, Eq. (5.23) has to be transformed to z-domain by

$$s = \frac{1 - z^{-1}}{T_s}, \tag{5.24}$$

T_s is the sample time.

To bring Eq. (5.24) to Eq. (5.23), this model in z-domain will be followed as Eq. (5.25)

$$(\frac{T}{T_s} + 1)y = \frac{T}{T_s} y z^{-1} + Ku. \tag{5.25}$$

According to $y(k)z^{-1} = y(k-1)$ (k: the kth sample time), Eq. (5.25) is transformed to the discrete time norm by

$$y(k) = \frac{T}{T + T_s} y(k-1) + \frac{T_s K}{T + T_s} u(k). \tag{5.26}$$

In Eq. (5.26), T and K are the only parameters to be defined for describing the first order model. It can be regarded as a nonlinear model when the set of parameters K and T varies as $u(k)$ does change. This is exactly what the mathematic model of the dynamic characteristics of CR response to exercise is. The relationships between the transient parameters (K and T) and $u(k)$ relating to SVR results can be found in section 4.4.

5.3.2 Switching control method

If a control system has two or more than two processes, switching control would be one of approaches commonly used in the multiply model control field. The switching control for discrete time models increases the control accuracy, lowers the system consumption

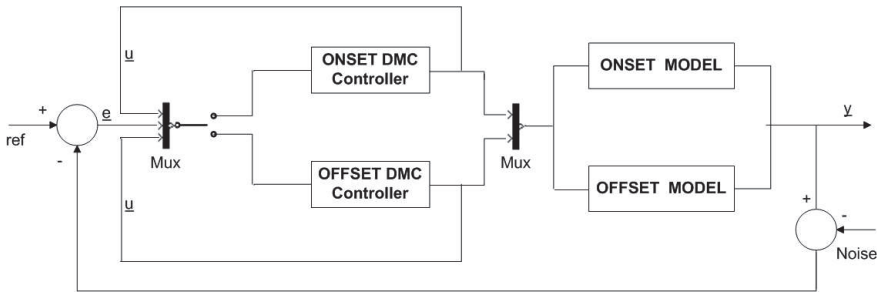

Fig. 5.4: Block Diagram for Double Model Predictive Switching Control System.

and raises the efficiency of control processing. Nevertheless, it also issues the risk on system robustness, because of the existing gap between models.

By the analysis of the previous experiment results in section 4.4, there are two nonlinear time invariant models being introduced for dynamic characteristics of HR response at onset and offset of exercises. Certainly, two unique DMC controllers also are established, each computing their own control actions. Although two models plus two controllers are employed in this work, the approach can easily be extended to include as many local models and controllers as the practitioner would like, seen as Fig. 5.4.

If $\triangle R(k) = R(k) - R(k-1)$ is the set point change, $\triangle u(k) = u(k) - u(k-1)$ is the input change of designed controller at kth sample time, u_{onset} is controller output for onset of exercises, u_{offset} is controller output for offset of exercise, y_{onset} is measured output of the process for onset of exercise and y_{offset} is measured output of the process for offset of exercise, then

If $\triangle R(k) > 0$ then

$$u_{meas} = u_{onset}, \tag{3.27a}$$

And if $\triangle u(k) > 0$

$$y_{meas} = y_{onset}, \tag{3.27b}$$

Otherwise

$$y_{meas} = y_{offset}, \tag{3.27c}$$

If $\triangle R(k) = 0$

And if $\triangle u(k) > 0$

$$u_{meas} = u_{onset}, \tag{3.28a}$$

$$y_{meas} = y_{onset}, \tag{3.28b}$$

Otherwise

$$u_{meas} = u_{offset}, \tag{3.28c}$$

$$y_{meas} = y_{offset}, \tag{3.28d}$$

If $\triangle R(k) < 0$ then

$$u_{meas} = u_{offset}, \tag{3.29a}$$

And if $\triangle u(k) > 0$

$$y_{meas} = y_{onset}, \tag{3.29b}$$

Otherwise

$$y_{meas} = y_{offset}, \tag{3.29c}$$

In this point of view, y_{meas} is the actual measured output of the control system and u_{meas} is the actual controller output after which controller is being selected by the above conditions. It should be mentioned that in the simulation stage the constraints for $u(k)$ and $e(k)$ have not been involved, which will be studies in the experiment validation stage.

5.3.3 Demonstration of tuned DMC parameters for control system of cardiorespiratory responses to exercise

The parameters consisting of the sample time (T_s), prediction horizon (P), moving horizon (M), model horizon (N), move suppression coefficient (λ), peak value of the reference profile (R_p) and number of samples (S) seen as Table 5.2, were tuned only based on the authors' experience and simulation results, which may vary at the experiment validation stage.

Table 5.2: Tuning Parameters for DMC Control System of Cardio-respiratory Response to Exercise.

	Controller for Onset Stage	Controller for Offset Stage
P	30	30
M	10	10
N	180	250
λ	300	3000
S	900	
R_p	30	
T_s	2	

According to previous studies in section 4.4, the range of a normal measured HR step response signal is approximately from 100 *btm* to 140 *btm*. Therefore, the reference scale (R_p) are kept around 30 as an expected value.

Due to its nonlinearity of this study, the DMC parameters usually are set by combination of practical training and theoretical philosophies. For example, in order to find a best value for the move suppression coefficient (λ), a test is carried out that employs 21 sets of steady state gain (K) and time constant (T) in terms of the SVR simulation results in section 4.4. These 21 different experiment data can be simply treated as 21 linear models. The method of practical training tends to tailor these linear models with a possible best value and evaluate them to find the final λ for nonlinear DMC controllers. The tuned values of for DMC onset and offset controllers through 21 sets of test data

Table 5.3: Tuning model horizon (N) for HR response at onset and offset of exercise.

Input (u)	Model Horizon (N) at Onset	Model Horizon (N) at Offset
1	30	166
2	43	145
3	113	251
4	179	367

analysis respectively amount to 300 and 3000.

The sample time (T_s) is set as 2 seconds based on the general heartbeat rate of human beings. The experiment period is about 30 minutes except 10 minutes for warm-up at the beginning of exercise. Hence, the number of samples (S) is 900. Considering about the larger T_s and S, prediction horizon (P) and moving horizon (M) are modulated to 30 and 10 severally. In addition, the tuned parameters T_s and N improve the system response time so as to the control effect can match with the sample time moves.

Model horizon (N) also needs to be tuned in order to reduce the system's computational time and enhance efficiency of DMC controller. In particular, N is defined as a dynamic array to keep storing and shifting the values of steady-state responses of the process until it stays at level. If the length of N is too long, it would be redundant. To cut the length of N for each controller, an experiment was performed where the two machine learning based nonlinear model for HR response to exercise were tested to get their own unit step response data respectively when input $u = 1$,$u = 2$,$u = 3$ and $u = 4$. The experiment data in Table 5.3 shows N for DMC onset controller is 180 and for DMC offset controller 250 is estimated.

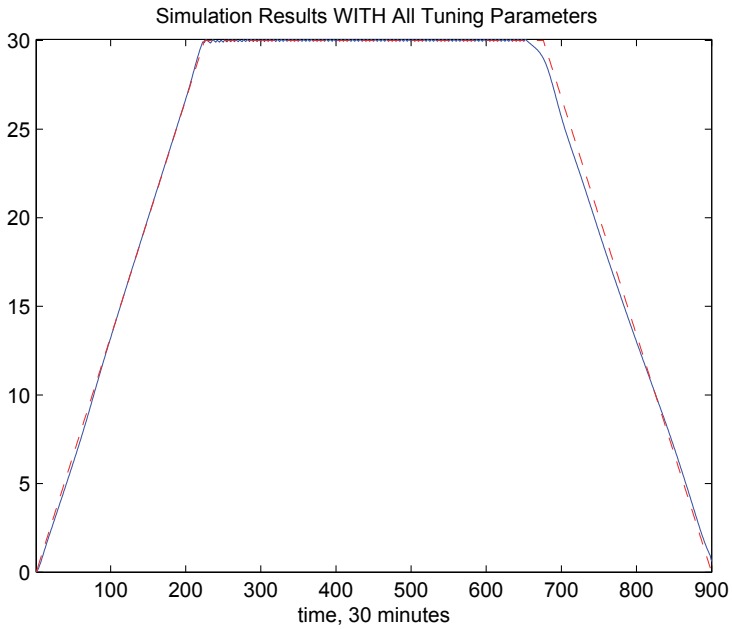

Fig. 5.5: Simulation results for machine learning based double nonlinear model predictive switching control for CR response to exercise with all tuning parameters (I).

5.3.4 Simulation

5.3.4.1 Simulation for double nonlinear model predictive switching control of cardiorespiratory responses to exercise

The simulation results for machine learning based double nonlinear model predictive switching control for CR response to exercise is demonstrated in Fig. 5.5 and Fig. 5.6. Based on these figures, the results are sound, even if a randomly disturbance is added into DMC controllers (see Figure 5.6), which also can efficiently avoid the distortion. In the experiment results, these complex nonlinear behaviors have been qualitatively optimized with high accuracy by using the double model predictive switching control approach.

On the other hand, switching control brings the slight oscillations at middle stage, seen as Fig. 5.7. As the amplitudes of these oscillations do not exceed the theoretical error

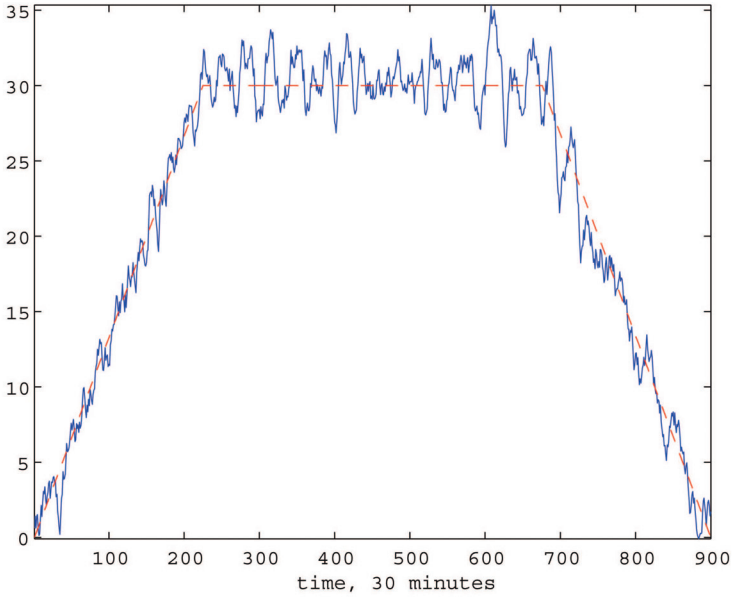

Fig. 5.6: Simulation results added noise for machine learning based double nonlinear model predictive switching control for CR response to exercise with all tuning parameters.

range ($\sigma \leq 5\%$), it should not be emphasize too much for the simulation work.

5.3.4.2 Experiment for a single nonlinear model control of cardiorespiratory responses to exercise

To visibly demonstrate the advantages of modeling the HR response at onset and offset of exercises separately, a comparative experiment for single Onset (Fig. 5.8) or Offset (Fig. 5.9) Nonlinear Model Predictive Control by Using SVR, are presented. The single onset nonlinear model control strategy (see Fig. 5.8) has a failed simulation result due to the bad performance at offset stage. Similar with the single offset one, it is regulated well at end but lose its control at beginning. This comparative experiment validated the necessity of the design of double models and the relevant regulations.

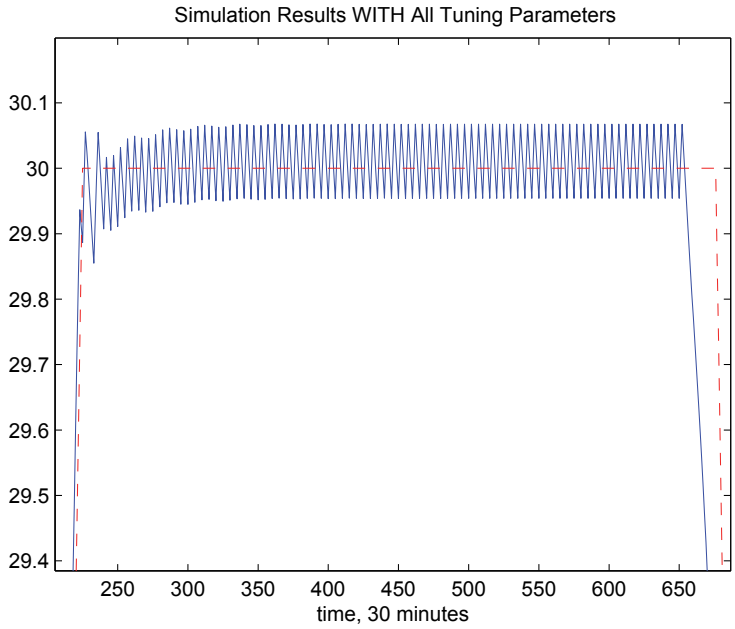

Fig. 5.7: Simulation results for machine learning based double nonlinear model predictive switching control for CR response to exercise with all tuning parameters (II).

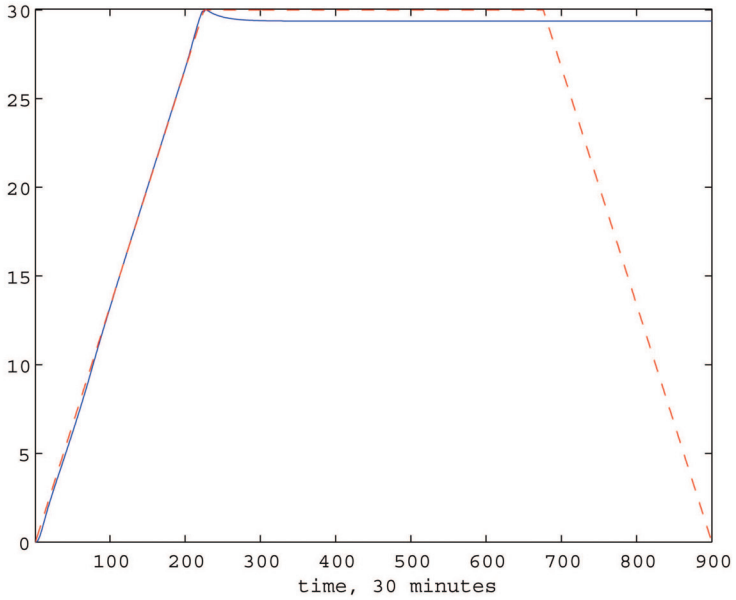

Fig. 5.8: Simulation results for machine learning based single onset nonlinear model predictive control.

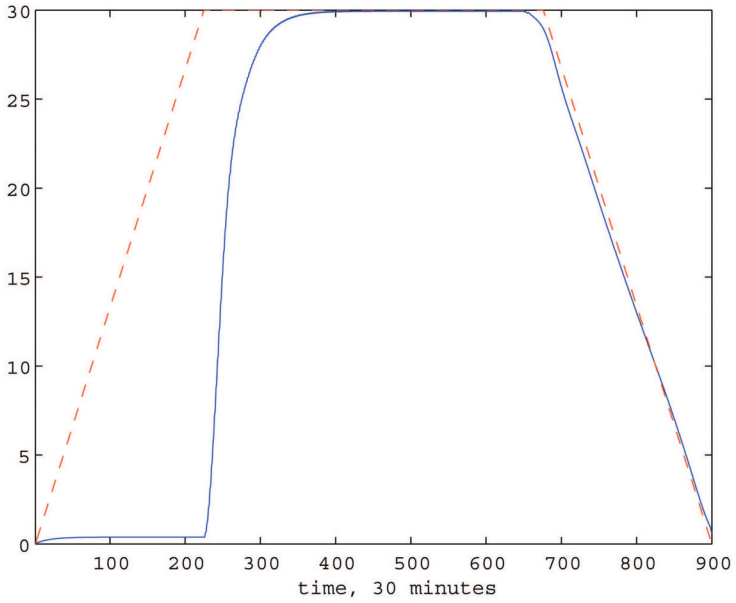

Fig. 5.9: Simulation results for machine learning based single offset nonlinear model predictive control.

5.4 Conclusion

In this study, a machine learning based nonlinear model predictive control for HR response to exercise is introduced.

As discussed in section 4.4, this nonlinear behavior of HR response to treadmill walking exercise can be effectively captured by using SVM regression. We investigated both steady state gain and the time constant under different walking speeds by using the data from an individual healthy middle aged male subject. The experiment results demonstrate that the time constant for recovery stage is longer than that at onset of exercise, which provide the essential to form double models method to describe the corresponding onset or offset of exercises.

Based on the established model, a novel switching model predictive control algorithm has been developed, which applied DMC algorithm to optimize the regulation of HR

responses at both onset and offset of exercises.

Simulation results indicate switching DMC controller can efficiently handle the different dynamic characteristics at onset and offset of exercise. However, it should be pointed out that the proposed approach, as most switching control strategy, also suffers from transient behavior during controller switching. For example, the simulation results in transition stage ($\triangle R = 0$, Fig. 5.7; Eq. (3.28a) , (3.28b), (3.28c) and (3.28d)) have slight oscillation due to the quick switching between two controllers. In the next step of this study, we will develop bump-less transfer controller to minimize the transient behavior and implement those methodologies in the real time control of HR response during treadmill exercises. In the future, the experiment validation of the SVM based nonlinear MPC control algorithm for HR response to exercise will be continuously explored.

Chapter 6

Multi-loop integral controllability analysis for nonlinear two-input single-output processes and its application to cardiorespiratory regulation for treadmill exercise

6.1 Introduction

One of the greatest public health challenges confronting many industrialized countries is the obesity epidemic. The safe, low-to-moderate intensity exercise, which is suitable for every fitness level (especially suitable for patients with existing chronic conditions such as diabetes, cardiovascular disease or arthritis), remains the healthiest and least risky way for losing weight [147] [3]. The development of automated exercise assisted equipments can greatly enhance the safety and reduce the requirement of supervision. For an automated treadmill system, and efficient method for exercise strength regulation is to stimulate exercisers' HR to follow a pre-designed HR profile. Paper [133] developed a non-switching, nonlinear anti-windup integral control for the long duration HR response to treadmill exercise; however, most studies [39] [100] [152] [155] consider only using one manipulate variable (treadmill speed or gradient) to regulate HR responses. In [80] [82], for exercise testing and rehabilitation of subjects with impaired exercise tolerance, ramp type protocols were proposed by simultaneously manipulating both speed

and gradient, which could produce a low initial metabolic rate that then increases the work rate linearly to reach the subject's limit of tolerance in approximately 10 minutes.

In [165], a multi-loop PID controller based HR tracking system has been presented which simultaneously tuned both treadmill speed and gradient in closed loop, and achieved good performance. However, in paper [165], it is assumed that the HR response to treadmill exercise is in a linear range, and only linear modeling and control approaches were presented. The advantages of using both speed and gradient to regulate HR are therefore only valid in a certain linear response range. The main purpose of this study is to theoretically analyze the advantage of using two manipulators in terms of nonlinearity near walking-running transition zone of treadmill exercise.

For most linear processes, the control of two correlated inputs and single output can be transferred as a SISO control problem by simply combining the two control inputs as one. However, in engineering practice, nonlinear systems with multiple control inputs are commonly encountered and sometimes it is not proper to combine them as a single input. Besides the process was investigated in this study, another example is the regulation of temperature of a container (such as a chemical reactor), which may apply multiple actuators (such as heaters and fans) to simultaneously control the temperature.

There are several advantages in practice for using multiple (redundant) actuators. Firstly, it can increase the non-saturation range. Real systems always have physical limitations and therefore have limited non-saturation range. If simultaneously execute multiple actuators, the output range can be extended. Secondly, it can increase the maximum gain of the actuator so that fast tracking or regulation of the manipulated variable can be achieved as shown experimentally in [165].

Furthermore, from reliability point of view, redundancy of actuators can facilitate fault accommodation for the implementation of fault tolerant control strategies. For the reg-

ulation of HR, multi-loop integral controllers were developed [165] in order to achieve zero steady state tracking error. For multi-loop integral control of square process, Skogestad and Morari [143] introduced the concept of DIC for evaluating the feasibility of a process to achieve Decentralized Unconditional Stability (DUS), a passive fault tolerant capability. DIC analysis [168] [30] [150] determines whether a multivariable plant can be stabilized by multi-loop controllers, whether the controller can have integral action to achieve offset free control, and whether the closed-loop system will remain stable when any subset of loops is detuned or taken out of service.

This study extended the DIC analysis for the nonlinear square process to this special non-square (a two-input single-output) process, and experimentally detected the HR range in which the MIC is valid/invalid. Simulation study is provided to show that simultaneous manipulating of treadmill speed and gradient can significantly improve the tracking performance near walking-running transition zone.

The organization of this chapter is as follows. Section 6.2 will define the MIC for a 2ISO nonlinear process, and present a sufficient MIC condition based on singular perturbation analysis [137] [88]. The MIC range as well as transition zone for HR tracking will be presented in this section as well. Section 6.3 concludes this chapter.

6.2 Multi-loop integral controllability

6.2.1 Multi-loop integral controllability analysis for HR response

In [165], multi-loop PID controller has been designed for the regulation of HR response to treadmill exercise. Based on the configuration in [165], we will introduce a definition of MIC for this special non-square process (2ISO), which is a direct extension of DIC

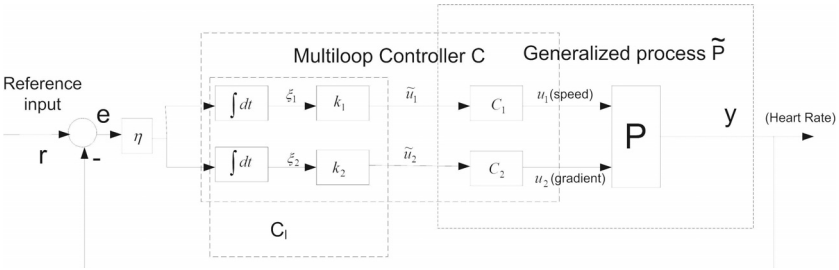

Fig. 6.1: MIC for a 2ISO system.

concept from square processes to non-square processes.

As shown in Fig. 6.1, we assume HR response can be described by the following nonlinear state variable equations with an input vector $u \in \mathcal{R}^2$ and an output vector $y \in \mathcal{R}^1$:

$$P \begin{cases} \dot{x} &= f(x,u) \quad x \in \mathcal{X} \subset \mathcal{R}^n, u \in \mathcal{U} \subset \mathcal{R}^2 \\ y &= g(x,u) \quad y \in \mathcal{Y} \subset \mathcal{R}^1. \end{cases} \tag{6.1}$$

It is assumed that the state $x(t)$ is uniquely determined by its initial value $x(0)$ and the input function $u(t)$. Another assumption made for convenience is that the system (6.1) has equilibrium at origin, that is, $f(0,0) = 0$, and $g(0,0) = 0$. If the equilibrium x_e is not at origin, a translation is needed by redefining the state x as $x - x_e$.

Definition 1 (Multi-loop integral controllability (MIC) for nonlinear 2ISO processes) Consider the closed loop system depicted in Fig. 6.1.

(i). For the nonlinear process P described by Eq. 6.1, if there exists a multi-loop integral controller C, such that the unforced closed loop system ($r = 0$) is Globally Asymptotically Stable (GAS) for the equilibrium $x = 0$.

(ii) Assume each individual loop is detuned independently by a factor k_i ($0 \leq k_i \leq 1$, $i = 1, 2$), and for each pair of multi-loop gain $\{k_1, k_2\}$ the closed loop system is still Asymptotically Stable (AS) for an equilibrium $\tilde{x}_e$ (not necessarily $\tilde{x}_e = x = 0$), then the nonlinear process P is said to be Multi-loop Integral Controllable.

The stability with detuning factor $\{k_1, k_2\}$ for the square process is the so-called 'decentralized unconditional stability' [155]. A closed-loop system which is decentralized unconditionally stable allows the gains of each controller subsystem to be modified independently by a factor in the range [0, 1] [155].

It should be noted that for the non-square process under multi-loop integral control the equilibrium varies when the ratio of the detuning factor k_1 and k_2 is changed, which is different with the decentralized integral control for the square process.

In Fig. 6.1, we assume the state equation of the general process $\tilde{P}$ (which includes original process P and the two scalar non-integral controllers c_1 and c_2) is modeled as below (with the same assumptions for process P in Eq. 6.1).

$$\tilde{P}: \begin{cases} \dot{x} &= f(x, \tilde{u}) \\ y &= g(x, \tilde{u}). \end{cases} \tag{6.2}$$

The state equation for the linear integral controller can be expressed as:

$$C_l: \begin{cases} \dot{\xi} = \begin{bmatrix} \dot{\xi}_1 \\ \dot{\xi}_2 \end{bmatrix} = \eta \begin{bmatrix} k_1 \\ k_2 \end{bmatrix} e = -\eta \begin{bmatrix} k_1 \\ k_2 \end{bmatrix} y \\ \tilde{u} = \xi. \end{cases} \tag{6.3}$$

In this paper, we assume the initial conditions of the two integrators in Fig. 6.1 are zero. Then, it is easy to see that the above equation can be simplified as follows:

$$C_l: \begin{cases} \dot{\xi} = -\eta y = \eta e \\ \tilde{u} = [\tilde{u}_1 \ \tilde{u}_2]^T = [k_1 \ k_2]^T \xi. \end{cases} \tag{6.4}$$

Theorem 1 (Sufficient steady-state MIC conditions for nonlinear 2ISO processes)

Consider the closed loop system in Fig. 6.1, and assume that the general process $\tilde{P}$ and the linear part of the controller C_l are described by Eq. 6.2 and Eq. 6.4 respectively. If the following assumptions are satisfied:

(i) The equation $0 = f(x, \tilde{u})$ obtained by setting $\dot{x} = 0$ in Eq. 6.2 implicitly defines a unique C^2 function $x = h(\tilde{u})$ for $\tilde{u} \in \tilde{\mathcal{U}} \subset \mathcal{R}^2$;

(ii) For any fixed $\tilde{u} \in \tilde{\mathcal{U}} \subset \mathcal{R}^2$, the equilibrium $x = h(\tilde{u})$ of the system $\dot{x} = f(x, \tilde{u})$ is Globally Asymptotically Stable (GAS) and Locally Exponentially Stable (LES);

(iii) Denote $\tilde{u} = [\tilde{u}_1 \ \tilde{u}_2]^T = [k_1\xi \quad k_2\xi]^T$, and suppose the steady-state input output function of the general process $\tilde{P}$ can be factorized as $g(h(\tilde{u}), \tilde{u}) = \psi(\tilde{u})(\tilde{u}_1 - \phi(\tilde{u}_2))$. Assume $\phi(\tilde{u}_2)$ is a unique C^2 function with $\frac{\partial \phi(\tilde{u}_2)}{\partial \tilde{u}_2} \leq \mu < 0$, and $\psi(\tilde{u}) \neq 0$ when $\tilde{u} \in \tilde{\mathcal{U}} \subset \mathcal{R}^2$;

Further assume

$k_1 \frac{\partial g(h(\tilde{u}),\tilde{u})}{\partial \tilde{u}_1} + k_2 \frac{\partial g(h(\tilde{u}),\tilde{u})}{\partial \tilde{u}_2} > \rho > 0$ (for some scalar $\rho > 0$) for in a neighborhood of $\tilde{u} = 0$,

then there exists $\eta > 0$, such that the equilibriums (under different k_1 and k_2) are GAS. That is, if the two scalar controllers $c_1$and $c_2$can be found such that the generalized process $\tilde{P}$ can satisfy Conditions i), ii) and iii), then the nonlinear 2ISO process is MIC.

Proof: We prove this theorem based on singular perturbation theory [137][88].
Consider the system of Fig. 6.1 described by Eq. 6.2 and Eq. 6.4. In order to analyse the Lyapunov stability of the unforced closed loop $(\tilde{P}, -C_l)$, the input signal r is set to zero. The state equation for the closed loop $(\tilde{P}, -C_l)$ can be expressed as:

$$(\tilde{P}, -C_l): \quad \begin{cases} \dot{x} &= f(x, [k_1\xi, k_2\xi]^T) \\ \dot{\xi} &= \eta\, e = -\eta\, y = -\eta\, g(x, \xi). \end{cases} \tag{6.5}$$

Equation 6.5 can be transformed into a standard singular perturbation form [137]: Let $\tau = \eta(t - t_0)$, so that $\tau = 0$ at $t = t_0$. As $\frac{d\tau}{dt} = \eta$, we have:

$$(\tilde{P}, -C_l): \quad \begin{cases} \eta \frac{d}{d\tau} x &= f(x, [k_1\xi, k_2\xi]^T) \\ \frac{d}{d\tau}\xi &= -g(x, \xi). \end{cases} \tag{6.6}$$

In order to be consistent with standard singular perturbation notation, we will for the moment use the notation $\dot{x}$ to denote the derivative on the *slow* time scale τ when we analyse singular perturbation models.

Now, for the standard singular perturbation model (see Eq. 6.6), based on Condition a) and b), the verification of the following two conditions (the first two conditions of Theorem 3.18 in [137]) is straightforward:

(i) The equation $0 = f(x, \xi)$ obtained by setting $\eta = 0$ in Eq. 6.6 implicitly defines a unique C^2 function $x = h(\xi)$.

(ii) For any fixed $\xi \in \mathcal{R}^m$, the equilibrium $x_e = h(\xi)$ of the subsystem $\dot{x} = f(x, \xi)$ is Globally Asymptotically Stable (GAS) [137] and Locally Exponentially Stable (LES).

We only need to prove Conclusion (iii) of Theorem 3.18 in [137], the stability (GAS and LES) of "slow time scale". That is, the following conclusion needs to be proved:

(iii) The equilibrium $\xi = 0$ of the reduced model (slow time scale) $\dot{\xi} = -g(h(\tilde{u}), \tilde{u})$ is GAS and LES. Where $\tilde{u} = [k_1\xi \quad k_2\xi]^T$.

To prove GAS, we select $V(\xi) = \frac{1}{2}(\tilde{u}_1 - \phi(\tilde{u}_2))^2 = \frac{1}{2}(k_1\xi - \phi(k_2\xi))^2$ as a Lyapunov function candidate for the "slow time scale" system. It can be seen that

$$\begin{aligned} \dot{V}(\xi) &= (\tilde{u}_1 - \phi(\tilde{u}_2)) \cdot (k_1 - k_2 \tfrac{\partial}{\partial \tilde{u}_2}\phi(\tilde{u}_2))(-g(h(\tilde{u}), \tilde{u})) \\ &= -\psi(\tilde{u})(\tilde{u}_1 - \phi(\tilde{u}_2))^2 \cdot (k_1 - k_2 \tfrac{\partial}{\partial \tilde{u}_2}\phi(\tilde{u}_2)) \end{aligned} \tag{6.7}$$

As $\psi(\tilde{u}) \neq 0$ when $\tilde{u} \in \tilde{\mathcal{U}} \subset \mathcal{R}^2$, it will be either **always** positive or negative:

1. When $\psi(\tilde{u})$ is positive and $\xi \neq 0$, it is easy to see that $\dot{V}(\xi) < 0$ as $(k_1 - k_2 \frac{\partial}{\partial \tilde{u}_2}\phi(\tilde{u}_2)) > 0$.

2. When $\psi(\tilde{u})$ is negative, we can change the sign of the general process $\tilde{P}$ by simply changing the sign of the two scalar non-integral controllers c_1 and c_2 simultaneously. Then, the steady state function $g(h(\tilde{u}), \tilde{u})$ becomes $-g(h(\tilde{u}), \tilde{u})$. Thus, when $\xi \neq 0$

$$\begin{aligned}\dot{V}(\xi) &= (\tilde{u}_1 - \phi(\tilde{u}_2)) \cdot (k_1 - k_2 \tfrac{\partial}{\partial \tilde{u}_2}\phi(\tilde{u}_2))(g(h(\tilde{u}), \tilde{u})) \\ &= \psi(\tilde{u})(\tilde{u}_1 - \phi(\tilde{u}_2))^2 \cdot (k_1 - k_2 \tfrac{\partial}{\partial \tilde{u}_2}\phi(\tilde{u}_2)) < 0.\end{aligned}$$

This ensures the 'slow time scale' system is GAS.

To prove Locally Exponential Stability (LES), we simply select $V_L(\xi) = \frac{1}{2}\xi^2$ as a Lyapunov function candidate for the 'slow time scale'. It can be seen that

$$\dot{V}_L(\xi) = -\xi\, g(h(\tilde{u}), \tilde{u}). \tag{6.8}$$

It is easy to check both $V_L(\xi)$and $\dot{V}_L(\xi)$ will satisfy the requirements for LES given that $k_1 \frac{\partial g(h(\tilde{u}),\tilde{u})}{\partial \tilde{u}_1} + k_2 \frac{\partial g(h(\tilde{u}),\tilde{u})}{\partial \tilde{u}_2} > \rho > 0$ for some scalar $\rho > 0$ in a neighborhood of $\tilde{u} = 0$. Specifically, for $\dot{V}_L(\xi)$, in a neighborhood of $u' = 0$

$$\dot{V}_L(\xi) = -\xi\, g(h(\tilde{u}), \tilde{u}) \approx -[k_1 \frac{\partial g(h(\tilde{u}), \tilde{u})}{\partial \tilde{u}_1} + k_2 \frac{\partial g(h(\tilde{u}), \tilde{u})}{\partial \tilde{u}_2}]\xi^2.$$

Now, we consider two cases again:

1. For $\psi(\tilde{u}) > 0$ ($\psi(0) = q_1 > 0$) and $\xi \neq 0$, in a neighborhood of $\tilde{u} = 0$, we have

$$\begin{aligned}\dot{V}_L(\xi) &= -\xi\, g(h(\tilde{u}), \tilde{u}) = -\psi(\tilde{u})(\tilde{u}_1 - \phi(\tilde{u}_2))\xi \\ &\approx\ -\psi(0) \cdot (k_1 - k_2 \tfrac{\partial}{\partial \tilde{u}_2}\phi(\tilde{u}_2))\xi^2 < -\rho_{l1}\xi^2,\end{aligned}$$

   where ρ_{l1} is a positive scalar.

2. For $\psi(\tilde{u}) < 0$ ($\psi(0) = q_2 < 0$), the sign of the general process $\tilde{P}$ has been changed by changing the sign of the two scalar non-integral controllers c_1 and c_2 simultaneously. Then, in a neighborhood of $\tilde{u} = 0$, we have:

$$\dot{V}_L(\xi)\ \approx\ \psi(0) \cdot (k_1 - k_2 \frac{\partial}{\partial \tilde{u}_2}\phi(\tilde{u}_2))\xi^2 < -\rho_{l2}\xi^2,$$

   where ρ_{l2} is a positive scalar.

Based on Definition 1, we can easily check that a necessary MIC condition for a 2ISO process is each single loop, a SISO system whose input is one of the inputs and output is the single output (with the other input fixed), is DIC respectively. For the HR regulation, the necessary condition is the speed-HR and gradient-HR loops are DIC respectively.

A sufficient DIC condition for a SISO system is its monotone increasing (or monotone decreasing) in steady state. It is easy to see the monotone increasing conditions for each loop (i.e. $\varepsilon_{imax} \geq \frac{\partial}{\partial \tilde{u}_i} g(\tilde{u}_1, \tilde{u}_2) \geq \varepsilon_{imin} > 0,\ i = 1,\ 2$) are sufficient to ensure $0 > -\varepsilon \geq \frac{\partial}{\partial \tilde{u}_2}\phi(\tilde{u}_2)$. In fact, from Condition iii) in Theorem 1, we can conclude that for the steady-state input output function of the general process $\tilde{P}$, $g(h(\tilde{u}), \tilde{u}) = 0$ implies that $\tilde{u}_1 = \phi(\tilde{u}_2)$. Then, we have $g(h(\phi(\tilde{u}_2), \tilde{u}_2)) = 0$. Thus, $[\frac{\partial g}{\partial \tilde{u}_1}\frac{\partial \phi}{\partial \tilde{u}_2}k_2 + \frac{\partial g}{\partial \tilde{u}_2}k_2]\xi = 0$, and $\frac{\partial \phi}{\partial \tilde{u}_2} = -\frac{\partial g}{\partial \tilde{u}_2} / \frac{\partial g}{\partial \tilde{u}_1}$. Considering that $\varepsilon_{imax} \geq \frac{\partial}{\partial \tilde{u}_i} g(\tilde{u}_1, \tilde{u}_2) \geq \varepsilon_{imin} > 0,\ i = 1,\ 2$, we have $0 > -\frac{\varepsilon_{2min}}{\varepsilon_{1max}} \geq \frac{\partial}{\partial \tilde{u}_2}\phi(\tilde{u}_2) \geq -\frac{\varepsilon_{2max}}{\varepsilon_{1min}}$.

For either purely walking (or purely running), it is not hard to see that the monotone increasing of speed or gradient respectively will lead to the monotone increasing in HR, i.e., each single loop is DIC in either walking zone or running zone. In [165], it is experimentally proved that in walking zone simultaneous manipulating both speed and gradient can achieve fast HR tracking.

However, due to the different motor patterns [32] of walking and running, HR response in walking/running transition zone would be non-monotone. In the following part, experiments are designed and implemented to investigate the heart rate response to walking and running around transition speed.

6.2.2 Experiments

In order to collect the HR data while walking or running on the treadmill, a portable and efficient device the Alive Heart Monitor (HM131), manufactured by Alive Technologies Pty Ltd, was used. This device is equipped with a HR sensor and a triaxial accelerometer. The ECG and accelerometer data is collected at a rate of 300 samples/sec and 75 samples/sec respectively. Data is transmitted in real time over a Bluetooth SPP connection. Data acquisition system was designed and implemented in the National Instrument LabVIEW 8.6, which provides easy synchronization and graphic user interface. The treadmill used in the experiment is powered by a DC motor and the controlled via the RS232 protocol using a serial port.

The physical characteristics of all three participants are presented in Table 6.1. The experiment scenario is shown in Fig. 6.2.

All subjects were asked to exercise on a motor-controlled treadmill, and they all selected 7 km/hour as the speed for which both walking and running are possible. Then, subject was asked to walk for 5 minutes at 7 km/hour for a certain gradient and followed 7

Table 6.1: Subjects Characteristics.

Subject No.	Age (Year)	Height (cm)	Weight (Kg)
1	24	170	52
2	26	175	55
3	27	173	53
Mean ± STD	25.7 ± 1.5	172.7 ± 2.5	53.3 ± 1.5

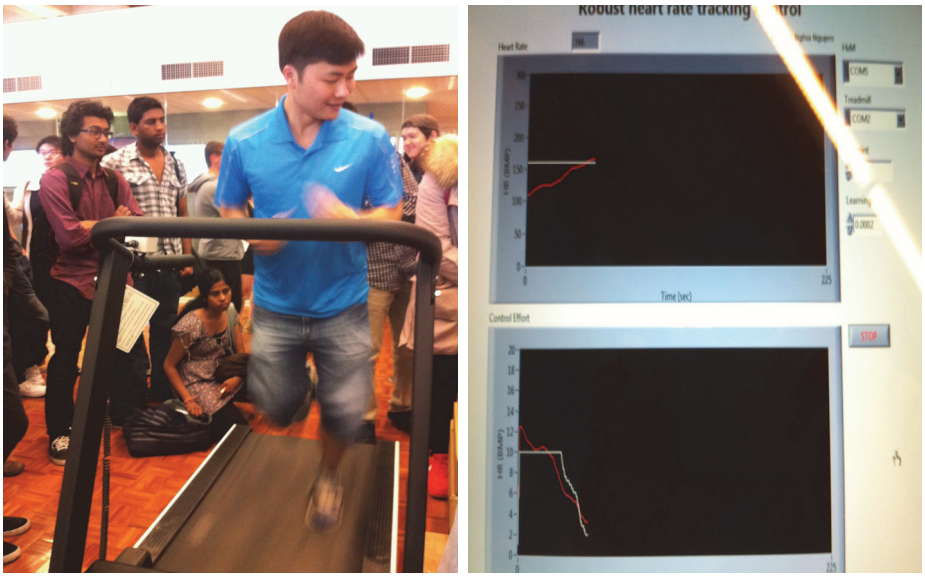

Fig. 6.2: The experiment environment.

minutes rest. This procedure was repeated for running as well as for different gradients. During experiments, HR response was recorded by the potable ECG monitor. The averaged steady state HR of the three subjects for both walking and running under different gradients is summarized in Table 6.2.

From Table 6.2, it can be seen that for a certain gradient, the HR for running is more than 15% higher than that for walking with speed 7 km/h. During exercise, the subjects may switch between walking and running when the treadmill speed is around 7 km/h. So, we find out, for example, when gradient is around 15 degree, the transition zone for HR is between 121 bpm and 144 bpm. When the reference HR is in the transition zone, simultaneous manipulation of speed and gradient would be beneficial as shown in the

Table 6.2: HR response at steady state.

Gradient (degree)	HR (bpm) Walking at 7 km/h	HR (bpm) Running at 7 km/h
0	102	125
15	121	144
25	137	171

following illustrative example by simulation.

6.2.3 Illustrative simulation study

Now, we provide simulation studies for the tracking of HR around transition zone. The reason why we use simulation rather than experiment is the fact that HR reflects not only the relative stress placed on the cardiopulmonary system due to activity, but it can also be elevated by emotional stress [153]. In the experimental condition, it is rather difficult to well control emotional stress of the exercisers around transition zone. On the other hand, in the simulation study, the irrelevant stimuluses of HR can be totally removed so that we can see the transition effects during HR tracking more clearly.

First, we discuss the model of HR response to treadmill exercises which will be used in the following simulation studies. In the control of HR, paper [3] assumed the HR response (vs. treadmill speed) can be described by a SISO Hammerstein model, i.e., a static nonlinear function followed by a linear dynamic system. In this study, both treadmill speed and gradient have been applied as control inputs. As shown in [80], for different speed $v(t)$ and gradient $\theta(t)$, external exercise work rate on treadmill can be simply quantified as: $p(t) = mgv(t)\sin(\theta(t))$.

Therefore, the two control inputs (speed and gradient) together only manipulate one control input variable, external exercise work rate $p(t)$. In order to simplify the analysis of HR response to treadmill exercise, similarly we depict this 2ISO system as a special

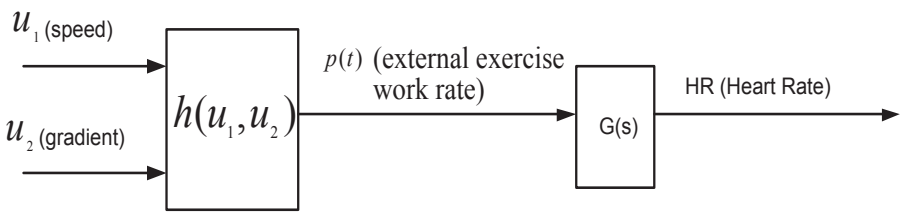

Fig. 6.3: The 2ISO Hammerstein system.

Hammerstein model as shown in Fig. 6.3. In Fig. 6.3, the linear dynamic part can be modeled as a first order SISO process [165] [155]: $G(s) = \frac{k}{Ts+1}$, with time constant $T = 35$ sec and steady state gain $k = 1$ as presented in [155].

For purely walking or purely running exercises, according to $p(t) = mgv(t)\sin(\theta(t))$, the static nonlinearity $g(\tilde{u}_1, \tilde{u}_2)$ can be approximately modeled as $p(\tilde{u}_1, \tilde{u}_2) = k_h \tilde{u}_1 \sin(\tilde{u}_2) + p_0$, where p_0 is the resting energy expenditure rate. Near the transition zone, it will be much complicated. In order to simplify the simulation, we consider the following simple function: $p(\tilde{u}_1, \tilde{u}_2) = p(v, \alpha) = \kappa \cdot [av^3 + bv^2 + cv][\sin(\alpha) + \eta]$, where $\kappa = 0.3487$, $a = 21.3221$, $b = -3.0516$, $c = 0.1453$, and $\eta = 0.75$. When the gradient is fixed as 15 deg ($\alpha = 15$ deg) and assuming the resting HR is 75 bpm, the steady state relationship between treadmill speed and HR is plotted in Fig. 6.4.

It should be clarified the parameters of the static nonlinearity presented above is not identified based on experimental data. To achieve a more accurate model of static nonlinearity which includes the walking/running transition, extensive experimental data together with sophisticated modeling methods are need. In this study, our focus is not the modeling of HR response. We investigate the control approach which will handle HR tracking around walking/running zone. Therefore, we constructed a third order polynomial to describe the fluctuation of HR due to the transition of running and walking. During simulation, we added random noisy ($\sigma = 0.8$ bpm) to the HR sensor.

As it can be easily checked that $g(h(\tilde{u}), \tilde{u}) = p(\tilde{u}_1, \tilde{u}_2) = p(v, \alpha) = \kappa \cdot [av^3 + bv^2 +$

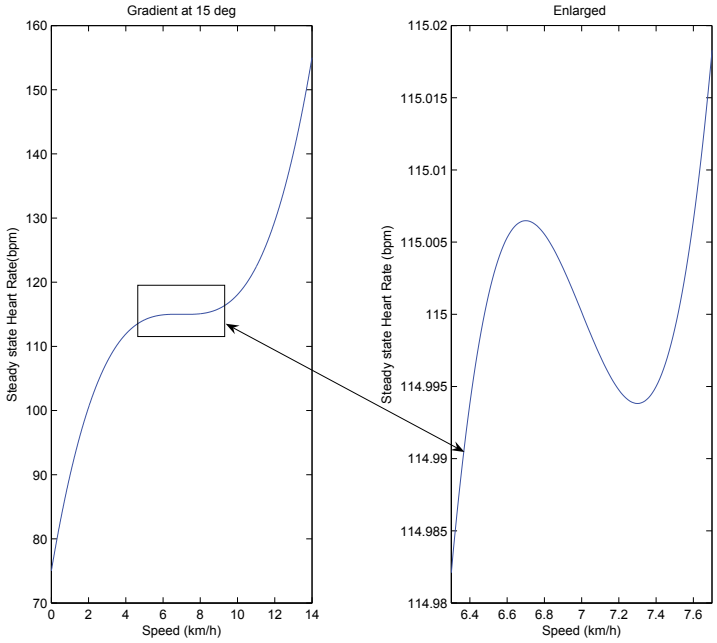

Fig. 6.4: Steady state response of HR.

$cv][\sin(\alpha) + \eta]$, when the HR reference is selected as r_0, and simply choose $\psi(\tilde{u}) = 1$ (see Theorem 1), then $\tilde{u}_1 = \phi(\tilde{u}_2)$ can be determined analytically or numerically. For the selected HR reference r_0 (115 bpm and 120 bpm), we numerically calculated the function $\tilde{u}_1 = \phi(\tilde{u}_2)$ for each reference HR respectively. As shown in Fig. 6.4, in the speed ranges (2 km/h $\sim$ 6.6 km/h) and (7.4 km/h $\sim$ 12 km/h), $\frac{\partial \phi(\tilde{u}_2)}{\partial \tilde{u}_2} < -\mu < 0$. However, in the speed range (6.6 km/h $\sim$ 7.4 km/h), the condition $\frac{\partial \phi(\tilde{u}_2)}{\partial \tilde{u}_2} < -\mu < 0$ is not valid.

The above Hammerstein model has been implemented by using MATLAB/Simulink. First, we fix treadmill gradient as $\alpha = 15$ deg, set the reference HR as 115 bpm, the initial speed as $v_0 = 6$ km/h, and select $\eta = 0.001$ and $k_1 = 0.5$ for the speed-HR loop integral controller. Fig. 6.6(a) shows the simulation result for which only speed has been manipulated. From Fig. 6.6(b) we can observe that although the regulated HR is quite close to reference HR, treadmill speed is swinging between 6.2 and 6.9 km/hour.

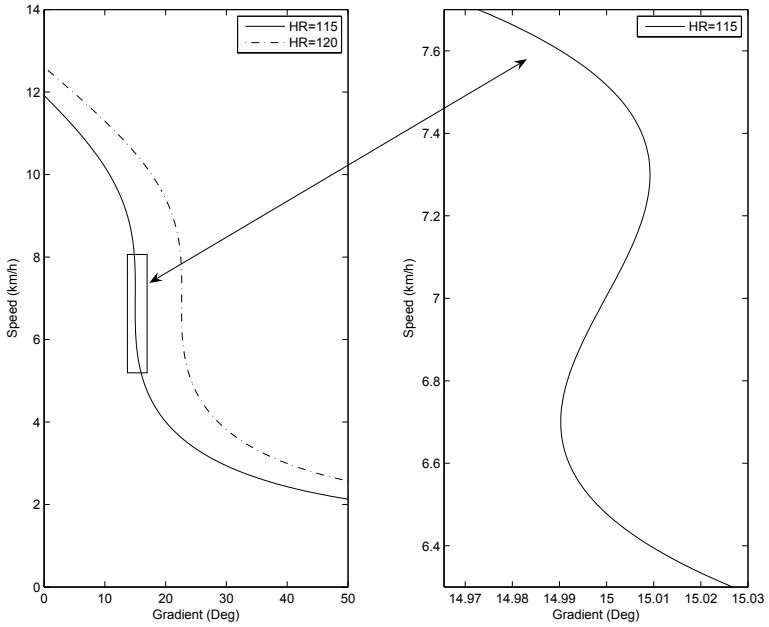

Fig. 6.5: The function $u_1' = \phi(u_2')$.

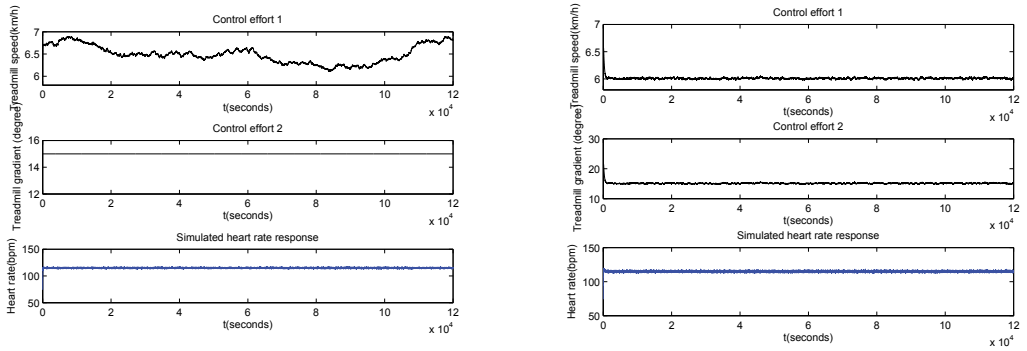

(a) Adjusting speed only (b) Adjusting both speed and gradient

Fig. 6.6: Simulation results.

It should also be noted that due to the closed loop system is multi-loop unconditional stable (MUS), the stability of closed loop system is guaranteed for any integral gains $k_1 \in [0, 1]$ and $k_2 \in [0, 1]$.

6.3 Conclusion

In order to analyze the advantage of using two manipulators in terms of nonlinearity existed near walking-running transition zone of treadmill exercises, a MIC analysis method for 2ISO processes was introduced. The proposed method extended the concept of nonlinear DIC to MISO nonlinear process, and presented a sufficient condition which only needs to check the steady state input-output relationship of under controlled processes. Based on the proposed condition, we investigate the new defined MIC for walking, running, and walking/running transition zones. Simulation study showed by simultaneously manipulating two control inputs, the automated control system can avoid the transition of motor patterns if the gains of the two multi-loop integral controllers are well tuned. Although the simulation work was sound enough, the experiment validation for simultaneously manipulating treadmill speed and gradient by using the proposed MIC analysis is also truly required in the future studies.

Chapter 7

Multi-loop integral controllability analysis for nonlinear multiple-input single-output processes

7.1 Introduction

Although various sophisticated control approaches have been developed, the most popular control strategy in engineering practice is perhaps still multi-loop integral control. Comparing with centralized control structure, the advantages of multi-loop control are its simplicity, effectiveness and potential for fault tolerance.

For multi-loop integral control of linear square process (the number of inputs and outputs is equal), Skogestad and Morari [143] introduced the concept of DIC. DIC analysis [30] [168] [150] investigates the possibility of a process to achieve decentralized unconditional stability [143], which determines whether a multivariable plant can be stabilized by multi-loop controllers, whether the controller can have integral action to achieve offset free control, and whether the closed-loop system will remain stable when any subset of loops is detuned or taken out of service.

Processes with more inputs than outputs occur commonly in engineering practice. This study extends the DIC analysis of nonlinear square processes [150] to a special non-square process, MISO processes, and presents a sufficient condition for the analysis of unconditional stability for nonlinear MISO processes.

MISO processes are met frequently in engineering practices, particularly in the topic of the monitoring and regulation of Human CR responses to exercise. For example, the regulation of CR responses to outdoor exercises, which may require multiple sensors (such as gas analyzer (CosmedÂ®), ECG, body temperature, tri-axial accelerometer, signals from a GPS, and micro-IMU) to simultaneously control the exercise intensity for improving the reliability of system.

The advantages of system having multiple inputs are evident. Firstly, real engineering processes always have physical limitations and therefore have limited non-saturation range. By simultaneously manipulating multiple inputs, the non-saturation range of the processes can be extended. Secondly, multiple inputs can increase the maximum gain of the actuator so that fast tracking can be achieved, which has been experimentally demonstrated in [165].

In engineering practice, MISO processes are often simplified as SISO systems by discarding some redundant control inputs. However, such simplification may greatly devalue the system as the discarded inputs have the potential to facilitate fault accommodation for fault tolerant control. In order to make fully use of the redundant control inputs, in this study, we extend the DIC analysis [143] [150] [168] to MISO processes, and presented an easy to use sufficient condition for MIC analysis. Based on this analysis, a practical multi-loop integral control design method is given, which can ensure offset free tracking under partial or complete failure of some actuators.

The organization of the chapter is as follows. In section 7.2 a definition of MIC is given, followed by a sufficient condition for the MISO process to achieve MIC. In section 7.3, the proposed approach is illustrated by using a real time temperature control system. Section 7.4 concludes the chapter.

7.2 Multi-loop integral controllability (MIC) and its sufficient conditions

We first introduce a definition of multi-loop integral controllability (MIC) for MISO processes. After that, we will provide sufficient MIC conditions for MISO processes, which can also be adapted to handle non-square processes with multiple outputs.

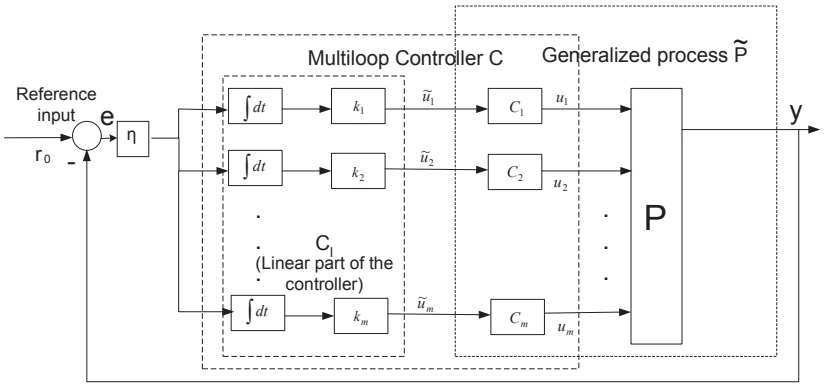

Fig. 7.1: MIC for a MISO system.

As shown in Fig. 7.1, assume the MISO system P can be described by the following equations with an input vector $u \in \mathcal{R}^m$ and a scalar output $y \in \mathcal{R}^1$:

$$P \begin{cases} \dot{x} &= f(x,u) \quad x \in \mathcal{X} \subset \mathcal{R}^n, u \in \mathcal{U} \subset \mathcal{R}^m \\ y &= g(x,u), \quad y \in \mathcal{Y} \subset \mathcal{R}^1, \end{cases} \tag{7.1}$$

It is assumed that the state $x(t)$ is uniquely determined by its initial value $x(0)$ and the input function $u(t)$. Under this assumption, in the following discussions, we further assume that the system (7.1) has equilibrium at origin, that is, $f(0,0) = 0$, and $g(0,0) = 0$. If the equilibrium x_e is not at origin, a translation can be performed by redefining the state x as $x - x_e$. In the following discussions, it is assumed such a translation has

been done whenever it is applicable.

In Fig. 7.1, the block η is a positive scalar, and the blocks $C_1, C_2, \cdots, C_m$ are all stable scalar controllers, which stand for the nonlinear part of the controller.

Definition 2 (Multi-loop Integral Controllability for nonlinear MISO processes) The nonlinear process P defined in Eq. (7.1) is said to be MIC with respect to a given reference $r = r_0$ if the closed loop system depicted in Fig. 7.1 satisfies the following conditions:

1. There exists a multi-loop integral controller C, such that the nominal closed loop system is Globally Asymptotically Stable (GAS) for the equilibrium $x = x_{e0}$ with respect to the given constant reference $r = r_0$.

2. When each individual loop is detuned independently by a factor k_i ($0 \leq k_i \leq 1$, $i = 1, 2, \cdots m$), for each set of fixed multi-loop gain $\{k_1, k_2, \cdots, k_m\}$ the closed loop system is Globally Asymptotically Stable (GAS) for an equilibrium $\tilde{x}_e$ (not necessarily $\tilde{x}_e = x_{e0}$).

Remark: In the above definition, the reference is a constant value r_0. For any other interested reference values, all statements should be valid for the new equilibrium with respect to the new reference. Different with DIC, for MIC, the equilibrium $\tilde{x}_e$ is not only determined by the reference input $r = r_0$. The ratio of detuning factors k_i ($0 \leq k_i \leq 1$, $i = 1, 2, \cdots m$) may also influence the equilibrium. We will discuss how the equilibrium $\tilde{x}_e$ can be calculated later.

In Fig. 7.1, we assume the state equation of the general process $\tilde{P}$ (which includes original process P and m stable scalar controllers $C_1, C_2, \cdots$, and C_m) is modeled as below (with the same assumptions for Eq. (7.1) of process P).

$$\tilde{P}: \begin{cases} \dot{x} &= f(x,\tilde{u}) \\ y &= g(x,\tilde{u}). \end{cases} \tag{7.2}$$

The state equation for the linear integral controller is expressed as:

$$C_l: \begin{cases} \dot{\varepsilon} = \begin{bmatrix} \dot{\varepsilon}_1 \\ \dot{\varepsilon}_2 \\ \vdots \\ \dot{\varepsilon}_m \end{bmatrix} = \eta e I_{m\times m} = -\eta y I_{m\times m} \\ \tilde{u} = diag\{[k_1, k_2, \cdots k_m]\}\varepsilon. \end{cases} \tag{7.3}$$

There are extensive research papers for DIC analysis. The reason that the MIC has not been explored may be due to its input multiplicity [88]. In order to cope with input multiplicity, we swap the bank of integrators with a single integrator in Fig. 7.1. That means, we use only one scalar variable (ξ) to take the role of all integral states (ε_i, $i = 1, 2, \cdots, m$) in Eq. (7.3) for the multi-loop controller.

If we assume the controller is with zero initial conditions (i.e. $\varepsilon_i(0^-) = 0, \quad i = 1,\ 2, \cdots m.$), Eq. (7.3) can be simplified as follows:

$$C_l: \begin{cases} \dot{\xi} = \eta\, e = -\eta\, y \\ \tilde{u} = \begin{bmatrix} k_1 \\ k_2 \\ \vdots \\ k_m \end{bmatrix} \xi. \end{cases} \tag{7.4}$$

The following theorem presented a sufficient condition for MIC for MISO processes:

Theorem 2 (Steady-state MIC conditions for nonlinear MISO processes)

Consider the closed loop system in Fig. 7.1, and assume that the general process $\tilde{P}$ and the linear part of the controller C_l are described by Eq. (7.2) and (7.4) respectively. If the following assumptions are satisfied:

a) The equation $0 = f(x, \tilde{u})$ obtained by setting $\dot{x} = 0$ in Eq. (7.2) implicitly defines a unique C^2 function $x = h(\tilde{u})$ for $\tilde{u} \in \tilde{\mathrm{U}} \subset \mathrm{R}^m$.

b) For any fixed $\tilde{u} \in \tilde{\mathrm{U}} \subset \mathrm{R}^m$, the equilibrium $x = h(\tilde{u})$ of the system $\dot{x} = f(x, \tilde{u})$ is Globally Asymptotically Stable (GAS) and Locally Exponentially Stable (LES).

c) When $\tilde{u} = [k_1\alpha \quad k_2\alpha \quad \cdots \quad k_m\alpha \ ]^T$ $(0 \leq k_i \leq 1,\ i = 1, 2, \cdots m)$, if the steady-state input output function $g(h(\tilde{u}), \tilde{u})$ (with respect to the reference input r_0) of the general process $\tilde{P}$ satisfies the following requirements:

$\alpha \cdot g(h(\tilde{u}), \tilde{u}) > 0$ (when $\alpha \neq 0$, and $\sum_{i=1}^{m} k_i \neq 0$)

and

$\alpha \cdot g(h(\tilde{u}), \tilde{u}) > \rho \cdot \alpha^2$ (when $\alpha \neq 0$, and $\sum_{i=1}^{m} k_i \neq 0$)

in a neighbourhood of $\alpha = 0$.

c') When $\tilde{u} = [k_1\alpha \quad k_2\alpha \quad \cdots \quad k_m\alpha \ ]^T$, if the steady-state input output function $g(h(\tilde{u}), \tilde{u})$ (with respect to its equilibrium point) of the general process $\tilde{P}$ satisfies the following requirements:

$k_1 \frac{\partial g(h(\tilde{u}),\tilde{u})}{\partial \tilde{u}_1} + k_2 \frac{\partial g(h(\tilde{u}),\tilde{u})}{\partial \tilde{u}_2} + \cdots + k_m \frac{\partial g(h(\tilde{u}),\tilde{u})}{\partial \tilde{u}_m} > 0$ (when $\alpha \neq 0$, and $\sum_{i=1}^{m} k_i \neq 0$)

and

$(k_1 \frac{\partial g(h(\tilde{u}),\tilde{u})}{\partial \tilde{u}_1} + k_2 \frac{\partial g(h(\tilde{u}),\tilde{u})}{\partial \tilde{u}_2} + \cdots + k_m \frac{\partial g(h(\tilde{u}),\tilde{u})}{\partial \tilde{u}_m}) > \rho > 0.$

Then there exists $\eta > 0$, such that the equilibriums are GAS. That is, if the scalar controllers c_1, c_2, and c_m can be found such that the generalized process $\tilde{P}$ can satisfy Conditions a), b) and c) or c'), then the nonlinear MISO process is MIC.

Proof The Proof of the above theorem (similar to that of Theorem 2 in [150]) is based on the singular perturbation theory [143]. By using singular perturbation theory, the overall dynamic system can be reduced as the integrator dynamics feedback with the steady state input-output mapping of the process. For details, see Appendix A.

Conditions a) and b) in Theorem 2, which require the stability of the open loop process, are easy to check even without the need of an explicit model of the processes. Condition c) is a sector condition with parameters k_i ($0 \leq k_i \leq 1$, $i = 1, 2, \cdots m$). If an explicit steady state model in the operation range cannot be obtained, Condition c) is not easy to be verified. Instead, we provide Condition c'), a sufficient condition of Condition c), which can be checked by experiments for real processes as this qualitative type condition does not need an explicit model to verify (see section 7.3). We present the following discussions for the proposed sufficient conditions in Theorem 2:

1. The proposed MIC conditions in Theorem 2 are only involved in steady state input-output function of the process. Models of the steady state behavior of processes are generally more accurate and readily available than are those of the transient [88]. Thus the proposed steady state sufficient condition is easy to use.

2. Similar to the sufficient condition for DIC of nonlinear square processes (see Condition iii) of Theorem 2 in [150]), both conditions c) and c') require the conditions of Local Exponentially Stable (LES) of the reduced model (slow time scale) around equilibrium point. Actually, the LES conditions are rather mild. For example, it is easy to check the following steady state input-output function: $g_1(h(\tilde{u}), \tilde{u}) = \tilde{u}_1^3 + \tilde{u}_1 + 5\tilde{u}_2^5 + 2\tilde{u}_2$ satisfies LES condition around $\tilde{u} = 0$. To see this, we only need check $\frac{\partial g(h(\tilde{u}),\tilde{u})}{\partial \tilde{u}_i} > \rho > 0$, for all $i = 1,\ 2,\ \cdots m$. (when $\alpha \neq 0$, and $\sum_{i=1}^{m} k_i \neq 0$) in a neighbourhood of $\alpha = 0$. It should be emphasized that although the function $g_2(h(\tilde{u}), \tilde{u}) = \tilde{u}_1^3 + 5\tilde{u}_2^5$ does not satisfy LES conditions in the planes

$\tilde{u}_1 = 0$ and $\tilde{u}_2 = 0$ (inflexion points), but it satisfies these conditions for any other points.

3. As Condition c') is a sufficient condition of c), some steady state functions satisfy Condition c) but may not satisfy Condition c') as shown in the following examples: $g_3(h(\tilde{u}), \tilde{u}) = \tilde{u}_1^3 + \frac{\sqrt{15}}{2}\tilde{u}_1^2 + \tilde{u}_1 + \tilde{u}_2^3 + 3\tilde{u}_2$ and $g_4(h(\tilde{u}), \tilde{u}) = \tilde{u}_1^3 + \tilde{u}_1^2\tilde{u}_2^3 + \tilde{u}_1 + \tilde{u}_2^3 + 3\tilde{u}_2$.

4. Although some functions cannot satisfy Condition c) or c') at all equilibriums, it can satisfy these conditions at some equilibriums. For example, $g_5(h(\tilde{u}), \tilde{u}) = \tilde{u}_1^2\tilde{u}_2^2$ cannot meet Condition c) and c') around zero, but it satisfies these conditions around the new equilibrium $[\tilde{u}_1, \tilde{u}_2]^T = [k_1\alpha_0, k_2\alpha_0]^T$(with $0 < c_0 < \alpha_0 < \infty$) in $\{(\tilde{u}_1, \tilde{u}_2) | \tilde{u}_1 \geq k_1 c_0 > 0, and\ \tilde{u}_2 \geq k_2 c_0 > 0\}$. As function $g_5(h(\tilde{u}), \tilde{u}) = \tilde{u}_1^2\tilde{u}_2^2$ can be rewritten as $\bar{g}_5(h(\tilde{u}), \tilde{u}) = (\tilde{u}_1 + k_1\alpha_0)^2(\tilde{u}_2 + k_2\alpha_0)^2 - k_1^2k_2^2\alpha_0^4$ by equilibrium translation, it is easy to check Condition c) and c') are valid around the new equilibrium.

All the above presented conditions and its discussions are around some specific equilibriums. For square processes, the equilibrium often can be determined by the reference input. For MISO processes, as discussed before, the equilibrium point for MISO systems is also influenced by the ratio of detuning factors k_i ($0 \leq k_i \leq 1$, $i = 1, 2, \cdots m$). We provide the following formulas to calculate the equilibrium:

1. Based on the reference input $r = ref$, we can calculate α_r by using the following equation:

$$g(h([k_1\alpha_r, \cdots, k_m\alpha_r]^T), [k_1\alpha_r, \cdots, k_m\alpha_r]^T) = ref \tag{7.5}$$

   (For simplicity, we assume there exists only one α_r in the interested range).

2. For the given detuning factors k_i ($0 \leq k_i \leq 1$, $i = 1, 2, \cdots m$), the equilibrium can

be calculated as follows:

$$x_e = h([k_1\alpha_r, \cdots, k_m\alpha_r]^T).$$

For the equilibrium x_e, if all the conditions in Theorem 1 are satisfied, the process is MIC for the reference input $r = ref$.

In Fig. 7.1, the initial conditions of all the integrators are assumed to be zero. If they are not zero, Eq. (7.5) needs to be adjusted as:

$$g(h([k_1(\alpha_r + \alpha_{10}), \cdots, k_m(\alpha_r + \alpha_{m0})]^T), \\ h([k_1(\alpha_r + \alpha_{10}), \cdots, k_m(\alpha_r + \alpha_{m0})]^T) = ref \quad (7.6)$$

where $\alpha_{10}, \cdots, \alpha_{m0}$ are the initial conditions of the integrators in Fig. 7.1.

It is easy to check that for stable linear systems all the conditions in Theorem 2 can be satisfied given that there are no zero items in the steady state input-output functions, and the equilibrium for linear system can be easily calculated. Assume a linear system is described by a state variable description$\{A, B, C, D\}$, then the equilibrium can be calculated in the following steps:

1. $G_0 = -CA^{-1}B + D$;
2. $\alpha_r = \{ref - G_0 \cdot diag([k_1, \cdots, k_m]) \cdot [\alpha_{10}, \cdots, \alpha_{m0}]^T\}/(G_0 \cdot [k_1, \cdots, k_m]^T)$;
3. $x_e = -A^{-1}B \cdot diag([k_1, \cdots, k_m]) \cdot \{[\alpha_{10}, \cdots, \alpha_{m0}]^T + \alpha_r\}$.

Now, based on Theorem 2, we discuss the advantages of using multiple inputs for the purpose of fault tolerant control. For square processes, the DIC condition actually can

guarantee offset free tracking under the faulty of loop gain decreasing. However, it cannot achieve offset free tracking when some of the actuators are totally out of order although closed loop stability is still maintained. For MIC MISO systems, when some of the actuators are totally out of order, if any other actuators are not fully failure broken then offset tracking is still ensured. Furthermore, even when some of the loop controller served as positive feedback (perhaps due to wrong connections), offset tracking as well as closed loop system stability can still be achieved given that the condition c) or c') is satisfied for a specific set of coefficients k_i, $i \in 1, 2, \cdots, m$.

7.3 Illustrative example

In this section, a pilot real time temperature control system, which has two actuators (a heater and a fan) and one output (the temperature of a sink), is introduced here for the simulation verification of the proposed method. It also should be pointed out that the RC modeling work proposed in Chapter 3 is not applicable because it is just a SISO model with switching, in which the treadmill speed is the only input.

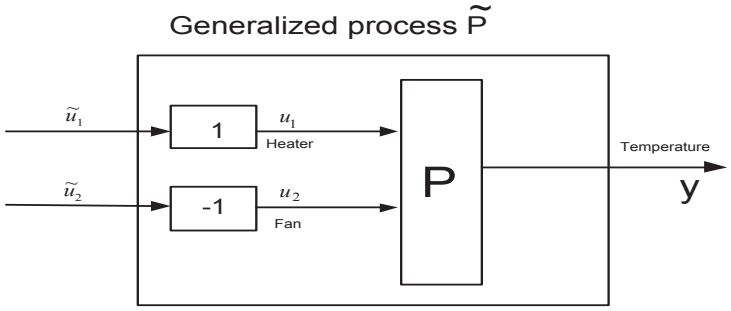

Fig. 7.2: Open loop block diagram of a pilot temperature control system.

We illustrated the proposed analysis approach by using a pilot real time temperature control system. This system has two actuators (a heater and a fan) for the control of the temperature of a sink. The output power of both heater and fan is adjusted by

tuning the duty cycles of two PWM generated by a PIC microcontroller (see Fig. 7.2). In Fig. 7.2, u_1 and u_2 are the incremental changes of duty cycles for heater and fan respectively, and y is the temperature of the sink.

For this two-input single output system, we actually need not to quantitatively identify the model for the verification of the sufficient Conditions a), b), and c') of MIC condition given in Theorem 2. Actually, for this real time system, we can easily derive that the steady state temperature of the sink will be a fixed value for two constant duty cycles if we assume no disturbances exists. This ensures that Condition a) is valid. Because the temperature of the sink is determined by the input powers of the heater and the fan, the open loop asymptotically stability is also evident. Furthermore, as the process is asymptotically stable, it is reasonable to assume the linearized dynamic system is strictly stable around equilibriums. That is the open loop process is LES around equilibriums. Thus, Condition b) is ensured.

Condition c') actually requires the incremental steady state gain from any one of the inputs to the single output is positive when the other input keeps a constant value in the interested working range.

In the interested temperature range (between 25 deg and 90 deg), it can be easily checked in steady state when the PWM duty cycle of heater increases, the temperature also increases incrementally if the power for the fan keeps constant. On the mean time, if the input power of the heater keeps a constant value, the increasing of the duty cycle of the fan will decrease of the temperature. If we design pre-compensators as $c_1 = 1$ and $c_2 = -1$ (see Fig. 7.2), then qualitatively we can see that the generalized process $\tilde{P}$ satisfies Conditions c'). Based on the above observations, we conclude that the system is MIC. Then, we can easily design a multi-loop PI controller for the generalized process.

The tuning of this multi-loop PI controller is quite simple as the generalized process is

MIC:

Initially select two small enough values for the two coefficients K_p and K_i for each loop so that the overall closed loop is stable. Then, gradually increase the values of the coefficients until desired tracking performance achieves. The overall real time control results are shown in Fig. 7.3.

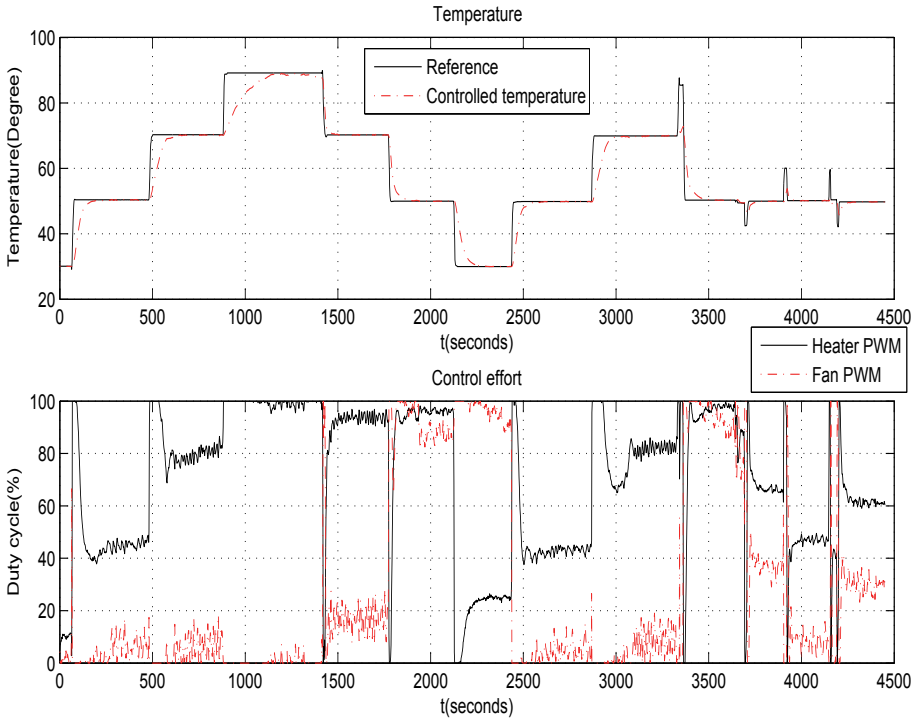

Fig. 7.3: Experimental results.

From Fig. 7.3 it can be seen that the overall tracking performance (from 30 degree to 90 degree) are satisfactory for both increasing and decreasing stages of the temperature. There are two interesting observations which should be emphasized:

If the heater is the only actuator of the system, the increasing of temperature is much faster than decreasing, which makes the process nonlinear (onset and offset of the process have different dynamics). From Fig. 7.3 we can see that the fan almost does not operate when the output temperature is tracking a high reference temperature, but nearly fully

operate when tracking a low reference temperature. The main functionality of the fan is the acceleration of the decreasing of temperature and thus compensating the nonlinear behavior of the process.

Another interesting phenomena showed in Fig. 7.3 is that for the same steady state temperature, the steady state duty cycles of fan and heater could be quite different, which is distinct with the control of square processes. Specifically, around 50 degree, after 3500 seconds, the duty cycles for heater and fan are (98% and 89%), (65% and 35%), (45% and 5%), and (60% and 25%) respectively when the detune factors k_i changed (we also deliberate generate some impulse style disturbances for the reference temperature) as well.

It should be pointed out as the provided MIC conditions can be verified qualitatively, throughout the design of this example, the explicit model of the process, which is often either difficult or time consuming to identify, does not need. After the verification of MIC, a simple but efficient multi-loop integral controller can be easily designed and tuned. We believe this practical approach will be useful in engineering practice.

7.4 Conclusion

This paper extends the concept of DIC analysis to MISO processes and presented easy to use sufficient conditions. A special phenomena for the multi-loop integral control of MISO processes is that the equilibrium of the overall closed loop system may change when the steady state loop gain is detuned, which is different with the case for square MIMO processes. We apply the proposed MIC analysis in the control of a real-time temperature control system and obtained anticipated results. We hope it can provide useful guidance for the experiment validation of offset free tracking controllers for nonlinear 2ISO processes.

Chapter 8

A future direction for outdoor exercise regulations

8.1 Introduction

The body-worn HR monitoring and regulation systems provide the intuitive guide for people in outdoor exercises and health rehabilitation. In clinical cases, however, the existing medical devices have disadvantages in terms of the safety and reliability issues. From exercise physiology point of view, a novel nonlinear multivariable model was successfully established (see the details in Chapter 2), which could completely estimate the body's metabolic rate during dynamic exercises. Following by this idea, this chapter describes a more individualised and auto-adaptive smartphone based HR monitoring, modeling and regulation system.

The aim of this study is to develop a smartphone-based real-time HR monitoring, modeling, and regulation system. It provides the real-time measure of HR and the automated exercise guidance system by communicating a wearable HR sensor with the smartphone via Bluetooth serial port protocol (SPP) and displaying them on an intuitive user interface (UI). The automated exercise guidance system has the ability to make its own decision of whether to increase or decrease the intensity of a workout in a given predefined exercise protocol. The proposed modeling work will be applied into this guidance system, as it can well describe HR dynamics during exercises. The established physical model uses a simple switchable resistance-capacitor (RC) circuit to unify the complex

dynamics at the human's onset and offset of exercise. It not only explains the body's energy-generating process, metabolism and CR responses during exercise, but also mathematically accounts for CR dynamics at the both onset and offset of exercise, in which the continuity of the output and states during switching is guaranteed [169]. Another feature of the developed system is the beeping sound notification. Currently, the boundary control method was implemented well in the guidance system to setup some sorts of exercise programs. Within the predefined program, different types of beeping will be triggered when subjects move from one HR zone to another.

The organization of this chapter is as follows. Section 8.2 introduces the devices applied (Zephyr®), experiment activities, and developed modeling and control methods. Section 8.3 outlines the exercise guidance results of the developed application under the outdoor exercise environment. The application will be tested and the test results will be shown in section 8.3. Section 8.4 concludes this chapter.

8.2 Methods

8.2.1 Modeling of human cardiorespiratory responses during indoor treadmill exercises

In order to test the reliability and accuracy of the completed Android mobile phone based network system, an indoor treadmill exercise was performed. A 27 years old healthy but untrained male subject participated in the experiment. The Zephyr Bluetooth HR chest strap was put on properly (see Fig. 8.1). During exercise the real-time HR data are sent to an Android mobile device via Bluetooth transmission. An intuitive user interface is provided to display and record the HR data and control efforts during workout, shown in the green and red coordinate planes of Fig. 8.2(b) respectively. The subject was

asked to have a light meal at least 2 hours before taking experiment. In the exercise session, the subject walks on a treadmill at 5 km/h for 6 minutes at the warming-up interval. Then, they begin running for 8 minutes at 9 km/h in the onset of exercise session. That consequently follows another 15 minutes walking at 5 km/h speed in the offset afterwards. The recorded data was precisely synchronized. Fig. 8.3 shows the experimental protocol (by red line) and the observed HR readings (by blue line).

Fig. 8.1: Experimental hardware: Zephyr Bluetooth HR chest strap.

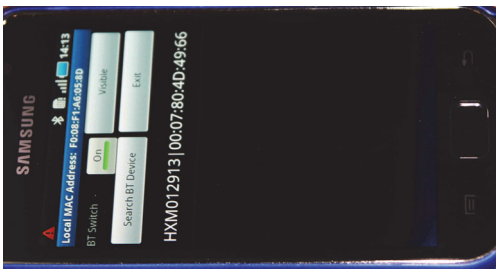

(a) The Android-based automated exercise guidance application UI - 1

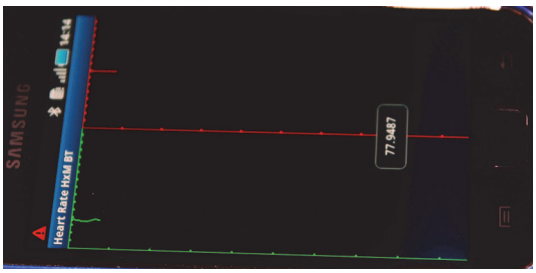

(b) The Android-based automated exercise guidance application UI - 2

Fig. 8.2: Experimental software: Android-based real-time HR measurement and regulation system.

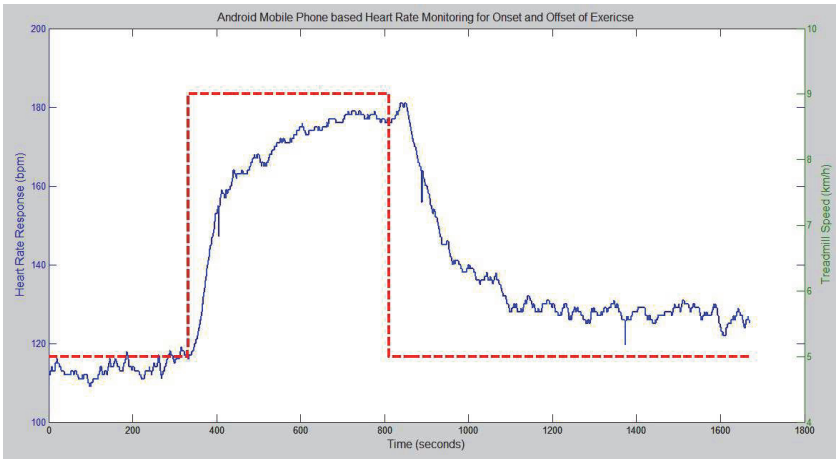

Fig. 8.3: Measured experiment data (HR) followed by the onset and offset exercise protocol.

8.2.2 Modeling of human cardiorespiratory responses for outdoor exercises

The treadmill exercise protocol was defined to analyze the step response of HR. The experiment results in Fig. 8.3 support our early observation [151]: time constant of HR response to exercise is influenced by the load of exercise, as well as by self conditions (e.g., during a constant exercise intensity, steady state gain and time constant of HR/VO_2 response to exercise were found to mostly still be varying in every single moment); in other words, the dynamic characteristics of HR response at onset and offset of exercise are notably different. A natural way to describe this variation is to set up two models for onset and offset dynamics separately, and unify these two models by using switching mechanism. However, how to guarantee the continuity of both output and states of established model is not trivial. Furthermore, to find a physical system that matches this switching model is more difficult. In this project, we proposed a physical system, a switching RC circuit, which can fully explain metabolic dynamics at both onset and offset of exercise. As far as the authors known, this kind of switching model has not been reported in literature till date [53]. More discussions about this modeling work

can be found in Chapter 2.

This modeling work overcame the fundamental difficulty that is the derivation of estimates of metabolic rate from non-invasive measured parameters, such as HR. In the next step, the model will be applied into this application for outdoor exercise.

8.2.3 Regulation of human cardiorespiratory responses during outdoor exercises

At this stage a boundary control system was used. The aim of this control system is to ensure that the subjects' exercise program stays within safe bounds for their level of fitness, and for the high-risk client, within their symptom limited metabolic range. The beeping duration will be adjusted when their HR move into a specific HR zone, and the received current HR value will be added into the blue coordinate of Fig. 8.2(b). In the control law, if the HR is lower than 100 bpm, a fast-paced sound is activated twice per second that allows the subject to have a higher intensity. Then the HR will be increased in every increment in exercise intensity. When the HR exceeds 100 bpm, the sound pattern repeats once per second. If the HR continues to increase over 120 bpm, it beeps at intervals of 3 seconds to alert subjects to stop or slow down exercising.

8.3 Application simulation

The Zephyr sensor transmits HR data to a paired Android mobile phone through SPP protocol. The Bluetooth adapter is configured to read the stream in every 100 milliseconds. Fig. 8.4 shows the recorded HR data (the green coordinate plane) and Boundary Level (BL) data (the red coordinate plane). The horizontal axis scale in both red and green coordinate planes of Fig. 8.4 is 10 seconds; the veridical axis scales are 10 and

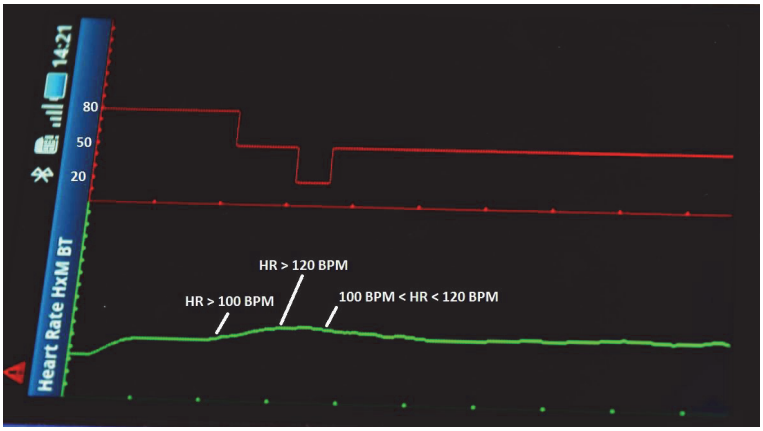

Fig. 8.4: The developed Android-based outdoor exercise regulation system test.

20, respectively. Once a valid HR data is received, its corresponding boundary level will be computed and both data of HR and BL will be plotted on their own planes synchronously. The beep duration will be a various time according to the different BLs. In addition, the current averaged HR value will be shown on the UI when users touch the screen. The results in Fig. 8.4 clearly demonstrate that the reliability of the constructed monitoring system, and the accuracy of the developed boundary control system.

8.4 Conclusion

The experimental results performed by using Zephyr HR belt have shown such device has good performance on multi-event synchronization, low noise interference and fast real-time computation. In the next step, a wireless network involving the smartphone application, the modeling and regulation methods developed in Chapters 3, 4, 5, 6 and 7, the multi-sensor signal processing (such as gas analyzer (Cosmed®), ECG, body temperature, tri-axial accelerometer, signals from a GPS, and micro-IMU), and a robust control approach that has the capability for fault detection and tolerance, will be established. Then, the proposed methods can be validated through the outdoor exercises.

Chapter 9

Conclusion and future work

Biomedical engineering is a discipline that address medical and biological problems through the use of theories borrowed from the physical sciences, and technologies inherited from engineering. Exercise-related biomedical engineering synthesizes data from exercise physiology, biomedicine, and engineering, utilizing exercise as the stressor to develop technologies for early detection, diagnosis, and rehabilitation of diseases.

Several difficulties inherent to the exercise-related biomedical fields, particular to modeling and control of human CR systems, have restrained the progress in the past, problems that make these systems much more difficult to tackle than practically all other types of systems met anywhere in science and engineering.

The goal of the work developed in this dissertation was to address some of these difficulties, of exercise-related biomedicine in general and of control engineering in particular, and to come up with a methodology that would make the optimal estimation and regulation of human CR responses for indoor and outdoor exercises in a portable noninvasive manner, and would utilize external information for exercise monitoring of CR responses based on these types of models and regulation mechanisms.

In a first step, a mathematic modeling methodology was developed. Two slight different exercise protocols were used for two different groups of subjects to investigate the dynamic characteristics of the HR and VO_2 responses to onset and offset of treadmill exercise. The portable gas analyzer K4b^2 was used to measure breath-by-breath VO_2 and beat-by-beat HR values. It was concluded that the dynamic characteristics of hu-

man CR responses at the onset and offset of exercise are distinctively different. Based on the experimental observations, we developed a *Switching Resistance-Capacitor (RC) Model* that can explicitly depict the dynamical characteristics of human CR responses at the onset/offset of exercise and the transition in between. In addition, the developed model provides the quantitative analyses for the terms of energy 'credits', 'deficit', and 'debt'. The validity of the proposed switching model is confirmed by comparing the simulated model outputs with the experimental results.

Second, a modeling and control integrated methodology has been used to demonstrate the validity of this methodology for dealing with the transient behaviors during controller switching. In this study, a machine learning based nonlinear model predictive control for HR response to exercise is introduced. The nonlinear behavior of HR response to treadmill walking exercise is effectively captured by using support vector regression. We investigate both steady state gain and time constant under different walking speeds by using the data from an individual healthy middle aged male subject. The experiment results demonstrate that the time constant for recovery stage is longer than that at onset of exercise. This motivates the use of a time variant model to describe the response to both onset and offset of exercises. Based on this time invariant model, a novel switching model predictive control algorithm has been developed, which applies DMC algorithm to optimize the regulation of HR responses at both onset and offset of exercises. Simulation results indicates switching DMC controller can efficiently handle the different dynamic characteristics at the onset and offset of exercise. However, it should be pointed out that the proposed approach, as most other switching control strategies, also suffers from transient behavior during controller switching. Simulation results in transition stage have slight oscillation due to the quick switching between two controllers.

While the performance of the developed SISO model and control methodology mentioned above was adequate, we believe that a MIMO model would be achieve a better estimate

of each of the desired CR variables, since all available input data will be utilized in each estimation. However, the mutivariable model based control is not trivial. In my PhD studies, the main objective is to develop a set of control methodologies providing zero offset tracking errors under faulty conditions, approaches that could be valid from SISO models to MIMO models, and from 2ISO nonsquare models to MISO nonsquare models.

We first analyzed the system controllability for 2ISO nonsquare processes that is extremely useful for improving fault tolerance ability, as two actuators are simultaneously manipulated. For instance, we proposed to use both control inputs, speed and gradient of treadmill, for regulation of treadmill exercise responses. The concept of nonlinear DIC was extended to 2ISO nonsquare processes, and a sufficient condition is presented. Based on this condition, the new defined MIC for walking, running, and walking/running transition zones was investigated. Simulation study showed the proposed 2ISO control system can avoid the transition of motor patterns if the gains of the two multi-loop integral controllers are well tuned, and ensure offset tracking errors under faulty conditions.

Following the results from 2ISO processes, MIC analysis for MISO processes was established. We presented easy to use sufficient conditions for MISO processes based on singular perturbation analysis. Following conditions, when some of the actuators are totally out of order, if any other actuators are not fully failure broken then offset tracking is still ensured. Moreover, even when some of loop controller served as positive feedback (perhaps due to wrong connections), offset tracking and closed loop system stability can still be achieved. We applied the proposed MIC analysis in the control of a real-time temperature control system and obtained anticipated results.

Finally, an exercise monitoring methodology on the portable and non-invasive measurements of CR responses to outdoor exercises was investigated. The exercise monitoring system developed in my PhD studies is a smartphone application, including interconnections of Bluetooth-connected portable instruments, sensors, and mobile phone. This

technique has been applied, until now, to a simply boundary control algorithm to regulate HR signals only. Outdoor exercise experiments have well validated the accuracy and reliability of the exercise monitoring system. The results obtained are encouraged enough to, in a near future, apply additional transducers to more advanced control algorithms.

Summarizing, the major contributions of this doctoral thesis are the following:

- A methodology for modeling of human CR responses to the onset and offset of exercise.
- A switching model to guarantee the continuity of the model output during model switching.
- A quantitative methodology for A. V. Hill's hypothesis on exercise metabolism during exercise and recovery [53].
- A methodology for the control of human CR responses to the onset and offset of exercise whose dynamics have time-variant properties.
- A sufficient condition for MIC of nonlinear 2ISO processes that has potential for zero offset tracking performance.
- A sufficient condition for MIC of nonlinear MISO processes that has potential for zero offset tracking performance.
- A methodology to closed-loop feedback control for linear MIMO processes involving DIC analysis.
- A methodology for non-invasively monitoring of human CR responses to outdoor exercise by means of interconnections of Bluetooth-based portable transducers and smartphone.

There are some problems that remain open to future research. Although the approach to the modeling and control of human CR responses to exercise has been established, see details in Chapters 3, 4 and 5, the experiment validation of such approach has not yet tackled. In addition, the modeling approach described in Chapter 3 , referred to as *Switching Resistance-Capacitor (RC) Model*, also has the contribution in multi-model switching control, and thus it will be used for the implementation of bump-less switching between two or more higher dimensional systems based on multi-realization theory [8] [149]. Moreover, the MIC analysis method for nonlinear 2ISO and MISO processes described in Chapter 6 and 7 respectively, should be validated through experiments in the future studies.

Another important issue in the outdoor exercise monitor of human CR responses is the reliability of the wireless network involving the smartphone applications and a set of portable and non-invasive sensors. Some current results described in Chapter 8 only surveyed the boundary control of HR signal (Zephyr®). The future studies will concern the multi-sensor signal processing such as ECG (electrocardiogram), respiration rate, body temperature, tri-axial accelerometery and signals from a GPS (Global Positioning System) device and micro-IMU (Inertial Measurement Unit), as well as a robust control approach that has the capability for fault tolerance.

We hope that, with this thesis, we have provided a significant contribution to the field of biomedical engineering, and that our results will prove to be useful for many other researchers dealing with exercise-related CR systems.

Appendix A

Appendix

Proof of Theorem 2.

Proof We prove this theorem based on singular perturbation theory [137][88].

Consider the system of Fig. 7.1 described by Eq. (7.2) and Eq. (7.3). In order to analyze the Lyapunov stability of the unforced closed loop $(\tilde{P}, -C_l)$, the input signal r is set to zero. The state equation for the closed loop $(\tilde{P}, -C_l)$ can be expressed as:

$$(\tilde{P}, -C_l): \quad \begin{cases} \dot{x} &= f(x,\xi) \\ \dot{\xi} &= \eta\, e = -\eta\, y = -\eta\, g(x,\xi). \end{cases} \tag{A.1}$$

Equation (A.1) can be transformed into a standard singular perturbation form [137]: Let $\tau = \eta(t - t_0)$, so that $\tau = 0$ at $t = t_0$. As $\frac{d\tau}{dt} = \eta$, we have:

$$(\tilde{P}, -C_l): \quad \begin{cases} \eta \frac{d}{d\tau} x &= f(x,\xi) \\ \frac{d}{d\tau}\xi &= -g(x,\xi). \end{cases} \tag{A.2}$$

In order to be consistent with standard singular perturbation notation, we will for the moment use the notation $\dot{x}$ to denote the derivative on the *slow* time scale τ when we analyse singular perturbation models.

Now, for the standard singular perturbation model (A.2), based on Condition a) and b), the verification of the following two conditions (the first two conditions of Theorem 2 in [137]) is straightforward:

(i) The equation $0 = f(x, \xi)$ obtained by setting $\eta = 0$ in Eq. (A.2) implicitly defines a unique C^2 function $x = h(\xi)$.

(ii) For any fixed $\xi \in \mathcal{R}^m$, the equilibrium $x_e = h(\xi)$ of the subsystem $\dot{x} = f(x, \xi)$ is Globally Asymptotically Stable (GAS) [137] and Locally Exponentially Stable (LES).

We only need to prove Conclusion (iii) of Theorem 2 in [137], the stability (GAS and LES) of "slow time scale". That is, the following conclusion needs to be proved:

(iii) The equilibrium $\xi = 0$ of the reduced model (slow time scale) $\dot{\xi} = -g(h(\tilde{u}), \tilde{u})$ is GAS and LES. Where $\tilde{u} = [k_1\xi \quad k_2\xi \quad \cdots \quad k_m\xi\ ]^T$.

To prove the above conclusion, select $V(\xi) = \frac{1}{2}\xi^2$ as a Lyapunov function candidate for the "slow time scale". It can be seen that

$$\dot{V}(\xi) = -\xi\, g(h(\tilde{u}), \tilde{u}). \tag{A.3}$$

It is easy to check both $V(\xi)$and $\dot{V}(\xi)$ will satisfy the requirements for GAS and LES given that Condition c) is satisfied.

Now, we prove that c') is sufficient to ensure c).

The steady state input-output function$g(h(\tilde{u}), \tilde{u})$can be rewritten as $g(h(\tilde{u}), \tilde{u}) = g(\tilde{u}_1, \tilde{u}_2, \cdots, \tilde{u}_m) = g(k_1\xi, k_2\xi, \cdots, k_m\xi)$. Then, its derivative with ξ is $\frac{\partial}{\partial\xi} g(k_1\xi, k_2\xi, \cdots, k_m\xi) = k_1\frac{\partial g}{\partial \tilde{u}_1} + k_2\frac{\partial g}{\partial \tilde{u}_2} + \cdots + k_m\frac{\partial g}{\partial \tilde{u}_m}$. Consider that $g(0, 0) = 0$, and $k_1\frac{\partial g}{\partial \tilde{u}_1} + k_2\frac{\partial g}{\partial \tilde{u}_2} + \cdots + k_m\frac{\partial g}{\partial \tilde{u}_m} > 0$. We have $\dot{V}(\xi) = -\xi\, g(h(\tilde{u}), \tilde{u}) < 0$ for $\xi \neq 0$. Furthermore, as $k_1\frac{\partial g}{\partial \tilde{u}_1} + k_2\frac{\partial g}{\partial \tilde{u}_2} + \cdots + k_m\frac{\partial g}{\partial \tilde{u}_m} > \rho > 0$ in a neighbourhood of $\xi = 0$, it can be concluded that $\xi \cdot g(h(\tilde{u}), \tilde{u}) > \rho \cdot \xi^2$ in a neighbourhood of $\xi = 0$.

Bibliography

[1] Exercise and diabetes mellitus. In *Exercise and Sports Sciences Reviews*. Baltimore: Lippincott, Williams & Wilkins, 1992. 45, 46

[2] Position statement: Nutritional recommendations and principles for people with diabetes mellitus. *Diabetes Care*, 17:519–22, 1994. 46

[3] *Clinical Practice Guidelines for the Mangement of Overweight and Obesity in Adults*. Australia: National Health and Medical Research Council, 2006. 113, 124

[4] R. Acharya, A. Kumar, I. P. Bhat, L. Choo, S. Iyengar, K. Natarajan, and S. Krishnan. Classification of cardiac abnormalities using heart rate signals. *Medical & Biological Engineering & Computing*, 42(3):288–293, 2004. 14, 71, 86

[5] J. Achten and A. E. Jeukendrup. Heart rate monitoring applications and limitations. *Sports Med.*, 33(7):517–538, 2003. 57

[6] Shaper AG, Wannamethee G, Macfarlane PW, and Walker M. Heart rate ischaemic heart disease: sudden cardiac death in middle-aged british men. *Br Heart J*, 70:49–55, 1993. 86

[7] Dallas AHA. *Heart and stroke statistical update*. Dallas AHA, 1998. 35, 36

[8] B. D. O. Anderson, S. W. Su, and T. S. Brinsmead. Multi-realization of linear multi-variable systems. *IEEE Transaction on Circuits and Systems II*, 52(8):442–446, 2005. 69, 152

[9] Richard G. Aseltine, Charles L. Feldman, John A. Paraskkos, and Romeo L. Moruzzi. A simple device for closed loop heart rate control during cardiac rehabilitation. *IEEE Transactions on Biomedical Engineering*, BME-26(8):456–464, 1979. 53

[10] American Diabetes Association. *Fact sheet on diabetes*. Alexandria, VA, 1985. 44

[11] American Heart Association. Statement on exercise. *Circulation*, 86:340–44, 1992. 39

[12] P.O. Astrand, T.E. Cuddy, B. Saltin, and J. Stenberg. Cardiac output during submaximal and maximal work. *J. Appl. Physiol*, 9:268–274, 1964. 53, 71, 86

[13] K. J. Astrom and B. Wittenmark. *Computer Controlled Systems, Theory and Design*. Thomas Kailath, Ed., Prentice-Hall Information and System Science Series, 1984. 101

[14] R. Bailon, G. Laouini, C. Grao, M. Orini, P. Laguna, and O. Meste. The integral pulse frequency modulation model with time-varying threshold: application to heart rate variability analysis during exercise stress testing. *IEEE Transactions on Biomedical Engineering*, 58(3):642–52, 2011. 13, 14, 53

[15] Raquel Bailon, Nuria Garatachea, Ignacio de la Iglesia, Jose Antonio Casajus, and Pablo Laguna. Influence of running stride frequency in heart rate variability analysis during treadmill exercise testing. *IEEE Transactions on Biomedical Engineering (in press)*, 2013. 14, 53

[16] C. Balderrama, G. Ibarra, J. De La Riva, and S. Lopez. Evaluation of three methodologies to estimate the vo_{2max} in people of different ages. *Applied Ergonomics*, 42:162–168, 2010. 32, 55

[17] Williams & Wilkins Baltimore: Lippincott. *ACSM's Guidelines for Exercise Testing and Prescription*. Baltimore: Lippincott, Williams & Wilkins, 2000. 42

[18] A.K. Barros and N. Ohnishi. Heart instantaneous frequency (hif):an alternative approach to extract heart rate variability. *IEEE Transactions on Biomedical Engineering*, 48(8):850–855, 2001. 53

[19] D. R. Bassett and A. J. Zweifler. Risk factors and risk factor management. In *Clinical Ischemic Syndromes*. St. Louis: C. V. Mosby, 1990. 46

[20] Tom Baster and Christine Baster-Brooks. Exercise and hypertension. *Healthy heart*, 34(6):419–24, 2005. 48, 49

[21] R. Beaglehole, R. Bontia, and T. Kjellstrom. *Basic Epidemiology*. Geneva: World Health Organization, 1993. 36

[22] K. E. Berg. *Diabetic's Guide to Health and Fitness*. Champaign, IL: Life Enhancement Publications, 1986. 44

[23] K. Birch, D. MacLaren, and K. George. *Sport & exercise physiology*. BIOS Scientific Publishers, 2005. 1, 2, 4, 35

[24] C. Bordons and E.F. Camacho. *Model predictive control, 2nd edition*. Springer-Verlag, London, 2004. 89, 90, 91

[25] R. B. Bradfield. A technique for determination of usual daily energy expenditure in the field. *The American Journal of Clinical Nutrition*, 24:1148–1154, 1971. 16, 56

[26] G. Brooks, T. Fahey, and T. White. *Exercise Physiology: Human Bioenergetics and Its Applications*. Mountain View, CA: Mayfield, 1996. 34

[27] A. Cabasson, O. Meste, and J.M. Vesin. Estimation and modeling of qt-interval adaptation to heart rate changes. *IEEE Transactions on Biomedical Engineering*, 59(4):956–65, 2012. 14, 53

[28] Aline Cabasson, Olivier Meste, Gregory Blain, and Stephane Bermon. Quantifying the pr interval pattern during dynamic exercise and recovery. *IEEE Transactions on Biomedical Engineering*, 56(11):2675–83, 2009. 13, 14, 53

[29] B. N. Campaigne and R. N. Lampman. *Exercise in Clinical Management of Diabetes*. Champaign, IL: Human Kinetics, 1994. 46

[30] P. Campo and M. Morari. Achievable closed-loop properties of systems under decentralized control: Conditions involving the steady state gain. *IEEE Transactions and Automatic Control*, 39(5):932–943, 1994. 115, 129

[31] D. C. Cantu. *Diabetes and Exercise*. Ithaca, NY: Movement Publications, 1982. 44

[32] R. Cappellini, YP Ivanenko, RE Poppele, and F. Lacquaniti. Motor patterns in human walking and running. *Journal of Neurophysiology*, 95:3426–3437, 2006. 122

[33] C. J. Caspersen. Physical activity epidemiology: Concepts, methods, and applications to exercise science. In *Exercise and Sport Science Reviews*. Baltimore: Williams & Wilkins, 1989. 39

[34] Angela Nebot Castells. Qualitative modeling and simulation of biomedical systems using fuzzy inductive reasoning. Doctoral thesis, 1994. 1, 2

[35] P. Castiglioni, G. Parati, A. Civijian, L. Quintin, and M. Di Rienzo. Local scale exponents of blood pressure and heart rate variability by detrended fluctuation analysis: Effects of posture, exercise, and aging. *IEEE Transactions on Biomedical Engineering*, 56(3):675–84, 2009. 53

[36] Weidong Chen, Steven. W. Su, Yi Zhang, Ying Guo, Nghir Nguyen, Branko G. Celler, and Hung T. Nguyen. Nonlinear modeling using support vector machine for heart rate response to exercise. In *Computational Intelligence and its Applications: Evolutionary Computation, Fuzzy Logic, Neural Network and Support Vector Machine Techniques*. World Scientific, 2010. 86

[37] Y. Chen and Y. Lee. Effect of combined dynamic and static workload on heart rate recovery cost. *Ergonomics*, 41(1):29–38, 1998. 71

[38] Michael Cheng. *Medical device regulations: global overview and guiding principles*. World Health Organization, 2003. 6

[39] T.M. Cheng, A.V. Savkin, B.G. Celler, S.W. Su, and L. Wang. Nonlinear modelling and control of human heart rate response during exercise with various work load intensities. *IEEE Trans. Biomed. Eng.*, 55(11):2499–2508, 2008. 13, 14, 53, 71, 113

[40] A. Coggin. Plasma glucose metabolism during exercise in humans. *Sports Medicine*, 11:102–124, 1991. 30

[41] R.A. Cooper, T.L. Fletcher-Shaw, and R.N. Robertson. Model reference adaptive control of heart rate during wheelchair ergometry. *IEEE Trans. Contr. Syst. Tech.*, 6(4):507–514, 1998. 72

[42] J. H. Coote. Cardiovascular responses to exercise: central and reflex contributions. In *Cardiovascular regulation*, pages 93–111. Portland, London, 1995. 5

[43] A. Cowley. Long-term control of arterial blood pressure. *Physiological Reviews*, 72:231–300, 1992. 26, 29

[44] M.A.Mc. Crory, P.A. Mole, L.A. Nommsen-Rivers, and K.G. Dewey. Between-day and within-day variability in the relation between heart rate and oxygen consump-

tion: effect on the estimation of energy expenditure by heart-rate monitoring. *The American Journal of Clinical Nutrition*, 66:18–25, 1997. 16, 56

[45] T. R. Dawber. *The Framingham Study.* Cambridge, MA: Harvard University Press, 1980. 36, 37

[46] Rebeka J. Donatello. Health, the basics. *Pearson Education, Inc.*, January 1985. 24

[47] Danielle Dougherty and Doug Cooper. A practical multiple model adaptive strategy for single-loop mpc. *Control Engineering Practice*, 11:141–159, 2003. xiii, 88, 93

[48] H. Drucker, C. Burges, L.Kaufman, A. Smola, and V. Vapnik. *Support vector regression machines.* Advances in Neural Information Procession Systems, M. Mozer, M. Jordan, and T. Petsche, Eds., Cambridge, MA. 73

[49] R. Duffield, B. Dawson, H. C. Pinnington, and P. Wong. Accuracy and reliability of a cosmed k4b^2 portable gas analysis system. *J Sci Med Sport*, 7(1):11–22, 2004. 57

[50] M.E. Duffy. Designing research the qualitative - quantitative debate. *Journal of Advanced Nursing*, 11(3):225–232, 1985. 7

[51] Richard M. Engeman, George D. Swanson, and Richard H. Jones. Input design for model discrimination: Application to respiratory control during exercise. *IEEE Transactions on Biomedical Engineering*, BME-26(10):579–85, 1979. 13, 53

[52] A. Alwan et al. Monitoring and surveillance of chronic noncommunicable diseases: progress and capacity in high-burden countries. *The Lancet*, 376:1861–1868, 2010. 3

[53] A. V. Hill et al. Muscular exercise, lactic acid and the supply and utilization of oxygen. *Proc. R. Soc. Lond. (Biol.)*, 96:438, 1924. 15, 54, 55, 62, 64, 65, 145, 151

[54] E. F. Coyle et al. Carbohydrate and fluid ingestion during exercise: Are there tradeoffs? *Medicine and Science in Sports and Exercise*, 24:671–678, 1991. 30

[55] Franklin et al. Exercise prescription of the myocardial infarction patient. *Journal of Cardiopulmonary Rehabilitation*, 6:62–79, 1986. 40, 41

[56] G. A. Brooks et al. *Exercise Physiology: Human Bioenergetic and Its Applications*. Mountain View, CA: Mayfield, 2000. 22, 24, 59, 60

[57] K. E. Powell et al. Physical activity and the incidence of coronary heart disease. *Annual Review of Public Health*, 8:253–87, 1987. 39

[58] M.S. Fairbarn, S.P. Blackie, N.G. McElvaney, B.R. Wiggs, P.D. Pare, and R.L. Pardy. Prediction of heart rate and oxygen uptake during incremental and maximal exercise in healthy adults. *Chest*, 105:1365–1369, 1994. 71, 86

[59] Heart Foundation. Hypertension management guide for doctors. *Heart Foundation. Available at: www.heartfoundation.com.au*, 2004. xv, 47, 48

[60] E. Fox, M. Foss, and S. Keteyian. *Fox's Physiology Basis for Exercise and Sport*. New York: McGraw Hill Companies, 1998. 35

[61] G. F. Franklin and J. D. Powell. *Digital control of dynamic systems*. Reading, MA: Addison-Wesley, 1980. 101

[62] M.E. Freedman, G.L. Snider, P. Brostoff, S. Kimelblot, and L.N. Katz. Effects of training on response of cardiac output to muscular exercise in athletes. *J. Appl. Physiol*, 8:37–47, 1955. 53, 71, 86

[63] E. Gaeta, G. Cea, M.T. Arredondo, and J.P. Leuteritz. Amirtem: A functional model for training of aerobic endurance for health improvement. *IEEE Transactions on Biomedical Engineering*, 59(11):3155–61, 2012. 53

[64] C. E. Garcia and A. M. Morshedi. Quadratic programming solution of dynamic matrix control (qdmc). *Chemical Engineering Communications*, 46:73–87, 1986. 97

[65] C. E. Garcia, D. M. Prett, and M. Morari. Model predictive control: Theory and practice-a survey. *Automatica*, 25(3):335–348, 1989. 87

[66] Leslie A. Geddes, Neal E. Fearnot, and Heidi J. Smith. The exercise-responsive cardiac pacemaker. *IEEE Transactions on Biomedical Engineering*, BME-31(12):763–770, 1984. 53

[67] I. Goethals., K. Pelckmans, J. Suykens, and B. De Moor. Identification of mimo hammerstein models using least squares support vector machines. *Automatica*, 41:1263–1272, 2005. 73

[68] P. Gollnick. Metabolism of substrates: Energy substrate metabolism during exercise and as modified by training. *Federation Proceedings*, 44:353–356, 1985. 30

[69] Google. $http://en.wikipedia.org/wiki/superposition_principle$. *Wikipedia*. 98

[70] N. F. Gordon, C. B. Scott, W. J. Wilkinson, J. J. Duncan, and S. N. Blair. Exercise and mild hypertension: Recommendations for adults. *Sports medicine*, 10:390–404, 1990. 49

[71] Y. Goren, LR. Davrath, I. Pinhas, E. Toledo, and S. Akselrod. Individual time-dependent spectral boundaries for improved accuracy in time-frequency analysis of heart rate variability. *IEEE Transactions on Biomedical Engineering*, 53(1):35–42, 2006. 14, 53

[72] S. Gunn, M. Brown, and K. Bossley. Network performance assessment for neuro-fuzzy data modelling. *Intelligent Data Analysis*, pages 313–323, 1997. 73

[73] Y. Guo, P. Bartlett, J. Shawe-Taylor, and R. Williamson. Covering numbers for support vector machines. *IEEE Trans. on Information Theory*, 48(1):239–250, 2002. 73

[74] M. Hajek, J. Potucek, and V. Brodan. Mathematical model of heart rate regulation during exercise. *Automatica*, 16:191–195, 1980. 13, 14, 53, 71

[75] JR. Halliwill, JA. Taylor, and DL. Eckberg. Impaired sympathetic vascular regulation in humans after acute dynamic exercise. *J Physiol*, 195:279–88, 1996. 49

[76] Terry J. Housh and Dona J. Housh. *Introduction to exercise science*. Allyn & Bacon, 2000. 1, 2, 3, 4, 5, 35

[77] E. T. Howley and B. D. Franks. *Health Fitness Instructor's Handbook*. Champaign, IL: Human Kinetics, 1997. 43

[78] E. T. Howley and S. K. Powers. *Exercise Physiology: Theory and Application to Fitness and Performance*. Dubuque, IA: Wm. C. Brown Publishers, 1990. 4

[79] E. Hultman and H. Sjoholm. Substrate availability. In *Biochemistry of Exercise, ed. H. Knuttgen, J. Vogel, and J. R. Poortmans*. Champaign, IL: Human Kinetics, 1983. 30

[80] K. J. Hunt. Treadmill control protocols for arbitrary work rate profiles conbining simultaneous nonlinear changes in speed and angle. *Biomedical Signal Processing and Control*, 3:278–383, March 12, 2008. 113, 124

[81] J. L. Ivy, T. W. Zderic, and D. L. Fogt. Prevention and treatment of non-insulin-dependent diabetes mellitus. In *Exercise and Sports Sciences Reviews*. Baltimore: Lippincott, Williams & Wilkins, 1998. 44

[82] L. P. Jamieson, K. J. Hunt, and D. B. Allan. A treadmill control protocol combining nonlinear, equally smooth increases in speed and gradient. *Med. Eng. Phys.*, 2007. 113

[83] Evaluation Joint National Committee on Detection and Treatment of High Blood Pressure. The sixth report of the joint national committee on detection, evaluation, and treatment of high blood pressure. *Report V. Arch Intern Med*, 157:2413–45, 1997. 47, 48

[84] W. B. Kannel. Contributions of the framingham study to preventive cardiology. *Journal of the American College of Cardiology*, 15:206–211, 1990. 36, 38

[85] F. Kao. An experimental study of the pathways involved in exercise hyperpnea employing cross-circulation techniques. In *The Regulation of Human Respiration, ed. D. Cunningham*. Oxford: Blackwell, 1963. 27

[86] Jason Karp. The three metabolic energy systems. *IDEA Fitness Journal*, 6(2):10–16, 2009. 22, 23, 59, 60, 61, 65

[87] F. W. Kemmer and M. Berger. Exercise and diabetes mellitus: Physical activity as a part of daily life and its role in the treatment of diabetic patient. *International Journal of Sports Medicine*, 4:77–88, 1983. 2, 44

[88] P. Kokotovic, H. Khalil, and J. Reilly. *Singular Perturbation Methods in Control: Analysis and Design*. Academic Press Inc, U. S. A, 1986. 115, 118, 133, 135, 153

[89] A. M. Kriska, S. N. Blair, and M. A. Pereira. The potential role of physical activity in the prevention of non-insulin-dependent diabetes mellitus: The epidemiologi-

cal evidence. In *Exercise and Sports Sciences Reviews*. Baltimore: Lippincott, Williams & Wilkins, 1994. 44

[90] R. M. Lampman and D. E. Schteingart. Effects of exercise training on glucose control, lipid metabolism, and insulin sensitivity in hypertriglyceridemia and non-insulin dependent diabetes mellitus. *Medicine and Science in Sports and Exercise*, 23:703–12, 1991. 46

[91] The Lancet. Frost & sullivan statistics. *Frost & Sullivan Statistics*, January 16, 2005. 47

[92] M. H. Laughlin. Cardiovascular response to exercise. *Am. J. Physiol.*, 277:S244–S259, 1999. 5

[93] V. R. Legrand, G. Laarman, N. Danchin, M. A. Morel, and P. W. Serruys. Diagnostic values of exercise electrocardiography and angina after coronary artery stenting. *American Heart Journal*, 133:240–48, 1997. 41

[94] A. Linder and R. Kennek. *Model predictive control for electrical drives*. Wuppertal University, Germany, 2005. 90

[95] L. Ljung. *System Identification Toolbox V4.0 for Matlab*. MA: The MathWorks, Inc., 1995. 76

[96] B. Macmahon and T. F. Pugh. *Epidemiology*. Boston: Little, Brown, 1970. 36

[97] E. Magosso and M. Ursino. Cardiovascular response to dynamic aerobic exercise: a mathematical model. *Med. Biol. Eng. Comput.*, 40:660–674, 2002. 13

[98] J. L. Marchetti, D. A. Mellichamp, and D. E. Seborg. Predictive control based on discrete convolution models. *Industrial & Engineering Chemistry, Processing Design and Development*, 22:488–495, 1983. 97

[99] A. D. Martin. Ecg and medications. In *Health/Fitness Instructor's Handbook*. Champaign, IL: Human Kinetic, 1986. 40

[100] Frederic Mazenc, Michael Malisoff, and Marcio de Querioz. Tracking control and robustness analysis for a nonlinear model of human heart rate during exercise. *Automatica, In Press*, 2011. 113

[101] William D. McArdle, Frank I. Katch, and Victor L. Katch. *Exercise Physiology: Energy, Nutrition, and Human Performance*. Lea & Febiger, 1981. 12, 15, 16, 30, 31, 53, 54, 57, 65

[102] Olivier Meste, Balkine Khaddoumi, Gregory Blain, and Stephane Bermon. Time-varying analysis methods and models for the respiratory and cardiac system coupling in graded exercise. *IEEE Transactions on Biomedical Engineering*, 52(11):1921–1930, 2005. 13, 14, 53

[103] A. M. Morshedi, C. R. Cutler, and T. A. Skrovanek. Optimal solution of dynamic matrix control with linear programming techniques (ldmc). *Proceedings of the American Control Conference, New Jersey: IEEE Publications*, pages 199–208, 1985. 97

[104] K. R. Muske and J. L. Rawlings. Model predictive control with linear models. *AICHE Journal*, 39:262–287, 1993. 87

[105] B. Nobel. *Physiology of Exercise and Sport*. St. Louis: C. V. Mosby, 1986. 29

[106] American College of Sports Medicine. *ACSM's Exercise Management for Persons with Chronic Diseases and Disabilities*. Champaign, IL: Human Kinetics, 1997. xv, 42, 48, 49, 50

[107] American College of Sports Medicine. *ACSM's Resource Manual for Guidelines for Exercise Testing and Prescription*. Baltimore: Lippincott, Williams & Wilkins, 1998. 42

[108] American College of Sports Medicine. The recommended quantity and quality of exercise for developing and maintaining cardiorespiratroy and muscular fitness and flexibility in healthy adults. *Medicine and Science in Sports and Exercise*, 30:907–91, 1998. 46

[109] World Health Organization. Prevention of diabetes mellitus. *Report of a WHO Study Group. Geneva: World Health Organization*, (844), 1994. 2, 44

[110] World Health Organization. World health statistics 2012. *World Health Organization*, pages 12–31, 2012. 47, 48

[111] R. S. Paffenbarger, R. T. Hyde, and A. L. Wing. Work activity and coronary heart mortality. *New England Journal of Medicine*, 292:545–50, 1975. 39

[112] X.R. Pan, G.W. Li, Y.H. Hu, J.X. Wang, W.Y. Yang, and Z.X. An. Effects of diet and exercise in preventing niddm in people with impaired glucose tolerance: The da qing igt and diabetes study. *Diabetes Care*, 20(4):537–544, 1997. 71

[113] M. Paradiso, S. Pietrosanti, S. Scalzi, P. Tomei, and C.M. Verrelli. Experimental heart rate regulation in cycle-ergometer exercises. *IEEE Transactions on Biomedical Engineering*, 60(1):135–39, 2013. 53

[114] D. H. Pawelczyk, B. Hanel, J. Warberg R. A. Pawelczyk, and N. H. Secher. Dynamic and steady-state respiratory responses to bicycle exercise. *J. Appl. Physiol.*, 73:1838–1846, 1992. 5

[115] Physician and Sports medicine. A roundtable: Physiological adaptations to chronic endurance exercise training in patients with coronary artery disease. *Physician and Sports medicine*, 15(9):129–56, 1987. 43

[116] H. C. Pinnington, P. Wong, J. Tay, D. Green, and B. Dawson. The level of accuracy and agreement in measures of f_eo_2, f_eco_2, and v_e, between the cosmed k4b^2 portable, respiratory gas analysis system and a metabolic cart. *Journal of Science and Medicine in Sport*, 4(3):324–335, 2001. 57

[117] M. L. Pollock and J. H. Wilmore. *Exercise in Health and Disease*. Philadelphia: W. B. Saunders, 1990. 43

[118] Scott K. Powers and Edward T. Howley. *Exercise Physiology: Theory and Application to Fitness and Performance*. McGraw Hill, 2001. xii, 4, 17, 25, 26, 27, 30, 32, 33, 36, 46

[119] National preventative health taskforce. *Obesity in Australia: a need for urgent action*. Commonwealth of Australia, 2008. 3

[120] B. A. Qgunnaike. Dynamic matrix control: A nonstochastic, industrial process control technique with parallels in applied statistics. *Industrial & Engineering Chemical Fundamentals*, 25:712–718, 1986. 97

[121] S.J. Qin and T. A. Badgwell. A survey of model predictive control technology. *Control Engineering Practice*, 11(7):733–764, 2003. 89

[122] S. Quaglietti and V. F. Froelicher. Physical activity and cardiac rehabilitation for patients with coronary heart disease. In *Physical Activity, Fitness, and Health*. Champaign, IL: Human Kinetics, 1994. 41

[123] Alfio Quarteroni. Modeling the cardiovascular system - a mathematical adventure: part i. *SIAM News*, 34(5):1–3, 2001. 5, 11

[124] J. Richalet. *Practque de la commande predictive.* The Institute of Electrical Engineers, Hermes, 1992. 92

[125] J Richalet. Industrial applications of model based predictive control. *Automatica*, 29(5):1251–1274, 1993. 87

[126] J. Richalet, A. Rault, J. L. Testud, and J. Papon. Model predictive heuristic control: Applications to industrial processes. *Automatica*, 14:413–428, 1978. 89

[127] E. R. Richter and H. Galbo. Diabetes, insulin, and exercise. *Sports Medicine*, 3:275–88, 1986. 44, 46

[128] R. A. Robergs and S. o. Roberts. *Exercise Physiology: Exercise, Performance, and Clinical Applications.* Boston: William C. Brown, 1997. 23, 24, 59, 60

[129] P. D. Roberts. *A brief of model predictive control.* The Institute of Electrical Engineers, UK, 1999. 91, 92

[130] I. H. R. Rockett. Population and health: an introduction to epidemiology. *Population Bulletin*, 49:1–48, 1994. 4, 36

[131] S. Rubin. Core temperature regulation of heart rate during exercise in humans. *Journal of Applied Physiology*, 62:1997–2002, 1987. 33

[132] J. Saul. Thermal and circulatory responses to repeated bouts of prolonged running. *News in Physiological Sciences*, 5:32–37, 1990. 27

[133] S. Scalzi, P. Tomei, and C.M. Verrelli. Nonlinear control techniques for the heart rate regulation in treadmill exercises. *IEEE Transactions on Biomedical Engineering*, 59:599–603, 2012. 113

[134] Stefano Scalzi, Patrizio Tomei, and Cristiano Maria Verrelli. Nonlinear control techniques for the heart rate regulation in treadmill exercises. *IEEE Transactions on Biomedical Engineering*, 59(3):599–603, 2012. 14, 53, 57

[135] B. Schlkopf and A. Smola. *Learning with kernels*. MIT Pres, Cambridge, 2002. 73, 76

[136] V. Seliger and J. Wagner. Evaluation of heart rate during exercise on a bicycle ergometer. *Physiol. Boheraoslov*, 18:41, 1969. 71

[137] R. Sepulchre, M. Jankovic, and P. Kokotovic. *Constructive Nonlinear Control*. New York: Springer Verlag, 1996. 115, 118, 119, 153, 154

[138] Serendip. *Regulation of Human Heart Rate*. Serendip, June 27, 2007. 27

[139] DL. Sherman. Exercise and endothelial function. *Coron Artery Dis*, 11:117–22, 2000. 48

[140] R. Shridhar and D. J. Cooper. A tuning strategy for unconstrained siso model predictive control. *Industrial & Engineering Chemical Research*, 36:729–746, 1997. 100, 102

[141] R. Shridhar and D. J. Cooper. A tuning strategy for unconstrained multivaribale model predictive control. *Industrial & Engineering Chemical Research*, 37:4003–4016, 1998. 100, 102

[142] D. S. Siscovick. Habitual vigorous exercise and primary cardiac arrest: Effect of other risk factors on the relationship. *Journal of Chronic Disease*, 37:625–31, 1984. 39

[143] Sigurd Skogestad and Manfred Morari. Variable selection for decentralized control. *Modeling, Identification and Control*, 13(2):113–125, 1992. 115, 129, 130, 135

[144] J. T. Soukup and J. E. Kovaleski. A review of the effects pf resistance training for individuals with diabetes mellitus. *Diabetes Education*, 19:307–12, 1991. 46

[145] R. A. Stallones. *Public health monograph 76*. Washington, D. C.:U. S. Government Printing Office. 36

[146] W. Stanley and R. Connett. Regulation of muscle carbohydrate metabolism during exercise. *FASEB Journal*, 5:2155–2159, 1991. 30

[147] S. Stewart, G. Tikellis, M. Carrington, K. Walker, and K. O'Dea. *Australia's Future Fat Bomb: A report on the long-term consequences of Australia's expanding waistline on cardiovascular disease*. Preventive Cardiology at the Baker Heart Research Institute, April 2008. 53, 113

[148] S. Su, L. Wang, B. Celler, A. Savkin, and Y. Guo. Identification and control for heart rate regulation during treadmill exercise. *IEEE Trans. Biomed. Eng.*, 54(7):1238–1246, 2007. 13

[149] S. W. Su, B. D. O. Anderson, and T. S. Brinsmead. The minimal multi-realization of linear multi-variable systems. *IEEE Transaction on Automatic Control*, 54(4):690–695, 2006. 69, 152

[150] S. W. Su, J. Bao, and P. L. Lee. Analysis of decentralized integral controllability for nonlinear systems. *Computers and Chemical Engineering*, 28(9):1781–1787, 2004. 115, 129, 130, 135

[151] S. W. Su, W. Chen, D. Liu, Y. Fang, W. Kuang, X. Yu, T. Guo, B. Celler, and H. Nguyen. Dynamic modelling of heart rate response under different exercise intensity. *The Open Medical Informatics Journal (In Press)*, 2010. 14, 53, 57, 145

[152] S. W. Su, S. Huang, L. Wang, B. G. Celler, A. V. Savkin, Y. Guo, and T. M. Cheng. Optimizing heart rate regulation for safe exercise. *Ann. Biomed. Eng.*, 38:758–768, 2010. 113

[153] S.W. Su, B.G. Celler, A. Savkin, H.T. Nguyen, T.M. Cheng, Y. Guo, and L. Wang. Transient and steady state estimation of human oxygen uptake based on noninvasive portable sensor measurements. *Medical & Biological Engineering & Computing*, 47(10):1111–1117, 2009. 53, 71, 86, 124

[154] S.W. Su, L. Wang, B. Celler, E. Ambikairajah, and A. Savkin. Estimation of walking energy expenditure by using support vector regression. *in Proceedings of the 27th Annual International Conference of the IEEE Engineering in Medicine and Biology Society (EMBS)*, pages 3526–3529, September, 2005, Shanghai, China. 71, 86

[155] S.W. Su, L. Wang, B.G. Celler, A.V. Savkin, and Y. Guo. Identification and control for heart rate regulation during treadmill exercise. *IEEE Trans. Biomed. Eng.*, 54(7):1238–1246, 2007. 57, 64, 78, 113, 117, 125

[156] J. Suykens, Van Gestel, J. De Brabanter, B. De Moor, and J. Vandewalle. Least squares support vector machines. *Singapore: World Scientific*, 2002. 73

[157] G.P. Talwar and L.M. Sriwastavaby. *Textbook of Biochemistry and Human Biology (3 ed.)*. Eastern Economy Edition, 2003. 34

[158] V. Tibes. Reflex inputs to the cardiovascular and respiratory centers from dynamically working canine muscles. *Circulation Research*, 41:332–41, 1977. 27

[159] C. L. Tommaso, M. Lesch, and E. H. Sonnenblick. Alterations in cardiac function in coronary heart disease, myocardial infarction, and coronary bypass surgery. In *Rehabilitation of the Coronary Patient*. New York: Wiley, 1984. 41

[160] J. Tuomilehto, J. Lindstrom, J.G. Eriksson, T.T. Valle, H. Hamalainen, P.Ilanne-Parikka, S. Keinanen-Kiukaanniemi, M. Laakso, A. Louheranta, M. Rastas, V. Salminen, and M. Uusitupa. Prevention of type 2 diabetes mellitus by changes in lifestyle among subjects with impaired glucose tolerance. n. engl. j. med. *Finnish Diabetes Prevention Study Group*, 344:1343–1350, 2001. 71

[161] V. Vapnik. *The Nature of Statistical Learning Theory*. Springer, New York, 1995. 73

[162] V. Vapnik and A. Lerner. Pattern recognition using generalized portrait method. *Automation and Remote Control*, 1963. 73

[163] M. Vranic and D. Wasserman. Exercise, fitness, and diabetes. In *Exercise, Fitness, and Health*. Champaign, IL: Human Kinetics, 1990. 46

[164] L. Wang, S.W. Su, B.G. Celler, G.S.H. Chan, T.M. Cheng, and A.V. Savkin. Assessing the human cardiovascular response to moderate exercise. *Physiological Measurement, Physiol. Meas.*, 30:227–244, 2009. 86

[165] K. Weng, B. Turk, L. Dolores, T. N. Nguyen, B. G. Celler, S. W. Su, and H. T. Nguyen. Fast tracking of a given heart rate profile in treadmill exercise. *Conf Proc IEEE Eng Med Biol Soc.*, 25:69–72, 2010. 114, 115, 122, 125, 130

[166] N. K. Wenger and H. K. Hellerstein. *Rehabilitation of the Coronary Patient*. New York: Churchill Livingstone, 1984. 42, 43

[167] N. K. Wenger and J. W. Hurst. Coronary bypass surgery as a rehabilitative procedure. In *Rehabilitation of the Coronary Patient*. New York: Wiley, 1984. 41

[168] C. Yu and M. Fan. Decentralized integral controllablility and d-stability. *Chemical Engineering Science*, 45:3299–3309, 1990. 115, 129, 130

[169] Yi Zhang, Steven W. Su, Azzam Haddad, Branko Celler, and Hung T. Nguyen. Onset and offset exercise response model in electronic terms. *Proceedings of the 9th IASTED International Conference on Biomedical Engineering, Innsbruck, Austria*, February 15-17, 2012. 15, 53, 54, 57, 143

[170] Yi ZHANG, Nadarajah Veluppillai, Steven Su, and Jordan Nguyen. Model predictive controller design for static var compensator. *Proceedings of the* 8^{th} *Asia-Pacific Conference on Control & Measurement*, 2008. 93

Index